

Molecular and functional characterization of communicating channels

Dissertation to obtain the degree
Doctor Rerum Naturalium (Dr. rer. nat.)
at the Faculty of Biology and Biotechnology
Ruhr-University Bochum

International Graduate School of Biosciences
Ruhr-University Bochum
Department of
Neuroanatomy and Molecular Brain Research

submitted by
Kathrin H. Engelhardt

from
Dortmund, Germany

Bochum
April 2011

Molekulare und funktionelle Charakterisierung kommunizierender Kanäle

Dissertation zur Erlangung des Grades
eines Doktors der Naturwissenschaften
der Fakultät für Biologie und Biotechnologie
an der Internationalen Graduiertenschule Biowissenschaften
der Ruhr Universität Bochum

angefertigt in der Abteilung
für Neuroanatomie und Molekulare Hirnforschung

vorgelegt von
Kathrin H. Engelhardt

aus
Dortmund

Bochum
April 2011

Table of Contents

Abbreviations	5
List of Figures	7
List of Tables	9
1. Introduction	10
1.1 The Pannexin protein family	10
1.1.1 Pannexins and gap junction proteins	11
1.1.2 Pannexins in the formation of channels or gap junctions	13
1.1.3 The structure of the channel pore	14
1.2 Functions and properties of Panx1	15
1.2.1 Regulation of pannexin channels	15
1.2.2 Panx1 in Ca ²⁺ signaling	16
1.2.3 Panx1 in perception	17
1.2.4 Panx1 in the immune system	18
1.2.5 ATP-induced ATP release	18
1.2.6 Panx1 and apoptosis	20
1.2.7 Panx1 in tumor suppression	21
1.2.8 Panx1 in ischemia	22
1.3 Functions and properties of Panx2	22
1.3.1 The size of Panx2	22
1.3.2 The influence of Panx2 on Panx1 trafficking	23
1.3.3 Panx1 and Panx2 in the possible formation of heteromeric channels	23
1.3.4 Panx2 in tumor suppression	24
2. Aims	25
3. Material	27
3.1 Organisms	27
3.1.1 Bacteria	27
3.1.2 Eukaryotic cell lines	27
3.1.3 Animals	27
3.2 Media, buffer and solutions	28
3.2.1 Solutions for cell culture	28
3.2.2 Solutions for protein biochemistry	29
3.2.3 Solutions for electrophysiology	29
3.2.4 Compounds for electrophysiology and kinetics	29

3.2.5 Solutions for Freeze fracture replica immunogold labeling (FRIL)	29
3.3 Reagents, enzymes and antibodies	30
3.3.1 Reagents	30
3.3.2 Reagent systems and kits	31
3.3.3 Enzymes	32
3.4 Nucleic acids	32
3.4.1 Oligonucleotides	32
3.4.2 Plasmids	34
3.4.3 Standards	34
3.5 Technical equipment	35
3.5.1 Equipment for cell culture and molecular biology	35
3.5.2 Equipment for microscopical analysis	35
3.5.3 Equipment for electrophysiology	36
4. Methods	37
4.1 Cytologic Methods	37
4.1.1 Cultivation of N2A cells	37
4.1.2 Transfection of N2A cells	37
4.1.3 Immunocytochemistry	37
4.1.4 Fluorescence activated cell sorting (FACS)	38
4.2 Methods for the preparation and analysis of DNA	38
4.2.1 Polymerase chain reaction (PCR)	38
4.2.1.1 Overlap Extension (OE) PCR	39
4.2.2 Agarose gel electrophoresis of DNA	39
4.2.3 Isolation of DNA from agarose gels	40
4.2.4 Ligation of DNA fragments	40
4.2.5 Transformation of competent bacteria	40
4.2.6 Preparation of plasmid DNA	41
4.2.7 Restriction of DNA	41
4.2.8 Determination of the concentration of nucleic acids	41
4.2.9 Sequencing of plasmid DNA	41
4.3 Methods for the preparation and analysis of RNA	42
4.3.1 RNA isolation from tissue	42
4.3.2 Synthesis of cDNA by reverse transcription	42
4.3.3 in vitro transcription	42
4.3.4 Agarose gelelectrophoresis of RNA	42
4.4 Protein biochemic methods	43
4.4.1 Immunohistochemistry	43
4.4.2 Immunocytochemistry	43
4.4.3 Confocal microscopy	44
4.4.4 Freeze fracture immunogold labeling (FRIL)	44

4.5 Methods for working with <i>Xenopus laevis</i> oocytes	45
4.5.1 Injection of <i>Xenopus</i> oocytes	45
4.5.2 Kinetic studies of <i>Xenopus</i> oocytes	45
4.5.3 Electrophysiology	45
4.5.4 Data analysis	46
5. Results	47
5.1 Simultaneous expression of Panx1 and Panx2 in <i>Xenopus laevis</i> oocytes for the analysis of heteromeric channel formation	47
5.2 Pannexin 2	50
5.2.1 Comparison of Panx2-664 and Panx2-674	50
5.2.2 Localization of Panx2-664 and Panx2-674 in N2A cells by immunocytochemistry	51
5.2.3 Localization of Panx2-664 and Panx2-674 in N2A cells via Freeze-fracture replica immunogold labeling (FRIL)	52
5.2.4 Electrophysiological properties of Panx2-664 and Panx2-674	54
5.2.5 Panx2-674 pharmacology	57
5.3 Chimeras	60
5.3.1 Comparison of Panx1 and Panx2 protein structure	60
5.3.2. Construction of the Panx1-Panx2 chimeras	61
5.3.3 Expression of the chimeras in N2A cells and <i>Xenopus laevis</i> oocytes	62
5.3.4 The role of the C-terminus of Panx1 and Panx2 for channel gating	64
5.4 Truncation of the Panx1 C-terminal domain	66
5.4.1 Design of Panx1 truncated versions	67
5.4.2 Electrophysiological characterization of truncated Panx1-forms in <i>Xenopus laevis</i> oocytes	68
5.4.3 The role of Panx1 truncation for cellular survival in <i>Xenopus laevis</i> oocytes	70
5.4.4 The role of Panx1 truncation for cellular survival in N2A cells	73
6. Discussion	75
6.1 Panx1 and Panx2 do not form functional heteromeric channels	75
6.2 Panx2-674 forms functional, voltage gated channels	77
6.2.1. Electrophysiology of Panx2	80
6.3 Transplantation of domains of Panx1 and Panx2 causes loss of function, whereas prolongation of Panx1 by a domain of Panx2 leads to gain of function	82
6.4 Truncation of Panx1 leads to differential effects on channel properties	84
6.4.1 Electrophysiology of truncated proteins	

not lethal after expression in oocytes	85
6.4.2 Mortality induced by truncation of Panx1	86
6.4.3 Panx1 Cbx sensitivity	88
7. Outlook	89
8. Summary	90
Zusammenfassung	93
9. References	97
Curriculum vitae	105
Acknowledgements	106
Erklärung	108

Abbreviations

A	Ampère
Å	Ångström
A. dest.	distilled water
AMPA	2-amino-3-(5-methyl-3-oxo-1,2-oxazol-4-yl)propanoic acid
ATP	adenosine triphosphate
BSA	bovine serum albumin
C	concentration
Cbx	carbenoxolone
CIAP	calf intestine alkaline phosphatase
CT	carboxy terminus
Cx	connexin
DNA	Deoxyribonucleic acid
<i>E. coli</i>	<i>Escherichia coli</i>
EDTA	Ethylenediaminetetraacetic acid
ER	endoplasmatic reticulum
FACS	fluorescence activated cell sorting
FCS	fetal calf serum
FRIL	freeze-fracture replica immunogold labeling
GC	ganglion cell layer
h	human
HEK 293	human embryonal kidney cell 293
IL-1 β	interleukin-1 β
IV	current/voltage
Inx	innexins
LB	Luria-Bertani broth
m	mouse
NEA	non-essential amino acids
N2A	Neuro2A
NFR	normal frog ringer
NGS	normal goat serum

Abbreviations

ni	not injected
NMDA	N-Methyl-D-aspartate
NO	nitric oxide
OE	Overlap Extension
OGD	oxygen/glucose deprivation
ON	over night
ORF	open reading frame
P2X ₇ R	P2X ₇ receptor
Panx	pannexin
PBS	phosphate buffered saline
PCR	polymerase chain reaction
PEG	polyethyleneglycol
PFA	paraformaldehyde
r	rat
RNA	Ribonucleic acid
RT	Room temperature
S	Siemens
SCAM	substituted cysteine accessibility method
TCEP hydrochloride	tris(2-carboxyethyl)phosphine
TEVC	two-electrode voltage clamp
UTP	Uridine triphosphate
V	Volt
zf	zebrafish

List of Figures

- Figure 1.1: Structural comparison of connexins, innexins and pannexins
- Figure 1.2: Structural organization of gap junction plaques
- Figure 1.3: Possible involvement of Panx1 in Ca²⁺ waves
- Figure 1.4: Gating of connexin and pannexin channels by ATP
- Figure 1.5: Panx1 in apoptosis
- Figure 4.1: Model for the generation of chimeric genes
- Figure 5.1: Representative IV-curves of Panx1 and Panx2 expressed alone or simultaneously in the *Xenopus laevis* oocyte system
- Figure 5.2: Electrophysiological characterization of Panx1 and Panx2 expressed alone or simultaneously in the *Xenopus laevis* oocyte system
- Figure 5.3: Comparison of Panx2-664 and Panx2-674
- Figure 5.4: Expression analyses of Panx2-664 and Panx2-674 in N2A cells
- Figure 5.5: Analysis of membrane localization of rPanx2 forms by FRIL
- Figure 5.6: Analysis of the cell surface localization of rPanx2 forms by FRIL
- Figure 5.7: Comparison of the IV-relationship in *Xenopus laevis* oocytes expressing Panx2-664 and Panx2-674
- Figure 5.8: Comparison of the electrophysiological properties of Panx2-664 and Panx2-674 in *Xenopus laevis* oocytes
- Figure 5.9: Effect of different compounds on Panx2-674
- Figure 5.10: Effect of different compounds on resting potential
- Figure 5.11: Effect of different compounds on Panx2-674 mediated currents
- Figure 5.12: Effect of ATP on resting potential
- Figure 5.13: Comparison of the Panx1 and Panx2 protein length
- Figure 5.14: Design of the Panx1/Panx2 chimeras
- Figure 5.15: Expression analyses of Panx1/Panx2 chimeras in N2A cells
- Figure 5.16: Expression analyses of Panx1/Panx2 chimeras in *Xenopus laevis* oocytes
- Figure 5.17: Representative IV-curves of Panx1/Panx2 chimeras 2 expressed in *Xenopus laevis* oocytes
- Figure 5.18: Electrophysiological characterization of chimeras of Panx1 and Panx2 expressed in *Xenopus laevis* oocytes
- Figure 5.19: Position of the amino acids chosen for the truncation of Panx1

- Figure 5.20: Comparison of the electrophysiological properties of truncated versions of Panx1 in *Xenopus laevis* oocytes
- Figure 5.21: Morphological appearance of *Xenopus* oocytes through expression of of Panx1-truncated versions
- Figure 5.22: Induction of cell death by expression of truncated versions of Panx1
- Figure 5.23: Induction of cell death in *Xenopus* oocytes by expression of Panx1-truncated versions
- Figure 5.24: Induction of cell death in N2A cells by expression of Panx1-truncated versions

List of Tables

- Table 3.1: List of antibodies
- Table 3.2: List of plasmids and respective oligonucleotides
- Table 3.3: List of backbone vectors used for the generation of recombinant plasmids
- Table 4.1: Cycling protocol for PCR with the Phusion-Taq Polymerase
- Table 5.1: Effect of different compounds on resting potential
- Table 5.2: List of constructs leading to breakdown of cellular homeostasis

1. Introduction

1.1 The Pannexin protein family

In the year 2000, Panchin and co-workers described a new family of proteins. This family of proteins displays considerable structural homology to the well characterized connexins as well as sequence homology to the innexins. Given the fact that these new proteins are expressed in vertebrates as well as in invertebrates, they were termed pannexins (Panxs). This name originates from the greek word 'pan' to point out the widespread expression of these proteins (Panchin et al. 2000).

The pannexin protein family consists of three members, namely Panx1, Panx2 and Panx3. All three proteins are integral membrane glycoproteins and were suggested to form hemichannels (Panchin et al. 2000; Dahl & Locovei 2006). In rat, Panx1 contains 426 amino acids and has a molecular weight of ~48 kDa. Panx2 consists of 674 amino acids and is ~70 kDa in molecular weight and Panx3 has 392 amino acids resulting in ~44.7 kDa (Ambrosi et al. 2010a). Studies on tissue distribution reveal large differences in the expression profiles for these three proteins. Panx1 is ubiquitously expressed in different cell types and organs, while Panx2 is found mainly in the central nervous system. Expression of Panx3 is restricted to the skin and cartilage tissue. (Baranova et al. 2004; Dvorianchikova et al. 2006a,b; Huang et al. 2007; Iwamoto et al. 2010; Ray et al. 2005; Vogt et al. 2005; Zappalà et al. 2007). During the past decade different experimental approaches have been dedicated to highlight the function of the pannexin proteins.

1.1.1 Pannexins and gap junction proteins

Given the homology to connexins, pannexins were considered to be capable of forming gap junctions or hemichannels and could therefore contribute to the electrical synapses in the central nervous system. In vertebrates, the electrical coupling is provided by connexins exclusively, while in invertebrates the electrical synapse is constituted by the innexins (Phelan & Starich 2001; Hua et al. 2003).

The topology of pannexins is similar to that of the larger family of connexin proteins, which consists of 20 different members in human (Bruzzone et al. 2003). Both families share common structural features in exhibiting intracellular amino and carboxyl termini, four transmembrane domains, and, consequently, two extra- and one intracellular loop (Baranova et al. 2004; Shestopalov & Panchin 2008).

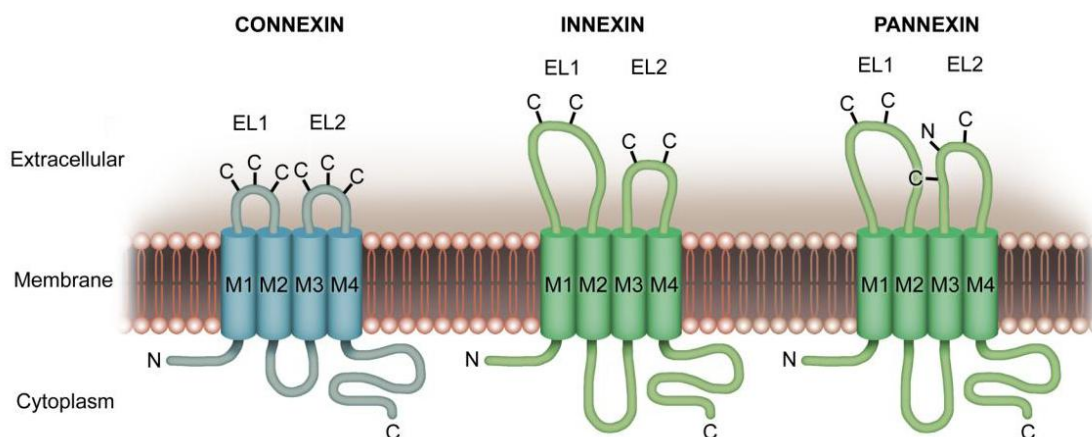


Figure 1.1: Structural comparison of connexins, innexins and pannexins. Gap junctions and corresponding hemichannels are formed by six proteins comprising a hexameric channel. The three protein types depicted exhibit intracellular amino and carboxyl termini (N and C, cytoplasmic), four transmembrane domains (M1-4), two extracellular loops (EL1, EL2) and one intracellular loop. Note the different number of cysteins (C) and glycosylation sites (N) conserved in the extracellular loops of pannexins. (Artwork provided by H.Schulze)

Gap junctions are formed by two channels apposed in the plasma membranes of two adjacent cells. In general, six monomeric proteins form a so called hemichannel, alternatively pannexon, connexon or innexon, respectively. These hemichannels are localized in defined regions in the plasma membrane, where they appear as clusters and form a so-called gap junction plaque, which is shown in figure 1.1 (Harris 2007; Scemes et al. 2009). A specific characteristic of gap junctions is, that they are prone to form heteromeric as well as heterotypic complexes (Elfgang et al. 1995; Werner et al. 1989).

For instance, a hexameric connexon can either be homo- or heteromeric, depending on the types of connexin assembled to form a connexon (Fig. 1.2, examples 1 and 2). Further, two heteromeric hemichannels or two different homomeric hemichannels can form a heterotypic junction (Fig. 1.2, examples 2 and 3).

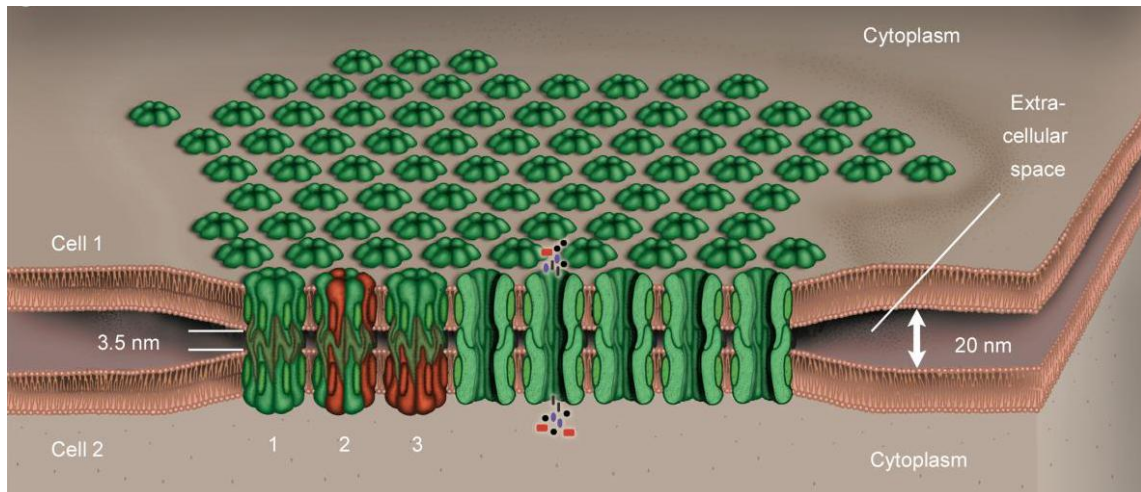


Figure 1.2: Structural organization of gap junction plaques. A typical gap junction plaque is depicted. Six connexin monomers assemble to a hexameric hemichannel, the connexon. Two apposing hemichannels in adjacent cells can form a gap junction channel that allows molecular exchange. The gap junction channel is either homotypic when formed by connexons of the same composition (1), or heterotypic when composed of heteromeric connexons (2) or two different homomeric connexons (3). (Artwork provided by H.Schulze.)

Prerequisite for this phenomenon is the expression of several connexins in one cell depending on the cell type (Dermietzel & Spray 1993). The gating properties of heteromeric and homomeric channels differ with regard to voltage dependence, rectification, conductivity and gating kinetics (Bennett & Zukin 2004; Cao et al. 1998; Harris 2001).

Regarding trafficking processes, connexins and pannexins can be retained in intracellular membrane pools, but are both predominantly trafficked to the plasma membrane (Penuela et al. 2007). While connexins form gap junction plaques, pannexins do not accumulate in clusters in the cell membrane.

Electron microscopy of canine kidney cells overexpressing Panx1 revealed a localization in the plasma membrane, but the expression of Panx1 appeared rather punctuate and did not reveal the plaque-like assembly that is typical for connexins (Boassa et al. 2007; Penuela et al. 2007).

This finding supports the hypothesis of pannexins being non-junctional channel proteins. While connexins are mediators of cell-cell communication via molecular transposition, pannexins are suggested to be involved in the molecular exchange of the intracellular and extracellular space (Harris 2007; MacVicar & Thompson 2010; Scemes et al 2009). Both protein families share a common trafficking pathway from the assembly inside the endoplasmic reticulum to the Golgi apparatus, but for pannexins the final target localization site in the plasma membrane is independent of the existence of cell-cell contacts (Bhalla-Gehi et al. 2010).

1.1.2 Pannexins in the formation of channels or gap junctions

The existence of gap junctions formed by pannexins is discussed controversially. In the following, a survey about the current state regarding the discussion of this topic is given. In 2003, Panx1 was reported to form gap junctions in the *Xenopus laevis* oocyte expression system. Oocytes overexpressing Panx1, Panx2 or both proteins in combination were used for recordings from paired oocytes and currents indicating gap junction formation could be measured (Bruzzone et al. 2003). These studies were followed by further experiments focusing on the influence of Panx1 on C6 glioma cells, where stable expression of Panx1 exhibited increased intercellular coupling (Lai et al. 2007). The same observation was made for glioma cells expressing Panx2 (Lai et al. 2009). Furthermore, Panx1 is considered to have the ability to form gap junctions mediating intercellular Ca^{2+} exchange (Vanden Abeele et al. 2006).

Although the above observations point out a functional role for Panx1 in the formation of gap junctions, there is far more evidence supporting the hypothesis that pannexins do not form intercellular channels. A feasible explanation for the above described finding of Panx1 to form gap junctions is that all data were obtained in pannexin overexpressing heterologous systems, where inherent capabilities become uncovered.

Up to now, no stringent evidence has been presented to confirm a role for pannexins as constituents of gap junction channels *in vivo*. Furthermore, Panx1 is expressed in cells that lack cell-cell contacts such as erythrocytes, a cell type where gap junction formation is negligible (Dubyak 2009). Therefore a non-junctional function of Pannexins is more likely than a junctional one. It now is common opinion, that pannexins, especially Panx1, form single membrane channels (Barbeet al. 2006; Boassa

et al. 2007; Dahl & Locovei 2006; Iglesias et al. 2008; Pelegrin & Surprenant 2006; Penuela et al. 2007; Zoidl et al. 2007). Because pannexons seem to exhibit single channel activity, the use of the term hemichannel must be regarded misleading; therefore, the term “pannexin channel” will be used in the present thesis instead of “pannexin hemichannel”.

1.1.3 The structure of the channel pore

To date, the topology of Panx1 is not fully understood. Further, only very few studies focused on the channel structure of Panx2, while almost nothing is known about the morphological characteristics of Panx3.

Ambrosi and colleagues were able to determine the size of Panx1 and Panx2 channels by electron microscopy. The study indicates that Panx2, with an oligomer diameter of ~183 and 190 Å (values calculated from two channels), forms larger channels than Panx1, that has an oligomer diameter of ~120 and 160 Å. The actual pore diameter was calculated as ~21 and 17 Å for Panx1 and ~29.5 and 30.5 Å for Panx2, respectively (Ambrosi et al. 2010a). Furthermore, the same authors suggested that Panx2 possibly forms an octameric channel instead of a hexameric channel like Panx1 (Ambrosi et al. 2010a; Boassa et al. 2007).

Recently, attempts were made to outline the topology of Panx1. Putatively pore lining amino acid residues were identified by the substituted cysteine accessibility method (SCAM). The study revealed that portions of the external part of the first transmembrane domain and the first extracellular loop line the outer part of the pore of Panx1 channels, which is a common feature in connexin hemichannels. (Wang & Dahl 2010). For connexons, a role of the first transmembrane domain and the first extracellular loop in lining the outer part of the pore could be demonstrated by domain swapping between different connexins, a phenomenon similar to Panx1 (Hu & Dahl 1999; Hu et al. 2006; Ma & Dahl 2006). Despite these similarities, in Panx1 channels the inner part of the pore is lined, at least partly, by the C-terminus of the protein.

1.2 Functions and properties of Panx1

In the family of pannexins, Panx1 has been analyzed most extensively. In the following passage, a survey about the functions of Panx1 shall be presented.

1.2.1 Regulation of pannexin channels

The functional regulation of Panx1 channels is mediated by a variety of different stimuli. Thus, Panx1 channels are activated upon depolarization to membrane potentials ≥ -20 mV (Bruzzone et al. 2003) in response to an increase in the intracellular Ca^{2+} concentration (Locovei et al. 2006a; Kienitz et al. 2010). Also, mechanical stress (Bao et al. 2004), elevation of the extracellular ATP concentration via the activation of purinergic receptors (Locovei et al. 2006b) and elevated extracellular concentrations of potassium ions (Silverman et al. 2009) activates Panx1 channels. Furthermore, Panx1 is reactive to exposure to reducing agents like tris(2-carboxyethyl) phosphine (TCEP) and the interaction with the potassium channel subunit $\text{Kv}\beta 3$ regulates the sensitivity of Panx1 channels to changes in the redox potential (Bunse et al. 2009).

To date, only one publication reports Panx2 to be a voltage-dependent functional channel. Ambrosi et al. (2010a) postulate that Panx2 forms a channel which can be activated by application of a voltage ramp shifting the membrane potential from -100 mV to +100 mV over a duration of 70s in *Xenopus* oocytes expressing Panx2. Furthermore, when Panx2 proteins were purified and incorporated into vesicles, channel opening could be monitored by intraliposomal reduction of cytochrome c by ascorbate after passing the bilayer through Panx2 pannexons (Ambrosi et al. 2010a). This reaction was sensitive to Carbenoxolone (Cbx), a commonly used unspecific gap junction blocker. Surprisingly, Cbx did not reduce Panx2 mediated currents in electrophysiological recordings.

While the authors did not find specific inhibitors of Panx2 in two electrode voltage clamp (TEVC) measurements, Panx1 mediated currents can be blocked by several agents. The Panx1 channel is inhibited by Cbx (Pelegriin & Surprenant 2006), mimetic peptides (Pelegriin & Surprenant 2006; Thompson et al. 2008), the gout remedy probenecid (Silverman et al. 2008), polyethylene glycol (PEG) with a molecular weight

up to 1500 kDa (Wang et al. 2007) and the antimalarial quinine derivative mefloquine (Iglesias et al. 2009).

Of all the agents mentioned, only probenidicid is considered to be specific for Panx1. All other reagents are cross-reactive with connexin proteins and even the use of mimetic peptides does not prevent cross-inhibition of both pannexin and connexin channels (Wang et al. 2007).

1.2.2 Panx1 in Ca^{2+} signaling

It also has been reported, that Panx1 is a mediator of the initiation and propagation of regenerative calcium waves (Locovei et al. 2006b). The propagation of Ca^{2+} waves depends on two signaling pathways. Once a Ca^{2+} wave is initiated, calcium-mobilizing second messenger molecules are following an intercellular route and pass through gap junctions formed by connexins or innexins (Scemes et al. 2007). In addition, proteins expressed on the cell surface can mediate an extracellular pathway by messenger molecules to propagate Ca^{2+} waves. After an initiating stimulus, i.e. by mechanical stress as depicted in figure 1.3, Panx1 channels open and ATP is released into the extracellular space.

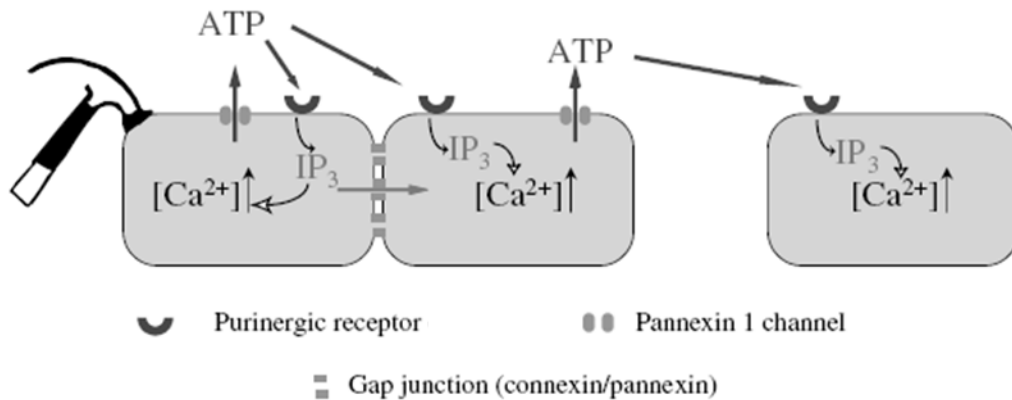


Figure 1.3: Possible involvement of Panx1 in Ca^{2+} waves. Upon stimuli like mechanical stress (indicated by the hammer symbol), the cell releases ATP through Panx1 channels that binds to purinergic receptors. A signal cascade leads to IP₃ synthesis, which causes Ca^{2+} release from intracellular compartments. IP₃ also passes gap junctions into adjacent cells. Here, the elevation of intracellular Ca^{2+} concentration leads to further opening of Panx1 channels, the signaling cascade is relayed. (Modified from Locovei et al., 2006b)

There, ATP binds to purinergic receptors either in an auto- crine or in a paracrine manner (Enkvist & McCarthy 1992; Hassinger et al. 1996). Recently, the ionotropic

P2X₇ receptor (P2X₇R) has been identified to be the main mediator of ATP release, a purinergic receptor forming a large pore complex together with Panx1 (Suadicani et al. 2006; Scemes et al. 2009). Among others, the P2Y₆ receptor is an additional receptor of this class and therefore also involved in this signaling cascade. (Nishida et al. 2008).

The binding of ATP to P2X₇R leads to a fast influx of extracellular Na⁺ and Ca²⁺ and efflux of cytosolic K⁺ ions. This results in an enhanced membrane permeability by opening of Panx1 and concurrent passage of molecules of ≤ 900 Da molecular weight (Dubyak 2009). This change in permeability evoked by P2X₇R plays an important role during the activation of leukocytes and therefore is involved in the regulation of the innate and the adaptive immune system (Ferrari et al. 2006).

1.2.3 Panx1 in perception

During the last years, pannexins have been considered to play a role in perception given their expression in peripheral sensory organs. Panx1 expression has been confirmed in the retina of mouse and zebrafish (Zoidl et al. 2008) by RT-PCR and in situ-hybridization. Further, Panx1 expression is validated for taste cells in the mouse (Huang et al. 2007). Up to now, intercellular communication necessary for the processing of taste signals prior to their transmission to the CNS was thought to be mediated by connexins. More recent studies now identified Panx1 to serve a trigger function for the initiation of Ca²⁺-waves and the ATP-mediated pathway described earlier. Studies on mouse taste buds demonstrated that Panx1 channels are necessary for the release of ATP from type II receptor cells. These cells transmit gustatory signals via G-protein coupled receptors for sweet, bitter and umami taste sensations. Previous studies showed that ATP release from type II receptor cells is not mediated by vesicular transmitter transport (Clapp et al. 2004; DeFazio et al. 2006), or at least to a small extent only, considering the presence of vesicular neurotransmitter transporters (Iwatsuki et al. 2009). Taken together, Panx1 has been identified as an important factor of ATP release and mediator of Ca²⁺ wave propagation in taste cells (Huang et al. 2007; Dando & Roper 2009).

In contrast, in the visual system Panx1 could not be linked to a specific function. Panx1 expression varies strongly during development. While in the adult murine visual system Panx1 is found mainly in retinal ganglion cells, in juveniles the expression is confirmed

for ganglion cells, amacrine cells and horizontal cells and in lens epithelial cells (Dvorianchikova et al. 2006; Ray et al. 2005). These results indicate that Panx1 has an important role in the development of the visual system and, beyond that, for vision in the adult.

1.2.4 Panx1 in the immune system

Panx1 has several roles in the regulation of the immune system, which will be summarized in the following.

First, Panx1 has been shown to activate leukocytes, which in turn leads to an activation of specific target cells. Depending on the type of leucocyte activated, different responses can be induced: i.e. host defense against infections, allergic responses by histamine release, activation of lymphocytes, monocyte migration or phagocytosis. Furthermore, the release of ATP from the leukocyte results in an autocrine regulation of the P2X₇ signaling pathway, as well as in paracrine activation of other immunologically active cells (Bianco et al. 2005).

Second, the interaction of Panx1 with P2X₇R leads to the release of interleukin-1 β (IL-1 β) from immunologically active cells like macrophages and T-lymphocytes (Pelegrin & Surprenant 2006; Schenk et al. 2008). IL-1 β is regarded as an initiator of acute inflammatory responses (Dinarello 2005). At sites of inflammation or injury, high concentrations of ATP lead to an activation of P2X₇R, which does not only result in an opening of P2X₇ itself, but also in a gradual opening of Panx1 channels over seconds to minutes. In this context, Panx1 acts as an upstream protein in the pathway of activation of the inflammasome. (Martinon & Tschopp 2004). Taken together, Panx1 can be considered as a regulator of IL-1 β release from macrophages after ATP-induced P2X₇R-activation (Pelegrin & Surprenant 2006; Locovei et al. 2007; Iglesias et al. 2008).

1.2.5 ATP-induced ATP release

ATP-induced ATP release is an exclusive function of Panx1. By this mechanism, cells are able to respond to different types of environmental stimuli like metabolic inhibition during ischemia, mechanical stress, and infection with microbes in response to bacterial lipopolysaccharides via leukocyte activation. The reaction to these stimuli can take

place very locally and can be restricted to the area of injury or inflammation (Scemes et al. 2007). Because Panx1 channels are large conduits for ATP, a mechanism is suggested to regulate ATP efflux through Panx1 channels in order to sustain ATP homeostasis.

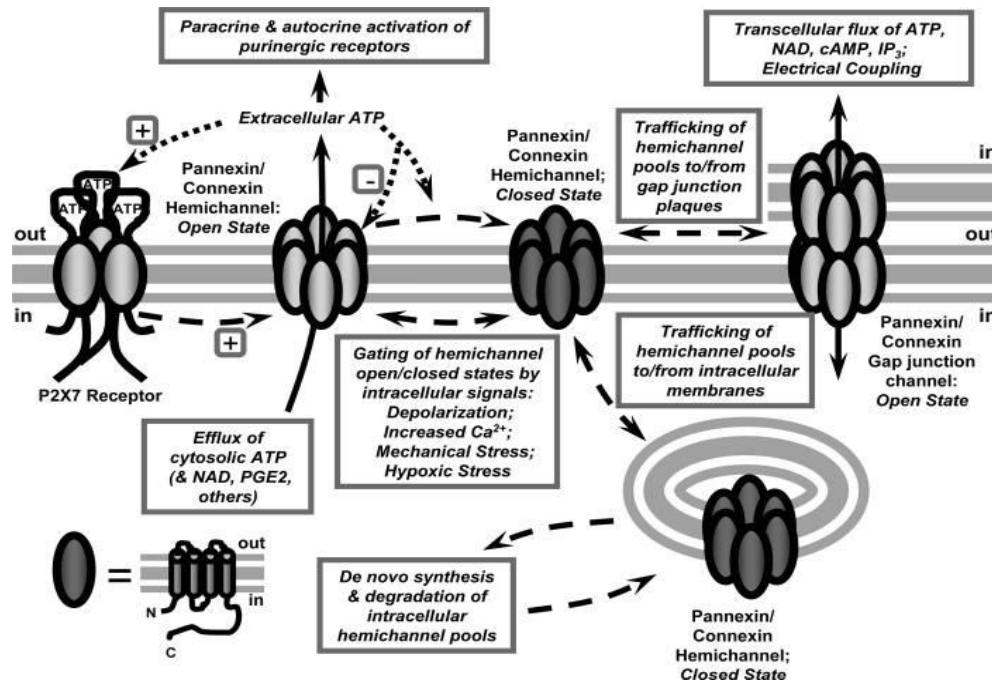


Figure 1.4: Gating of connexin and pannexin channels by ATP. Panx1 channels, like connexin hemichannels, are permeable for ATP and other molecules. The gating of the channels induced by ATP binding to purinergic receptors is shown. The mechanism of ATP-induced ATP-gating is marked (+), while the negative allosteric function of ATP on Panx1 channels is marked (-). (Picture taken from Dubyak 2009).

Recently, Thompson and colleagues postulated that intracellular ATP would be necessary for a suppression of Panx1 channel opening. The depletion of the intracellular ATP reservoir is supposed to abrogate the suppressive effect and to therefore mediate uncontrolled Panx1 opening (Thompson et al. 2006). Consistent with these findings it was postulated, that intracellular ATP could pass Panx1 channels and accumulate at the outer part of the pannexon, where it, once extracellular, inhibits Panx1 opening (Dubyak 2009).

In contrast, other groups did not observe any influence of the presence of intracellular ATP on channel gating when analyzing the electrophysiology of Panx1 channels (Ma et al. 2009). Nevertheless, the release of ATP due to the interaction of P2X₇R and Panx1 would lead to a complete loss of the intracellular ATP stores and consecutively to cell death if the mechanism was not inhibited. Recent studies revealed an inhibitory effect of

ATP on the activity of Panx1 channels, where ATP is described as an allosteric modulator of Panx1. Studies performed on Panx1 expressing *Xenopus* oocytes explored ATP as a regulator of its own permeation pore (Qiu & Dahl 2009; Dubyak 2009). The interaction of positive and negative regulation pathways of ATP on Panx1 channels is summarized in figure 1.4. Further experiments were performed using mammalian expression systems. Results from HEK293 cells expressing Panx1 confirmed the inhibitory effects of ATP, but further unraveled that UTP and GTP also suppress Panx1 channel activity (Ma et al. 2009).

1.2.6 Panx1 and apoptosis

New findings reveal an important role for Panx1 in apoptosis. Apoptosis is one form of programmed cell death, where so-called effector caspases play a crucial role. Recently, experimental evidence indicated that during apoptosis cells release the nucleotides ATP and UTP (Fig. 1.5). This release was observed at a time when the cells were still intact and did not release other substances.

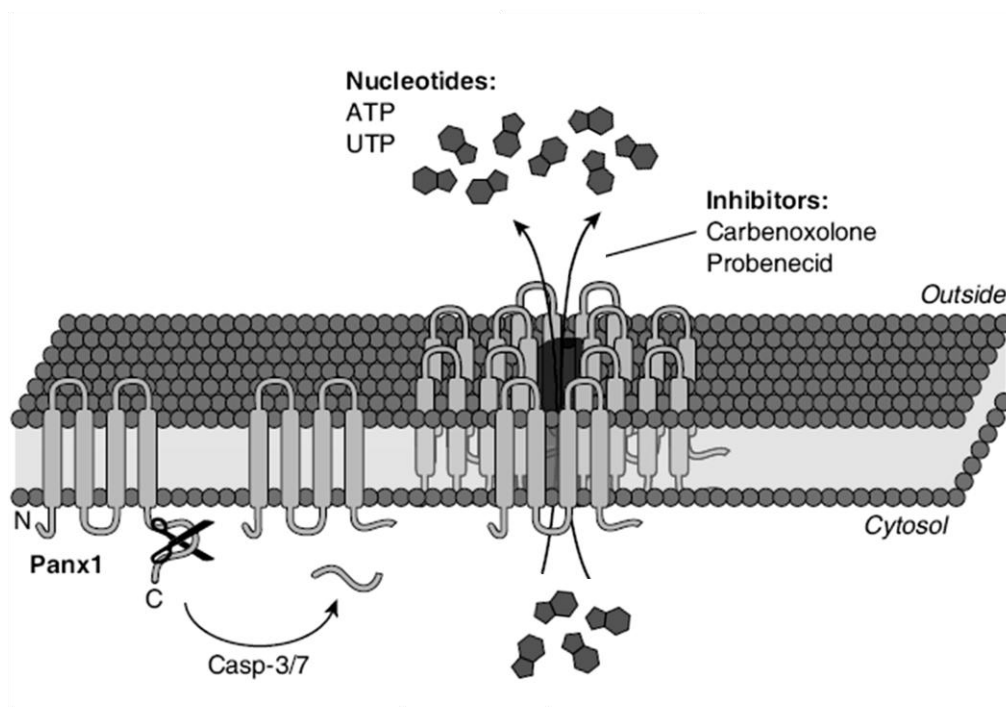


Figure 1.5: Panx1 in apoptosis. Cleavage of Panx1 by Caspases 3/7 lead to irreversible channel opening and therefore to the release of the nucleotides ATP and UTP (Picture modified from Peter et al. 2010).

It was postulated that the nucleotide release must have been mediated through a channel in the plasma membrane (Elliott et al. 2009). Only one year later, the same group was

able to unravel Panx1 channels being responsible for the release of ATP and UTP. Using proteom analysis tools, the authors identified two putative caspase cleavage sites in the Panx1 amino acid sequence.

By mutagenesis studies a cleavage site in the protein's C-terminal domain was identified as a target for the caspases 3 and 7, two caspases known to be upregulated during apoptosis. The crucial cleavage site is located at aa 376 – aa 379 in the Panx1 sequence.

It turned out that the typical tetrapeptide sequence DXXD has been highly conserved in Panx1 during evolution, giving a hint for the importance of this mechanism.

Panx1 cleavage by caspase 3/7 leads to a constitutively open channel. The channel cannot close anymore, the reaction is irreversible. The cell consequently releases ATP and UTP through Panx1 channels, which both act as so-called “find-me” signals and lead to phagocyte recruitment. Thus, monocytes, macrophages and dendritic cells migrate to the site of impairment. The apoptotic cell can then be degraded and engulfed, a process also known as phagocytic clearance (Chekeni et al. 2010a).

With these findings a main question in the understanding of apoptosis was answered. It was well known before that apoptotic cells are able to influence their extracellular environment by the release of nucleotides, but the underlying pathway was unknown.

Still, the mechanism of Panx1 channel gating remains unknown. The fact that cleavage of the C-terminus at position aa378 by caspase3/7 results in an irreversibly open channel leads to the question about the impact of the C-terminal sequence on channel gating.

1.2.7 Panx1 in tumor suppression

Panx1 has been shown to be tumor-suppressive. In recent studies, a down-regulation of all three pannexin proteins in rat C6 glioma cells has been shown. RT-PCR analysis of primary astrocytes, the non-cancerogenic counterpart to C6 glioma cells has shown that these cells are positive for pannexin genes. Therefore, the influence of Panx1 and Panx2 expression was investigated recently. The group of C. Naus was able to show an effect of pannexin expression on tumor progression. In a first study, a stable overexpression of Panx1 in C6 gliomas was induced and further assays on tumor growth induced by these cells were done. Also, the effect of Panx1 on tumorigenicity was investigated *in vitro*.

Taken together, the authors revealed that Panx1 expression in C6 glioma cells reduced cell proliferation, altered cell morphology and reduced motility. *In vivo* tumor growth was decreased significantly. Therefore it was postulated that Panx1 downregulation can be linked to tumor development, while an artificial expression of Panx1 has a tumor-suppressive role (Lai et al. 2007).

1.2.8 Panx1 in ischemia

Incidences like heart attack or stroke can lead to cerebral ischemia due to disturbances in blood supply of the brain. This may lead to severe neuronal damage and tissue loss, mainly caused by excitotoxicity. As a consequence, enhanced glutamate release leads to an overactivation of NMDA and AMPA receptors and a large Na⁺ and Ca²⁺ influx into the cells within the affected area causes membrane depolarization. Finally, a breakdown of the cells ionic homeostasis may result in cell death.

Under ischemic conditions, the expression of Panx1 is upregulated and the channel is activated under oxygen/glucose deprivation (OGD) (Thompson et al. 2006). The opening of Panx1 channels leads to severe neuronal degeneration by providing a large death pore. In this context the participation of Panx1 in redox regulation is of special importance, because the redox potential changes under ischemic conditions (Bunse et al. 2009; Zhang et al. 2008). The occurrence of neuronal cell death caused by ischemic conditions has been linked to elevated levels of reactive oxygen species like nitric oxide (NO). Panx1 acts as a sensor for redox potential changes induced by OGD that occurs during ischemia.

Therefore, Panx1 is an important factor in pathophysiological processes like stroke.

1.3 Functions and properties of Panx2

1.3.1 The size of Panx2

Until 2007, Panx2 was described as a protein consisting of 664 amino acids. In that year, the protein sequence published on the website of the National Center for Biotechnology Information (NCBI) was updated. The new Panx2 sequence contained ten additional amino acids at the N- terminus. So far, there is a huge inconsistency in literature regarding the use of the long version comprising 674 aa or the short version

consisting of 664 residues. Until now, it is not clear whether the long version or the shorter one is naturally expressed *in vivo*. In the following parts of this thesis Panx2 will be referred to as either Panx2-664 or Panx2-674, whenever it is necessary to distinguish between both forms.

1.3.2 The influence of Panx2 on Panx1 trafficking

Pannexins are glycoproteins and the glycosylation sites are found on their extracellular loops (Boassa et al. 2008). Panx2 was shown to influence the trafficking of Panx1 depending on its glycosylation status. Studies addressing the reciprocal influence of both proteins revealed that interactions are not or not only confined to the fully glycosylated forms of Panx1 and Panx2, but also occur between certain intermediate states.

Panx1 shows three glycosylation states, and only two of them, namely the core and high-mannose forms of Panx1 interact with the Panx2 protein, which leads to an increased membrane localization of Panx2 (Penuela et al. 2009). Panx2 itself is glycosylated to a high-mannose form and seems to be localized in intracellular compartments when expressed in HEK293 cells, but co-expression with Panx1 increases the plasma membrane localization of Panx2 by two-fold (Penuela et al. 2009). Thus, by use of immunolabeling and co-immunoprecipitation methods the evidence was provided that Panx1 and Panx2 influence each other's trafficking process.

1.3.3 Panx1 and Panx2 in the possible formation of heteromeric channels

In 2003, the possible formation of heteromeric channels consisting of both Panx1 and Panx2 was investigated (Bruzzone et al. 2003). cRNAs encoding the two proteins were injected into *Xenopus* oocytes and differences in electrophysiological properties were examined. The authors were able to induce the formation of Panx1 channel expression, but no signs for functional Panx2 channels were obtained. In TEVC measurements, recordings from oocytes coinjected with both cRNAs showed current responses that differed from oocytes expressing Panx1 only. Further, investigations on paired oocytes lead to the conclusion that that a connection of both cells similar to gap junction coupling was possible (Bruzzone et al. 2005). Based on this observation, the authors

postulated that Panx1 and Panx2 are able to form heteromeric channels because an attenuation of the current response was observed.

1.3.4 Panx2 in tumor suppression

Since Panx1 was shown to have tumor suppressive effects, Lai and colleagues performed similar experiments on Panx2. Overexpression of Panx2 in C6 glioma cells resulted in data comparable to the results obtained from Panx1 overexpression. *In vitro* assays revealed a decrease in cell proliferation and growth, tumor growth was reduced *in vivo* (Lai et al. 2007). Further evidence on tumor suppressive effects was given by cDNA microarray analysis of human brain tumor tissue that revealed reduced gene expression of Panx2 in glial tumors. Furthermore, an upregulation of Panx2 could be linked to post-diagnosis survival in patients suffering from gliomas (Litvin 2006). Interestingly, in both publications the authors reported about increased cell-cell contacts and dye coupling induced by Panx1 as well as by Panx2 expression. Also, an intracellular localization of Panx2 was reported.

Taken together, Panx1 and Panx2 seem to have beneficial effects on the reduction of tumor growth and progression. Both proteins are supposed to have tumor-suppressive functions.

2. Aims

The proteins Panx1 and Panx2 have been identified to play several roles in the organism. Since most functional studies performed so far focused on Panx1, more different functions have been attributed to this protein than to Panx2. Panx2 is shown to be tumor suppressive when exogenously expressed in gliomas (Lai et al. 2009). However, apart from that, Panx2 has been mainly described in correlation with Panx1. Both proteins interact in trafficking processes. Furthermore, preceding this thesis, the possible formation of heteromeric channels consisting of Panx1 and Panx2 was under debate. While different interactions of both proteins such as heteromeric channel formation or the reciprocal influence on trafficking were described (Bruzzone et al. 2003; Penuela et al. 2009), the interactions of Panx1 and Panx2 domains and subunits on the level of quarternary structure have not been addressed. It was a main goal of this thesis to focus on the reciprocal influence of Panx1 and Panx2. The existence of heteromeric channels should be studied and, if verified, the contribution of these channels to cellular conductance should be ruled out.

Panx2 has been described to exert a potential inhibitory effect on Panx1 channel gating. Coexpression of both proteins in *Xenopus* oocytes should highlight the possible formation of heteromeric channels, and coexpression of both proteins in different ratios should reveal a putative reciprocal inhibition or enhancement of cellular conductivity.

A second goal was to investigate the function of certain domains of both Panx1 and Panx2. Therefore, transplantation of domains, the exchange of parts or the prolongation or truncation of domains, were performed. Thus, the special focus of this part of the thesis was on the impact of the huge difference in the size of the C-terminal domains of Panx1 and Panx2 and the study of possible interactions between certain domains was facilitated.

As a third aim, the formation of functional Panx2 channels was examined. Panx2 had been postulated not to be capable of forming voltage or ligand gated channels. Apart from that, during the experimental work of this thesis two sequences occurred in literature, leading to proteins differing in the length of the N-termini. While a final conclusion about which of these proteins represents the native form of Panx2 was not possible, neither based on the nucleotide nor on amino acid sequence, a functional differentiation was achieved. Furthermore, localization studies should highlight a

putative involvement of the N-termini in trafficking, considering the localization of signal sequences in this domain of integral membrane proteins in general. Finally, the influence of the length of the C-terminal domain of Panx1 came into focus. At the same time as experiments for this thesis were performed, the importance of this domain for Panx1 channel function was addressed by others. Furthermore, recent publications strongly suggested an involvement of Panx1 in apoptosis by caspase hydrolysis. The influence of the size of the Panx1 C-terminal domain induced by this cleavage was analyzed in the present thesis. Several truncations of the protein allowed to analyze the function of domains and even just few residues on Panx1 channel formation, voltage dependent gating, development and extent of mortality, and Cbx sensitivity.

In summary, this thesis was aimed to a better understanding of the function of Panx1 and Panx2 channels, with special regard to the importance of certain protein domains.

3. Material

3.1 Organisms

3.1.1 Bacteria

Escherichia coli (*E. coli*) K-12: DH5 α (Invitrogen):

F- Φ 80dZ Δ M15 Δ (*lacZYA-argF*) U169 *recA1* *hsdR17*(rk-, mk+) *phoA* *supE44* λ - *thi-1* *gyrA96* *relA1*

E. coli: Turbo Competent *E. coli* “High Efficiency” (New England Biolabs)

F' *proA*⁺*B*⁺ *lacI*^f Δ *lacZ* M15/ *fhuA2* Δ (*lac-proAB*) *glnV* *gal* R(*zgb-210::Tn10*)Tet^S *endA1* *thi-1* Δ (*hsdS-mcrB*)5

3.1.2 Eukaryotic cell lines

Neuro2A (N2A) cells are derived from a murine neuroblastoma (*mus musculus*) (Klebe & Ruddle 1969). Cells have been kindly provided by Dr. David Spray (Albert Einstein College, NY, USA).

3.1.3 Animals

The South African clawed frog *Xenopus laevis* was used for production of oocytes for experiments with the Roboocyte® system. Therefore, defolliculated oocytes were purchased from EcoCyte Bioscience.

Rats were used for the production of cryosections or for the generation of cDNA from tissue. The strain Wistar was achieved from Charles River.

3.2 Media, buffer and solutions

3.2.1 Solutions for cell culture

Growth medium	D-MEM (+ 4.5 g/l glucose, + L-glutamin, - pyruvate; Gibco, Invitrogen, Carlsbad, CA, USA) + 1% L-glutamin + 1% non essential amino acids (NEA) + 1% penicillin/streptomycin (10.000U/ml / 10 mg/ml) + Na-pyruvate (1 mM) + 5% fetal calf serum (FCS) for N2A cells
Phosphate buffered saline (PBS)	138 mM NaCl, 2.8 mM KCl, 10 mM Na ₂ HPO ₄ , 1.8 mM KH ₂ PO ₄ , pH 7.4
Trypsin-EDTA	0.05% trypsin, 0.02% EDTA

3.2.2 Solutions for molecular biology

RNA loading buffer	95% formamide 0.025% xylene cyanol, 0.025% bromophenol blue 18 mM EDTA 0.025% SDS
DNA loading buffer	0,5 M EDTA 66% glycerin 0.025% xylene cyanol, 0.025% bromophenol blue
TAE	1.0 mM EDTA, 40 mM Tris-acetate
LB medium	1% tryptone, 0.5% yeast extract, 0.5% NaCl

3. Material

LB agar	LB medium + 1 % agar
SOC medium	2% tryptone, 0.5% yeast extract, 10 mM NaCl, 2.5 mM KCl, 10 mM MgCl ₂ , 20 mM glucose

3.2.2 Solutions for protein biochemistry

Blocking solution for immunocytochemistry and immunohistochemistry of tissues	1% BSA, 3% normal goat serum (NGS) in PBS
---	---

Blocking solution for immunohistochemistry of oocytes	10% NGS, 0.1% Triton X-100 in PBS
---	-----------------------------------

3.2.3 Solutions for electrophysiology

Normal frog ringer (NFR; EcoCyte Bioscience)	90 mM NaCl, 2.0 mM KCl, 2.0 mM CaCl ₂ , 1.0 mM MgCl ₂ , 5.0 mM HEPES, pH 7.4
--	--

3.2.4 Compounds for electrophysiology and kinetics

ATP, Carbenoxolone, CoCl₂, LaCl₃, Mefloquine, Octanol, and PEG 1500 have been diluted in 1x NFR in concentrations ready to use depending on the experimental situation.

3.2.5 Solutions for Freeze fracture replica immunogold labeling (FRIL)

TBS	150 mM NaCl, 50 mM Tris-HCl, pH 7.4
Blocking solution	5% donkey serum in TBS
Detergent solution	2.5% SDS, 30 mM sucrose, 10 mM Tris-HCl pH 8.3

3.3 Reagents, enzymes and antibodies

3.3.1 Reagents

Agarose	FMC BioProducts
Ampicillin	AppliChem
Ammonium chloride	Merck
Blocking buffer Odyssey	Licor Biosciences
Blocking reagent	Roche
Bovine serum albumin (BSA)	PAA
Bromphenol blue	Riedel-de Haën
Calcium chloride	Baker
Carbenoxolone (Cbx)	Sigma
Chloroform	Baker
Donkey serum	Jackson ImmunoResearch Laboratories
Ethanol	Baker
Ethidium bromide	Sigma
Ethylenediaminetetraacetic acid (EDTA)	Merck
Fetal calf serum	BiochromKG
Glucose	Baker
Glycerol	Baker
Glycine	AppliChem
H ₂ O	Gibco
Hoechst 33342	Invitrogen
Kanamycin	AppliChem
LB-medium and LB-agar	AppliChem
L-glutamine	PAA
MEM Non essential Amino Acids	PAA
Methanol	Baker
Nitrogen, liquid	RUB chemical facility
Normal goat serum	PAN Biotech
Paraformaldehyde	Sigma
Penicillin	PAA

Phenol	AppliChem
Polyethylene glycol (PEG)	Fluka
Potassium acetate	Baker
Potassium chloride	Merck
Potassium dihydrogen phosphate	Baker
ProLong Gold Antifade reagent	Molecular Probes, Invitrogen
Propane, liquid	RUB chemical facility
protease inhibitor	Sigma
Streptomycin	PAA, Sigma
Sodium chloride	Baker
Sodium hydrogen phosphate	Baker
Sodium pyruvate	PAA
Tissue freezing medium	Leica Microsystems
Tris(hydroxymethyl)aminomethane (Tris)	AppliChem
Triton X-100	AppliChem
Trizol	Invitrogen
Trypsin-EDTA	PAA
Tween 20	AppliChem

3.3.2 Reagent systems and kits

Effectene transfection kit	Qiagen
Phusion High Fidelity DNA Polymerase Kit	NEB
PrimeScript TM Rev. Transcriptase	TAKARA
Qiaquick Gel Extraction Kit	Qiagen
Plasmid DNA Miniprep	Fermentas
Nucleobond Xtra Midi	Clontech
Nucleobond Xtra Maxi EF	Macherey & Nagel
mMESSAGE mMACHINE SP6 or T7 Kit	Ambion

3.3.3 Antibodies

Table 3.1 List of antibodies.

Name	Species	Origin	Specificity
Primary antibodies			
Panx1 4515	chicken	Aves Labs (Tigard, OR, USA); kindly provided by G. Dahl	mouse Panx1
Panx2 SB	rabbit	RUB, Dept. of Neuroanatomy	rat Panx2
c-myc (clone 9E10)	mouse	Sigma	c-myc- tag
Secondary antibodies			
Alexa Fluor 488 anti mouse	goat	Molecular Probes, Invitogen	against mouse with Alexa Fluor 488-tag
Alexa Fluor 568 anti rabbit	goat	Molecular Probes, Invitogen	against rabbit with Alexa Fluor 568-tag
Alexa Fluor 568 anti chicken	goat	Molecular Probes, Invitogen	against chicken with Alexa Fluor 568-tag
anti rabbit 18 nm gold	donkey	Dianova	against rabbit IgG tagged with 18 nm gold particles

3.3.3 Enzymes

All restriction enzymes used for molecular cloning were purchased from Fermentas and used according to manufacturer's instructions.

3.4 Nucleic acids

3.4.1 Oligonucleotides

Oligonucleotides used for molecular cloning or sequencing are listed in Table 3.2 and were purchased from biomers. All primer sequences are depicted in 5`-3` direction.

Table 3.2 List of plasmids and respective oligonucleotides.

Recombinant plasmid vector	Primer sense	Primer reverse	Primer Overlap Extension sense	Primer Overlap Extension reverse
pCS2+rPanx1	gcattctgagccaccatg gccatgcccacc tggccac	gcattctagattag caggatgaattcag	-	-

3. Material

pCS2+rPanx2-674	gcatctcgagccaccatg caccacctctggag cagtcgg	cgtatctagattaaaactcc acagtactacaactgttct	-	-
pCS2+C1	gcatctcgagccaccatg gccatgcccacc tggccac	tctagaaaactcca cagtactaca	cgcaagagcaactcatttt tgacaagctg	aaaatgaagttgctcttgcg gacgaagagcgtgta gatga
pCS2+C2	gcatctcgagccaccatg gccatgcccacc tggccac	tctagaaaactcca cagtactcac	ctggccattatgcgcgtag aaaacagcaagactgag	tctacgcgcataatggccaga gagcaggatgaattcagaa gtcgc
pCS2+C3	gcatctcgagccaccatg gccatgcccacc tggccac	tctagactgctcctt gaaggctgtg	cgcaagagcaactcatttt tgacaagctgcacaa	aaaatgaagttgctcttgcg gacgaagagcgtgtag atga
pCS2+C4	gcatctcgagccaccatg caccacctctgga gcagtcgg	atgctctagattagcagga tgaattcagaagtcg ctggcg	ccgttccggcagaaga cggacgt	cgtcttctgccggaacggga agatgaagaggtg gatgagg
pSC-myc.his-C1	gcatctcgagccaccatg gccatgcccacc tggccac	gcattctagaccaaac tccacagtactcac	-	-
pSC-myc.his-C2	gcatctcgagccaccatg gccatgcccacc tggccac	gcattctagaccaaactcc acagtactcac	-	-
pSC-myc.his-C3	gcatctcgagccaccatg gccatgcccacc tggccac	gatctctagaccctgctct tgaaggctgtgg	-	-
pSC-myc.his-C4	gcatctcgagccaccatg caccacctctggag cagtcgg	atgctctagaccgcaggat gaattcagaagtc gctggcg	-	-
pCS2+rPanx1-307	gcatctcgagccaccatg gccatgcccacc tggccac	gcattctagattataccttg aggacgtcgtct	-	-
pCS2+ rPanx1-327	gcatctcgagccaccatg gccatgcccacc tggccac	gcattctagattacaagtc gttgtagccttcag	-	-
pCS2+ rPanx1-347	gcatctcgagccaccatg gccatgcccacc tggccac	gcattctagattaaagaca ctgtacgatttga	-	-
pCS2+ rPanx1-367	gcatctcgagccaccatg gccatgcccacc tggccac	gcattctagattaagtcag aagtaacatggggtc	-	-
pCS2+ rPanx1-370	gcatctcgagccaccatg gccatgcccacc tggccac	gcattctagattagcctag gttgtcagaag	-	-
pCS2+ rPanx1-374	gcatctcgagccaccatg gccatgcccacc tggccac	gcattctagattacatetta atcatgcctagg	-	-
pCS2+ rPanx1-377	gcatctcgagccaccatg gccatgcccacc tggccac	tctagattaaatgacgtc catcttaatcatgc	-	-
pCS2+ rPanx1-380	gcatctcgagccaccatg gccatgcccacc tggccac	gcattctagattattttc catcaatgacgtcca	-	-
pCS2+ rPanx1-383	gcatctcgagccaccatg gccatgcccacc tggccac	gcattctagattacatggg gacttttccatcaatga	-	-
pCS2+ rPanx1-387	gcatctcgagccaccatg gccatgcccacc tggccac	gcattctagattaggtetgt aggacatggggac	-	-
pCS2+ rPanx1-389	gcatctcgagccaccatg gccatgcccacc tggccac	gcattctagattatccctt ggtctgtagggaca	-	-
pCS2+ rPanx1-	gcatctcgagccaccatg gccatgcccacc	gcattctagattagtcctct cccttggtctgtaggg	-	-

3. Material

391	tggccac			
pCS2+ rPanx1-393	gcattctgagccaccatg gccatgcccacc tggccac	gcattctagattagecc tggctctcctt	-	-
pCS2+ rPanx1-395	gcattctgagccaccatg gccatgcccacc tggccac	gcattctagattactgg ctgccctggctctt	-	-
pCS2+ rPanx1-397	gcattctgagccaccatg gccatgcccacc tggccac	gattcttagattacattctt ggctgccctggctctt	-	-
pCS2+ rPanx1-407	gcattctgagccaccatg gccatgcccacc tggccac	gcattctagattactcgtg ctcaggccaatc	-	-
Sequencing of pCS2+	gattccatcgattc gaattca	ggtttgtccaaactca tcaatg		

3.4.2 Plasmids

Plasmid vectors used as backbone for molecular cloning are listed in table 3.3 .

Table 3.3 List of backbone vectors used for the generation of recombinant plasmids.

Backbone vector	Purpose	Source
pCS2+	Protein expression in mammalian cells and <i>Xenopus</i> oocytes, template for <i>in vitro</i> transcription for the generation cRNA over SP6 promoter	S. Bunse (Dept. Neuroanatomy, RUB)
pRK5	Protein expression in mammalian cells	R. Bruzzone (HKU-Pasteur Research Centre, Hong Kong)
pSC-mychis	Protein expression in mammalian cells, template for <i>in vitro</i> transcription for the generation cRNA over T7 promoter, vector provides a C-terminal c-myc-tag and 6His-tag	M. Tenbusch (Dept. of Virology, RUB)

3.4.3 Standards

Standards used for analysis of DNA-fragments in agarose gels were the 1kb ladder Plus and the 100 bp ladder Plus from Fermentas.

3.5 Technical equipment

3.5.1 Equipment for cell culture and molecular biology

Incubator HeraCell	Heraeus
Laminar flow unit LaminAir 1.2	Heto-Holten
Bacterial shaker	Thermo Forma
Electroporation of <i>E. coli</i> cells MicroPulser	BioRad
Incubator Kelvitron t	Heraeus
PCR PTC-200	MJ Research
Superspeed tabletop refrigerated centrifuge	Sorvall DuPont, Thermo Fisher
Sorvall Super T21 centrifuge; STH50 rotor, SL-205-T rotor	
UV spectrometer Ultraspec 3000	Amersham pharmacia biotech
UV/Visible spectrometer	
UV gel documentation system	Amersham pharmacia biotech
ImageMasterVDS	

3.5.2 Equipment for microscopical analysis

Light microscope Olympus BH-2	Olympus
Microscope digital camera Olympus DP71	Olympus
Fluorescence microscope Axiophot	Zeiss
Axiovert 200M	Zeiss
Confocal Laser Scanning Microscope LSM510-Meta	Zeiss
Cryostat Leica CM 3050 cryostat	Leica Microsystems
Slides SuperfrostPlus slides	Menzel
Microtome UltracutE Microtom	Reichert-Jung
Electron microscope Philips EM 420	Philips
120kV transmission electron microscope	
Grids for electron microscopy Nickel grids	Plano
Freezing device JFD 030 Cryo-jet	Balzers AG

Freeze fracture machine	Balzers AG
Balzers' freeze etching device	
Grids for FRIL Formvar-coated copper grids	Plano

3.5.3 Equipment for electrophysiology

Automated oocyte injection and recording Roboocyte ®	Multi Channel Systems
---	-----------------------

4. Methods

4.1 Cytologic Methods

4.1.1 Cultivation of N2A cells

All cell lines were incubated in 10 ml of appropriate medium at 5% CO₂-atmosphere, 90% relative humidity and 37°C. After microscopic estimation of cell density the cells have been splitted in an 1:5 to 1:10 dilution consecutively all 48 to 72 hours.

For splitting, cells were washed with 1x PBS, detached from the cell culture plate by addition of Trypsin/EDTA, resuspended and afterwards diluted in fresh medium.

4.1.2 Transfection of N2A cells

Transient transfection was performed by use of the Effectene Transfection Reagent Kit from Qiagen according manufacturer's instructions. For immunocytologic stainings 30.000 to 50.000 cells were transfected on poly-L-Lysin coated coverslips in 24-well-plates. For FRIL-Experiments 6 x 500.000 cells were transfected in 6cm-dishes. For FACS-analysis, 300.000 – 400.000 cells were transfected in 6-well-plates. In all cases except FACS-experiments, medium was changed after 24 h to enhance transfection efficiency.

4.1.3 Immunocytochemistry

N2A cells were fixed 48 h post transfection by incubation in 500 µl 4% paraformaldehyde in PBS for 20 min at RT. After dual washing in 500 µl 1x PBS cells have been permeabilized by use of 500 µl 0,2 % Triton X-100 for 10 min and washed again twice with 1x PBS. Blocking of free accessible binding sites was performed with 600 µl 1 % BSA / 3% NGS per well for 1h at RT.

The first antibody was diluted in blocking reagent and specimen were incubated for 1h at RT or ON at 4°C. Following three washing steps with 1x PBS the incubation with a species specific secondary antibody diluted in PBS or blocking reagent together with Hoechst staining followed for 1h at RT. After two washing steps with 1x PBS, the cover

slips were mounted in ProLongGold Antifade Reagent and afterwards stored in the dark at 4°C until analysis at the confocal microscope.

4.1.4 Fluorescence activated cell sorting (FACS)

For the analysis of cells via FACS, 350.000 N2A cells have been transfected with pEGFP and the plasmid vector encoding the protein of interest. Cells were collected 24h post transfection with cell scrapers, resuspended in PBS and washed twice by centrifugation and resuspension in fresh PBS. Then, 5 µl 7-AAD-solution was added to 1ml cell suspension and cells were sorted by the FACS machine.

4.2 Methods for the preparation and analysis of DNA

4.2.1 Polymerase chain reaction (PCR)

Polymerase chain reactions were performed by use of Phusion Taq High Fidelity Polymerase from NEB following the manufacturer's instructions. Reactions were assembled according to the following scheme:

- 20ng template DNA
- 200 µmol dNTP
- 10 µl 5x PCR-buffer
- 0,01 U Phusion Taq-Polymerase

Table 4.1 Cycling protocol for PCR with the Phusion-Taq Polymerase.

cycling step	2-step-protocol		3-step-protocol		cycles
	temp.	duration	temp.	duration	
initial denaturation	98°C	30s	98°C	30s	1
denaturation	98°C	5-10s	98°C	5-10s	25-45
hybridisation	-	-	55-65°C	10-30s	
elongation	72°C	15-30s/1kb	72°C	15-30s/1kb	
final elongation	72°C	5-10min	72°C	5-10min	1
	4°C	hold	4°C	hold	

4.2.1.1 Overlap Extension (OE) PCR

Overlap Extension PCR was performed using a modified protocol from Wurch and colleagues. Figure 4.1 gives an overview about the technique.

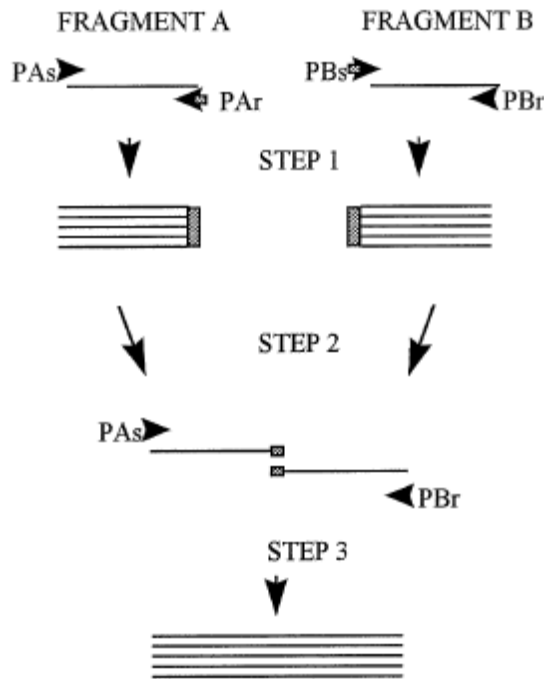


Figure 4.1: Model for the generation of chimeric genes. A first PCR leads to the creation of two products, that can be assembled in a second PCR. PAs / PBs= primer for PCR product A/B sense, PAr / PBr= primer for PCR product A/B reverse. (Picture from Wurch et al. 1998).

In a first PCR the fragments A and B are amplified. Primer PAs (formerly referred to as OE1, see table 3.2) is designed having an overlapping sequence complementary to a part of primer PBs (formerly referred to as OE2). In a second PCR, the PCR products A and B are assembled. While Wurch et al. (1998) describe to amplify this fusion product in a third PCR, during this thesis the assembly of A and B and the amplification of the fused product was performed in the same PCR by addition of Primers PAs and PBr.

4.2.2 Agarose gel electrophoresis of DNA

The size of DNA fragments or the purification of fragmented DNA was performed via horizontal gel electrophoresis. According to the size of investigated DNA, 0,7 – 2 % Agarose in 1 x TAE buffer and 0,4 µg/ml ethidium bromide was used. After addition of

1/10 Vol. loading buffer probes were loaded into the gels cavities and separated at a constant voltage of 6 V/cm electrode distance for a duration of 1-2 h. The estimation of the DNA fragments was performed by the use of the DNA standards GeneRuler 1 kb Ladder and 100 bp LadderPlus (Fermentas). The ImageMaster was used for digital documentation.

4.2.3 Isolation of DNA from agarose gels

Gel fragments containing DNA of interest were excised from agarose gels under UV light ($\lambda = 366$ nm) with a sharp scalpell. Elution and purification was performed with the QIAquick Gel Extraction Kit (Qiagen) according to manufacturer's instructions.

4.2.4 Ligation of DNA fragments

The ligation of DNA fragments was performed with a recombinant T4 DNA Ligase (Fermentas) according to manufacturer's instructions. For that purpose a 1:1 up to a 5:1 molar ratio of insert DNA to vector DNA was chosen, PEG 4000 was added for increasing the rate of ligation efficiency at a concentration of 5% (w/v). The mixture was incubated ON at 10°C or at RT for 1h.

4.2.5 Transformation of competent bacteria

For the preparative production of *in vitro* recombinated plasmid DNA the *Escherichia coli*-strains NEB-TURBOcompetent and DH5 α were used. Both strains had been made competent via treatment with CaCl₂ in advance. Chemical transformation was performed via heat shock at 42°C for 30 s. In 1 ml SOC medium an antibiotic resistance could develop. Bacteria could be through resistance genes selected for a positive transformation result on LB agar plates and via LB medium through the addition of an appropriate antibiotic.

The incubation of agar plates was carried out ON at 37°C, while colonies transferred into fluid LB growth medium were incubated in a horizontal shaker ON at 37°C and 225 rpm.

4.2.6 Preparation of plasmid DNA

For analytic and preparative purposes, plasmid DNA was purified from *E. coli* cells by the use of different isolation kits. The choice of the kit was given by the amount of DNA to be prepared. The used kits for mini-, midi- or maxipreparation, which equals 20µg, 100µg or 500µg nucleic acid, were obtained from fermentas, clontech or macherey & nagel, manufacturer's instructions were followed. The purification method is based on an alkaline lysis of bacterial cells and a consecutive binding of the DNA to a matrix of siliciumoxide

4.2.7 Restriction of DNA

For linearization of plasmids or for excision of defined fragments of interest specific type II restriction endonucleases were used. The analytic restriction was used for the analysis of recombinant plasmids, while the preparative restriction was achieved when the production of recombinant DNA was necessary. In the reaction assembly 1 unit endonuclease was used per 1 µg DNA in the appropriate buffer and incubated at 37°C for 5-30 min regarding manufacturers guidelines.

4.2.8 Determination of the concentration of nucleic acids

To assess the concentration of DNA or RNA the absorption at 260 nm (A_{260nm}) was measured. The concentration was calculated with the following formula:

c (nucleic acid) = absorption coefficient $\times A_{260nm} \times dilution \times \mu g/ml$ while the absorption coefficient at a path length of 1 cm equals 50 for dsDNA and 40 for ssRNA.

Contaminations with protein were determined by use of the quotient A_{260nm}/A_{280nm} . At a quotient of $> 1,8$, solutions were considered to be not contaminated.

4.2.9 Sequencing of plasmid DNA

Sequencing of recombinant plasmid DNA was performed at the sequencing facility of the Ruhr University of Bochum using the ABI PRISM 377 DNA Sequencer technology

with BigDye Terminator v1.1 Cycle Sequencing Kits and appropriate analysis software (Sequence Scanner; Applied Biosystems, Foster City, CA, USA).

4.3 Methods for the preparation and analysis of RNA

4.3.1 RNA isolation from tissue

RNA was isolated and purified from tissue via the trizol-method. 100mg tissue were homogenized in 1ml Trizol. An addition of 1/5 Vol. chloroform followed. High speed centrifugation separated the phase containing RNA from cellular protein. The RNA precipitation was performed by use of isopropanol and a subsequent centrifugation step, the pellet was washed with 70% ethanol and resuspended in RNase free water.

4.3.2 Synthesis of cDNA by reverse transcription

The synthesis of DNA complementary to mRNA was performed by use of the Kit PrimeScript from TAKARA according to manufacturers guidelines. In advance, 1µg of the RNA intended for transcription was treated with 1 µg DNase for 15 min at RT. Afterwards the DNase was inactivated through addition of 1µl EDTA and incubation at 65°C for 10 min.

4.3.3 *in vitro* transcription

The synthesis of cRNA for the injection into *Xenopus* oocytes was performed by use of the mmessage mmachine Kit from Ambion according to manufacturers guidelines.

4.3.4 Agarose gelelectrophoresis of RNA

The analysis of RNA was performed with 1-2% agarose gels supplemented with 0,4 µg/ml ethidium bromide. Probes were provided with RNA loading buffer (1µl probe + 6µl buffer), heated to 95°C for 2 min and separated at a constant voltage of 6 V/cm electrode distance for a duration of ~1h. The ImageMaster was used for digital documentation.

4.4 Protein biochemic methods

4.4.1 Immunohistochemistry

Xenopus oocytes were fixed in 2% PFA for 10 min 48-72h post injection of cRNA, washed in PBS and embedded in tissue freezing medium. Cells were frozen quickly in liquid nitrogen. Then, 12 µm thick cryosections were cut with a cryostat and placed onto microscope glass slides. Blocking of unspecific binding sites was performed in blocking buffer for 1h at RT. The incubation with the primary antibody diluted in blocking reagent was performed ON at 4°C. After three consecutive washing steps with 1x PBS the incubation with secondary Alexa Fluor coupled species specific antibodies was performed at RT for 1-2 h. After repeated washing steps oocytes were mounted in ProLong Gold Antifade reagent.

All antibodies were diluted in blocking buffer. In all experiments, stainings omitting the first or the second antibodies were performed to serve as negative controls.

4.4.2 Immunocytochemistry

Immunocytochemistry on transfected N2A was performed two days post transfection. After removal of DMEM cells were fixed 4% PFA for 10 min at RT and washed with 1x PBS.

Afterwards, a permeabilization step followed by use of 1% Triton X-100 in 1x PBS for 10 min. Blocking of unspecific binding sites was performed in blocking buffer (3%NGS/1%BSA) for 1h at RT. Incubation with the primary antibody was performed ON at 4°C. After consecutive washing steps with 1x PBS, the incubation with secondary Alexa Fluor coupled species specific antibodies was performed at RT for 1-2 h. After rinsing the cells with PBS, probes were mounted in ProLong Gold Antifade reagent on glass coverslips.

All antibodies were diluted in blocking buffer. Hoechst 33342 staining dye was added to the secondary antibody solution in a 1:10.000 dilution to achieve a staining of the cell nuclei.

4.4.3 Confocal microscopy

Confocal imaging was performed by use of a Laser scanning microscope LSM 510-Meta from Zeiss. Pictures were obtained with argon and HeNe lasers, a laser diode (emission wavelength: 405 nm), 20x, 40x and 63x (NA 1.4) objectives. If oil was used, it was purchased from Zeiss. Picture analysis was done with the LSM 510 Meta software, images were taken using the single track or multitrack mode as 512x512 or 1024x1024 pixels.

4.4.4 Freeze fracture immunogold labeling (FRIL)

For FRIL experiments, 5x 500,000 N2A cells were transfected with 2-4 µg plasmid DNA in 6 cm dishes. Cells were collected 48 h post transfection by use of cell scrapers after washing in PBS and pelleted by centrifugation. Then cells were either fixed with 1% PFA for 10 min or untreated. Cells were frozen in a JFD 030 Cryo-jet freezing device in liquid propane at -180°C. Afterwards cells were freeze-fractured and shadowed with platinum / carbon in a 45° angle. The replica was generated with carbon in a Balzers' freeze-etching device and released from the device by thawing in PBS. Afterwards the probe was incubated in detergent solution for 1-12 h under constant shaking. Thereby, a film of macromolecules absorbs to the replica and is therefore accessible for antibody staining and immunogold labeling. Then, replicas were washed in TBS several times and incubated in blocking solution for ½ h afterwards. The incubation of the first antibody was performed in 1% BSA in TBS for 1 – 2½ h at RT or ON at 4°C. Three subsequent washing steps in 1% BSA in TBS followed. A second blocking in 5% donkey serum in blocking solution for 30 min was performed. Immunogold labeling was done by incubation of the specimen with species specific gold-labeled secondary antibodies in 1% BSA in TBS for 1 h at RT or 4°C ON.

After subsequent washing in TBS, replicas were fixed with 0.5% glutaraldehyde in 0.1 M phosphate buffer for 10 min. Two washing steps in A. dest. followed. Then, replicas were mounted on formvar-coated copper grids and analyzed by electron microscopy.

4.5 Methods for working with *Xenopus laevis* oocytes

4.5.1 Injection of *Xenopus* oocytes

All oocytes used in this work were obtained from EcoCyte Bioscience. The cells were defolliculated and plated in 96-well plates ready to use. Injection of cDNA or cRNA was performed by use of the Roboocyte® automated oocyte injection and recording system. In case of injection of cDNA, 50 nl solution with a concentration of 250µg/µl were injected into the oocytes nucleus. When cRNA was injected, 50 nl solution with a concentration of 1 µg/µl was injected into the cells ooplasm. Preceding TEVC recordings, an incubation time of approximately 60 hours was maintained, the oocytes were kept in NFR at 17°C.

4.5.2 Kinetic studies of *Xenopus* oocytes

For generation of survival curves of oocytes expressing possibly harmful proteins, oocytes were injected with corresponding cRNA and incubated in NFR or NFR containing 50µM Cbx at 17°C. The oocytes were observed every 3 hours with help of a binocular microscope. The protrusion of ooplasm from the oocyte was taken as marker for cell death.

4.5.3 Electrophysiology

Xenopus oocytes were used for electrophysiological measurements by use of the two electrode voltage clamp (TEVC) technique. Recordings were performed with the Roboocyte ® system and Roboocyte TEVC measuring heads. Electrodes were filled with 2.5 M potassium acetate providing an electrode impedance of ~1 MΩ. During recording, oocytes were superfused with NFR (3-4 ml/min). For pharmacological treatment, substances were diluted in NFR and applied by use of a gravity based 8-channel perfusion system. Recordings always took place at RT. In TEVC recordings, oocytes were clamped to a voltage of -70mV, voltage steps were applied from -100 mV to 60 mV in 20 mV increments with a duration of 2 sec / step and currents were monitored by the Roboocyte® system.

4.5.4 Data analysis

Data acquired in TEVC measurements were analyzed with the Microsoft Excel and the GraphPad Prism5 software. Microsoft Excel was used for analyzing the maximum current at +60mV in current voltage relationship curves, the calculation of the inhibitory effects of pharmaceuticals and for readout of the resting potential. Statistical analyses were performed by use of the GraphPad Prism5 software. For the analysis of two groups of samples, paired t-test (Mann-Whitney-test) was performed, for the analysis of three or more groups One-way ANOVA (Kruskal-Wallis-test) was used. In all cases, Gaussian distribution was not assumed.

5. Results

5.1 Simultaneous expression of Panx1 and Panx2 in *Xenopus laevis* oocytes for the analysis of heteromeric channel formation

Pannexons are described to be multimeric protein channels (Boassa et al. 2007). The formation of heteromeric pannexons consisting of both Panx1 and Panx2 in various ratios was described to occur in *Xenopus* oocytes, but detailed analyses regarding channel properties have not been performed. Furthermore, it has not been tested so far whether the ratio of Panx1 to Panx2 protein forming the hexamer influences channel gating. In order to verify the existence of heteromeric Panx1/Panx2 channels, cRNAs were produced by *in vitro* transcription from the plasmids pRK5-rPanx1 and pRK5-rPanx2 (kindly provided by R.Bruzzone, Institute Pasteur, Paris, France) and were injected into *Xenopus* oocytes. To gain information about possible interactions of Panx1 and Panx2-664, cells were injected with both cRNAs in different ratios to perform TEVC measurements. Thus, if heteromeric channels were formed, the influence of the respective proteins on the pannexons channel properties could be investigated. Regarding the amount of Panx1 and Panx2-664 cRNAs a constant total RNA quantity of 50 ng per oocyte was maintained.

Current-voltage relationships (IV-curves) were recorded by using the Roboocyte® system and the TEVC method. Oocytes were clamped to -70 mV and voltage steps were applied in 20 mV increments resulting in membrane potentials from -100 mV to +60 mV. Cbx was used as an inhibitor for Panx1 evoked currents. With this protocol the maximum current amplitude at +60mV was measured. Also, the remaining current after Cbx application was calculated and the influence of heterologous protein expression on the cells resting potential was investigated. In figure 5.1 A-D representative IV-relationships are shown for coinjected oocytes with cRNAs for Panx1 and Panx2-664 as reference, for uninjected cells as a negative control, and for cells injected with cRNA encoding Panx1 and Panx2 in a 1:1 ratio.

Oocytes expressing Panx1 were characterized by an exponential increase in the slope of the IV-curve at membrane potentials of about ≥ -20 mV. This is regarded as a result of channel opening (Ma et al. 2009). The increase in conductance upon depolarization

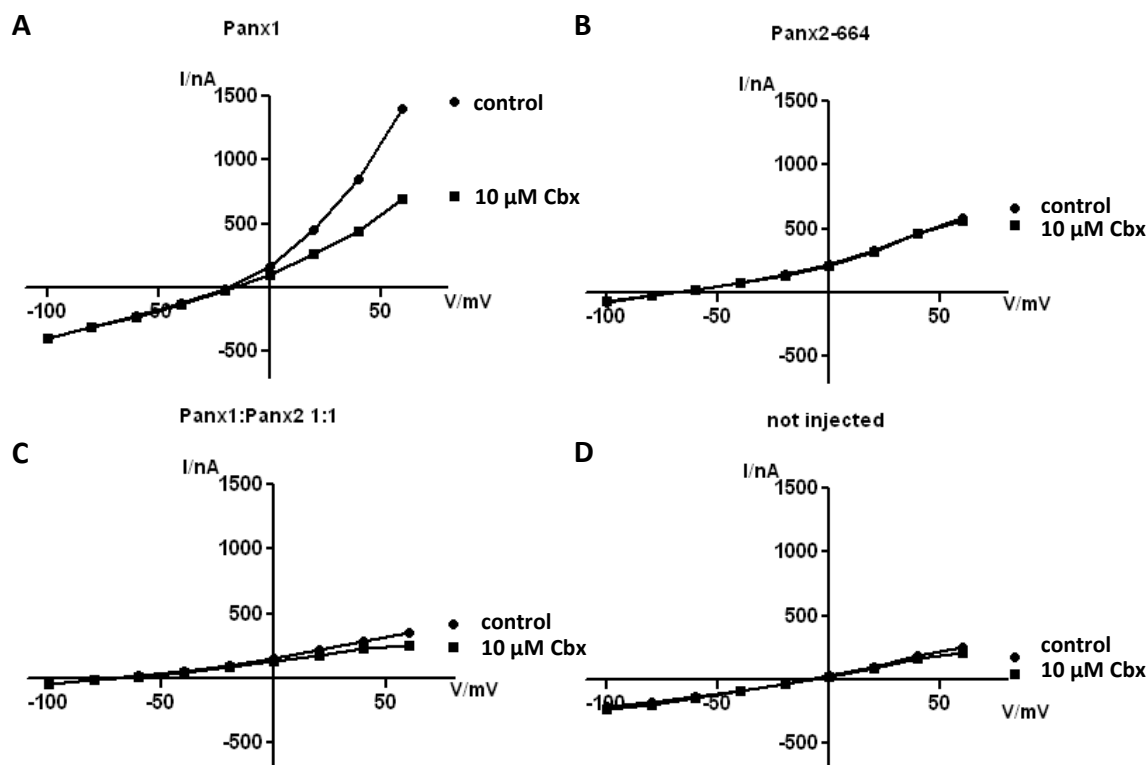


Figure 5.1: Representative IV-curves of Panx1 and Panx2 expressed alone or simultaneously in the *Xenopus laevis* oocyte system. Whole cell membrane currents from cRNA injected *Xenopus laevis* oocytes were recorded using the TEVC technique. Oocytes were clamped to -70 mV, voltage steps starting from -100 mV to $+60$ mV membrane potential were applied subsequently. IV-curves were calculated from corresponding current responses. ni = not injected. (A,B) Representative IV-curves from oocytes expressing either Panx1 or Panx2. After application of a first voltage step protocol, the influence of $10 \mu\text{M}$ Cbx was documented in a second measurement. (C) IV-curve from an oocyte expressing both Panx1 and Panx2. (D) IV-curve from a not injected oocyte as negative control. For potentials ≥ -20 mV, an exponential increase can be observed under control conditions in A, but not in B, C or D.

can be blocked by application of $10 \mu\text{M}$ Cbx. In the presence of Cbx, the maximum current at $+60$ mV on average is reduced to 73,4%. This is highly significant in comparison to uninjected cells (Fig. 5.1). In these negative controls the slope of the IV-curves is rather linear and constant throughout the membrane potential range tested (Fig. 5.1 D). Similar to the uninjected oocytes, the slope of the IV-curve of Panx2 expressing oocytes is almost linear (Fig. 5.1 B). Simultaneous expression of Panx1 and Panx2 did not alter the shape of the IV-curves (Fig. 5.1 C).

Throughout all *Xenopus* oocyte measurements a variability in the current amplitude could be observed, which did not correlate with heterologous protein expression, because this variance occurred in uninjected cells as well.

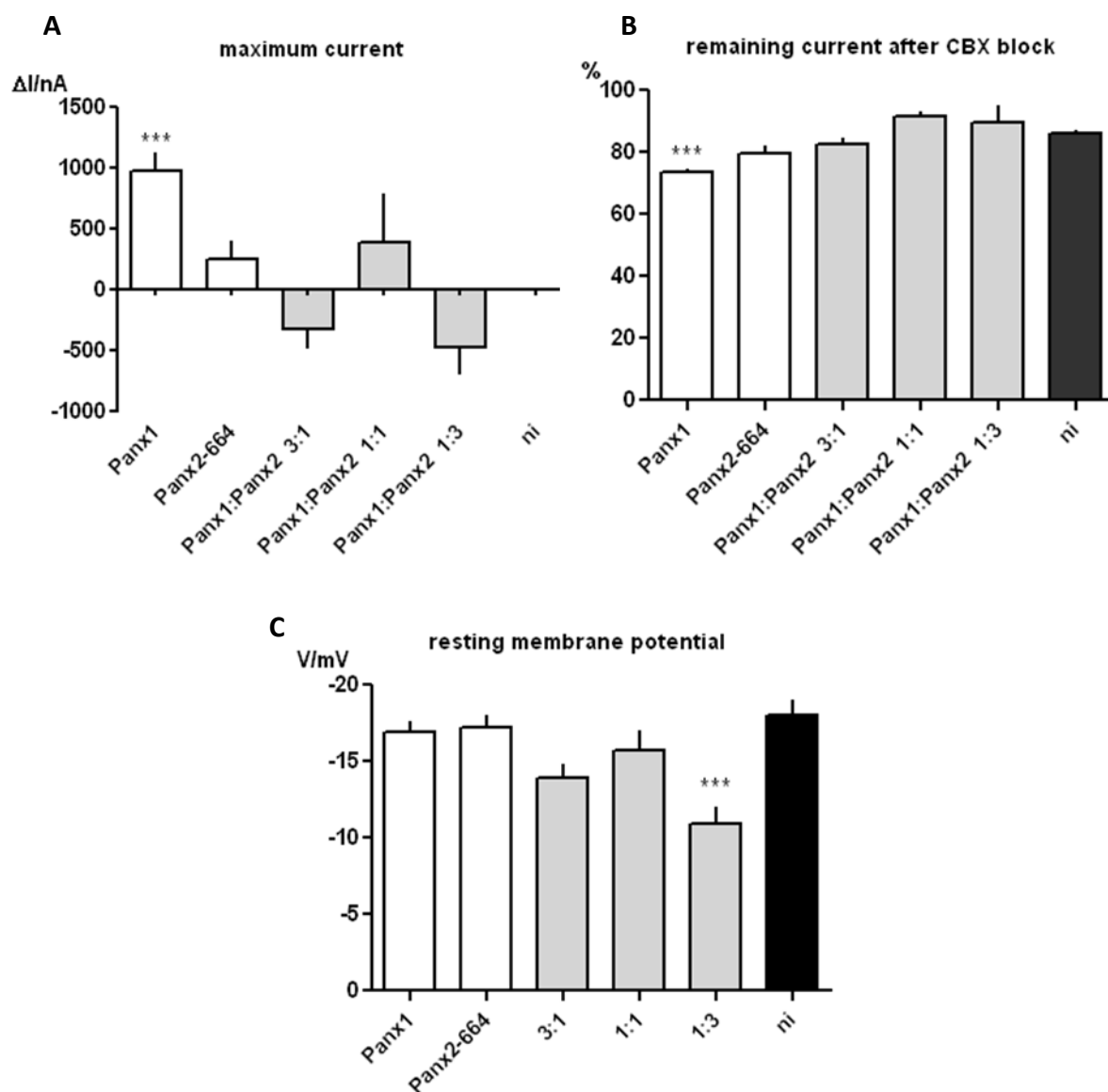


Figure 5.2: Electrophysiological characterization of Panx1 and Panx2 expressed alone or simultaneously in the *Xenopus laevis* oocyte system. (A) Quantitative analysis of the maximum current measured at a membrane potential of +60 mV. Currents were normalized to negative controls. (B) Quantitative analysis of the remaining current after inhibition of channel activity with Cbx (in % of control). (C) Quantitative analysis of the resting membrane potential. Panx1 n=232, Panx2-664 n=59, Panx1: Panx2 1:3 n=21, Panx1: Panx2 1:1 n=19, Panx1: Panx2 3:1 n=32, ni n=106. ***P<0.001 **P<0.01 *P<0.05, SEM, significance vs. ni

In fact, variations correlated with the day of recording. Possible explanations for this phenomenon were general differences in oocyte quality or an inconstant temperature of the NFR used, which could not be controlled during recording due to the experimental setup.

To avoid inconsistencies between different experimental days, the currents recorded from uninjected oocytes on a specific experimental day were averaged and subtracted

from all currents recorded from injected oocytes of the particular day. Thus, the currents for uninjected cells are normalized to zero and currents from injected oocytes are plotted as $\Delta I/nA$.

Figure 5.2 shows that a significant increase of maximum currents was observed for Panx1 expressing oocytes only. Consequently, a significant Cbx inhibition can also be observed for Panx1 expressing oocytes only. As far as resting membrane potential is concerned, a significant change can be observed only for a Panx1:Panx2 ratio of 1:3. However, this change is in a range of ~5 mV, which suggests that this difference is not biologically relevant.

5.2 Pannexin 2

5.2.1 Comparison of Panx2-664 and Panx2-674

The genomic nucleotide sequence encoding the Panx2 protein contains two putative start codons, resulting in two different possible open reading frames (ORF). A first ATG, which could be used as start codon for translation, is localized 30 nucleotides upstream a second ATG, which could be used as start codon as well.

The Panx2 protein originally was described as a protein consisting of 664 amino acids (Bruzzone et al. 2003). After an update of the NCBI and *ensembl* databases in 2007, the revised sequence occurred to be ten amino acids longer, a phenomenon that can be ascribed to a usage of the first codon mentioned. The experiments described in chapter 5.1 (see above) regarding possible interactions of Panx1 and Panx2 expression, when expressed at different ratios, were performed using the shorter version of Panx2, referred to as Panx2-664. A possible functional difference between Panx2-664 and the longer version, Panx2-674, was investigated by electrophysiological measurements in *Xenopus* oocytes. Additional experiments were performed to address the question if the prolonged N-terminus of Panx2-674 alters the intracellular localization of the protein, if it influences membrane trafficking efficiency, and which of the possible two isoforms are naturally occurring.

The start codons for Panx2-674 and for Panx2-664 are both localized on exon2 in the mRNA. Therefore, it is not possible to use common techniques like RT-PCR or RACE-

PCR for discrimination on mRNA level or cDNA level, respectively (Buettner et al. 2000).

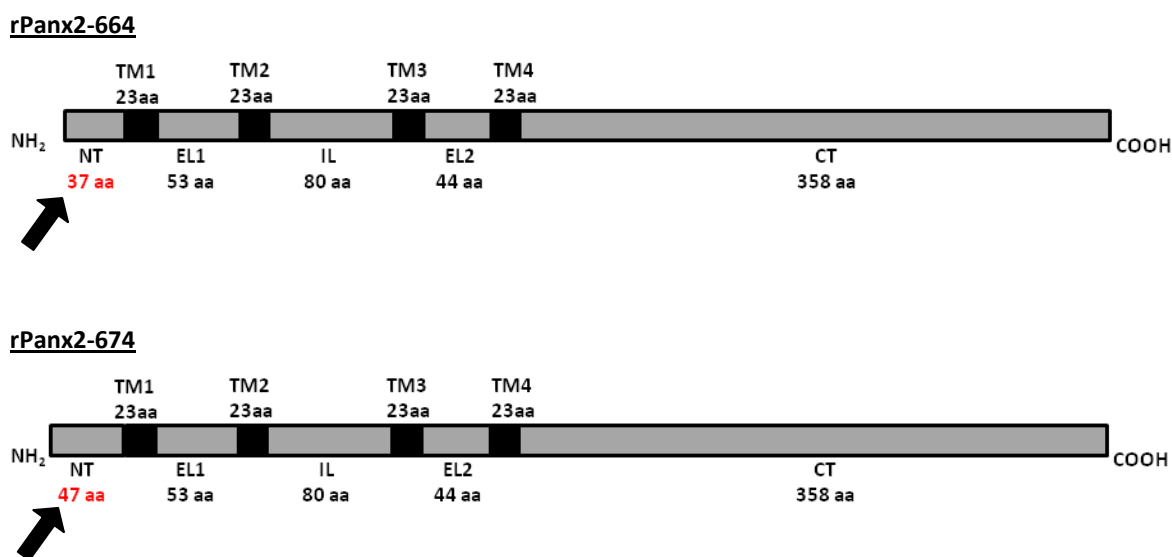


Figure 5.3: Comparison of Panx2-664 and Panx2-674. Definition of domain borders for both Panx2 forms corresponding to *ensembl* data. Note the difference in the N-terminus of the proteins (indicated by arrows). Linear representation of the protein domains are drawn to scale, the lengths reflect actual amino acid numbers. The transmembrane domains (TM), the extra- and intracellular loops (EL, IL) as well as the amino and carboxyterminal domains (NT, CT) are indicated.

Therefore, these methods are not appropriate for discrimination and since antibodies for immunocytochemical detection are not available, a functional comparison between the two differently sized Panx2 proteins was used. mRNA was purified from rat whole brain tissue via the trizol/chloroform-method and transcribed into cDNA. This cDNA was applied as template for PCR to amplify the ORF of Panx2-674. Afterwards, this sequence was used as an insert for molecular cloning into the plasmid vector pCS2+, which allows expression in mammalian cells as well as *in vitro* transcription for the generation of cRNA used for oocyte injection.

5.2.2 Localization of Panx2-664 and Panx2-674 in N2A cells by immunocytochemistry

In general, the N-terminus of proteins localized in cellular membranes is responsible for a correct trafficking to the target compartment by comprising arbitrate signal sequences (Blobel et al. 1984). Because the difference in length between the two Panx2 forms is found in the N-terminal domain, possible differences in membrane internalization have to be analyzed when Panx2-664 and Panx2-674 are expressed. In a

first experiment, both proteins were overexpressed in N2A cells and visualized by immunocytochemical staining.

The immunocytochemical stainings of both Panx2 forms reveal a different labeling. Panx2-664 was found to be localized in the cytoplasm of transfected cells. In contrast, Panx2-674 was primarily localized the cell membrane, a cytoplasmic localization was less evident.

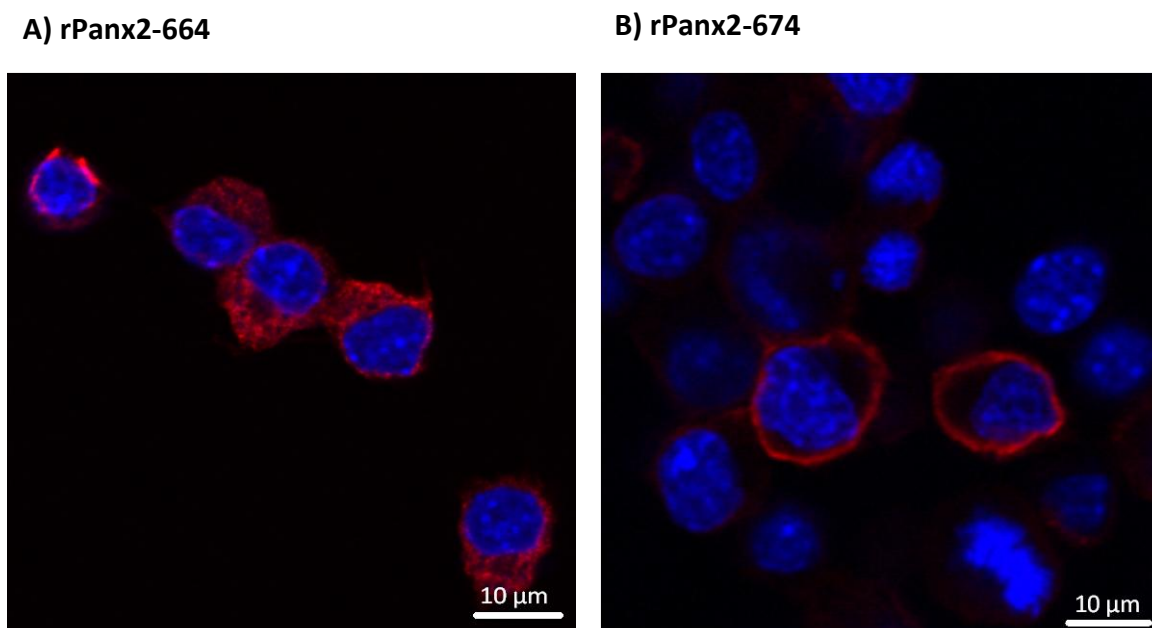


Figure 5.4: Expression analyses of Panx2-664 and Panx2-674 in N2A cells. N2A cells were transfected with pRK5-rPanx2-664 or pCS2+rPanx2-674 and stained against Panx2 48h post transfection. Images were taken with a confocal microscope. The signal derived from staining of the Panx2 proteins is depicted in red. The cell nuclei are stained with Hoechst 33342, the signal resulting is shown in blue. Bars as indicated, 10µm.

These results suggested that the prolonged N-terminus of Panx2-674 seems to be necessary for an appropriate trafficking of the protein to the cell membrane.

5.2.3 Localization of Panx2-664 and Panx2-674 in N2A cells via Freeze-fracture replica immunogold labeling (FRIL)

The FRIL technique allows the combination of freeze-fracture electron microscopy with the specificity of an immunocytochemical staining. In the standard freeze fracture preparation, cells are frozen quickly after collection and subsequently broken. The fracture is irregular and occurs along lines of weakness like the plasma membrane or

surfaces of organelles. By breaking the lipid bilayer, two monolayers with associated proteins termed P-face (protoplasmic leaflet) and E-face (extraplasmic leaflet) occur. A thin layer of carbon is evaporated onto the surface of the specimen, later on the surface is shadowed with a platinum vapor. To allow a staining of proteins with first antibodies of choice and immunogold labeled secondary antibodies, in FRIL the probe is not digested completely when generating the replica.

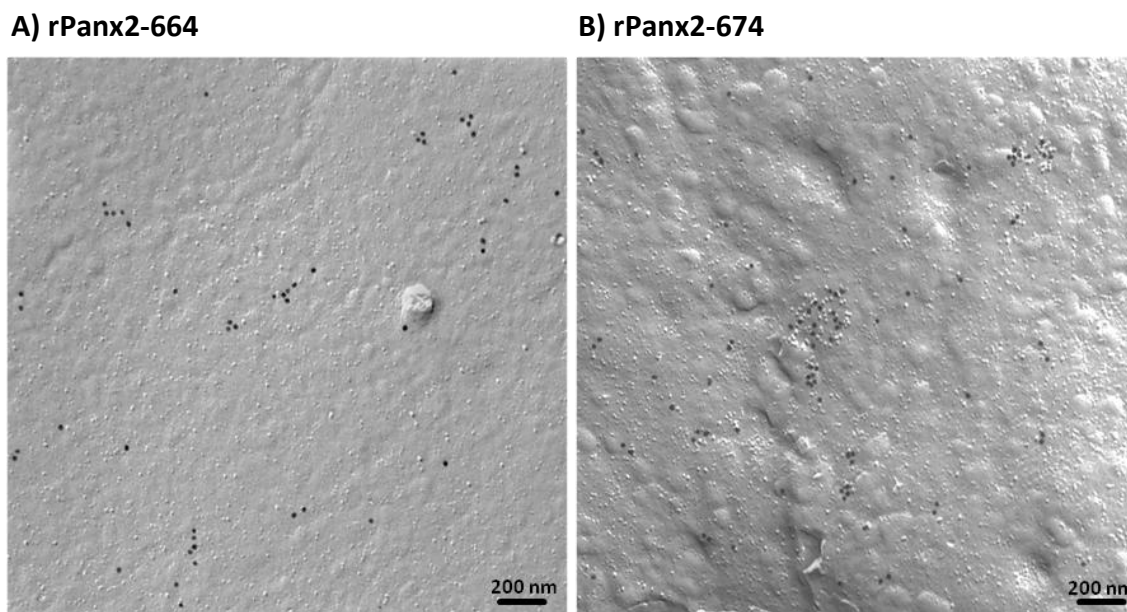


Figure 5.5: Analysis of the membrane localization of rPanx2 forms by FRIL.

N2A cells were transfected with pRK5-rPanx2-664 (A) or pCS+rPanx2-674 (B) and subjected to FRIL two days after transfection. Bars as indicated, 200 nm.

By that treatment, proteins still remain on the surface of the replica and are accessible for antibody staining techniques.

To further investigate the membranous localization and the structural organization of Panx2, N2A cells were transfected with pRK5-rPanx2-664 and pCS2+rPanx2-674. Stainings were performed by use of a rabbit-anti-Panx2 antibody generated in the department (Bunse 2009). Figure 5.5 shows representative membranes patches from N2A cells expressing either the long or the short version of Panx2. In both micrographs, P-faces are stained.

A quantification of the expression rate of Panx2-674 and Panx2-664, indicated by the density of gold particles calculated with respect to the analyzed region, is given in figure 5.6 A.

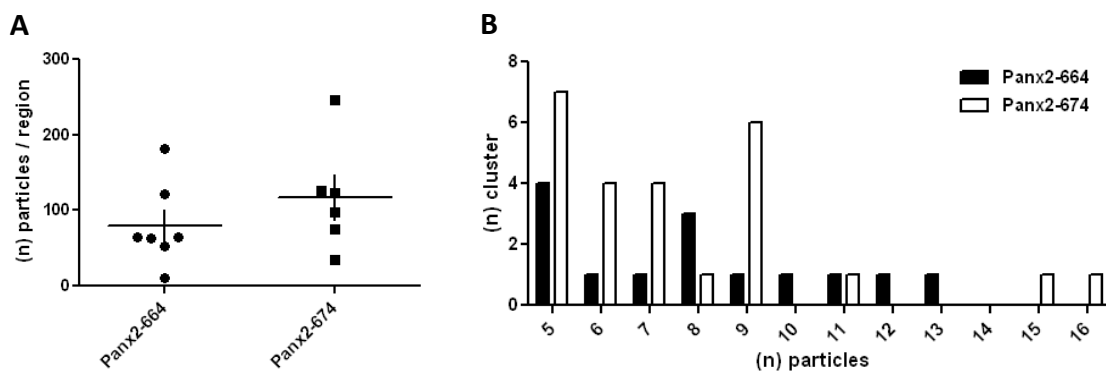


Figure 5.6: Analysis of the cell surface localization of rPanx2 forms by FRIL. Electron microscopic micrographs showing immunogold labeling of either Panx2-664 or Panx2-674 were used for quantification of the expression rate and clustering of both proteins. **(A)** Immunogold labeled proteins were counted / region (statistic: mean, SEM). **(B)** The number of particles / cluster was counted. Note the tendency of Panx2-674 to form more clusters with higher particle number. Panx2-664 n= 6 pictures, Panx2-674 n=7 pictures.

The average expression rate for Panx2-664 is 80,01 particles / region, while the expression rate of Panx2-674 is 117,15 particles / region. Resulting from a high variance in particle density / region a statistical significance could not be calculated, however, a tendency of Panx2-674 to show a higher particle density / region is evident. Furthermore, the micrographs in figure 5.5 demonstrate that the Panx2 protein is organized in clustered structures. A quantification (Fig. 5.6 B) reveals a tendency of Panx2-674 to form more clusters, that, at least in parts, are consisting of more proteins than Panx2-664 clusters. A significant difference could not be detected, the results obtained from the FRIL analysis of Panx2-664 and Panx2-674 are comparable. Considering the results obtained by analysis of the confocal imaging (Fig. 5.4), the similarity in the expression rate on the cell surface is an intriguing finding.

5.2.4 Electrophysiological properties of Panx2-664 and Panx2-674

The ability of Panx2 to form functional channels has been elusive. Instead, it was supposed to serve accessory functions in Panx1 trafficking (Penuela et al. 2009b). Recently, Ambrosi and colleagues postulated that Panx2-mediated currents can be observed, when a voltage ramp protocol from -100 mV to +100 mV with a duration of 70 s is applied to *Xenopus* oocytes expressing Panx2-674. Furthermore, the authors were able to reconstitute Panx2-674 channels in vesicular structures, and channel activity could be recognized via monitoring molecules passing from the outside to the

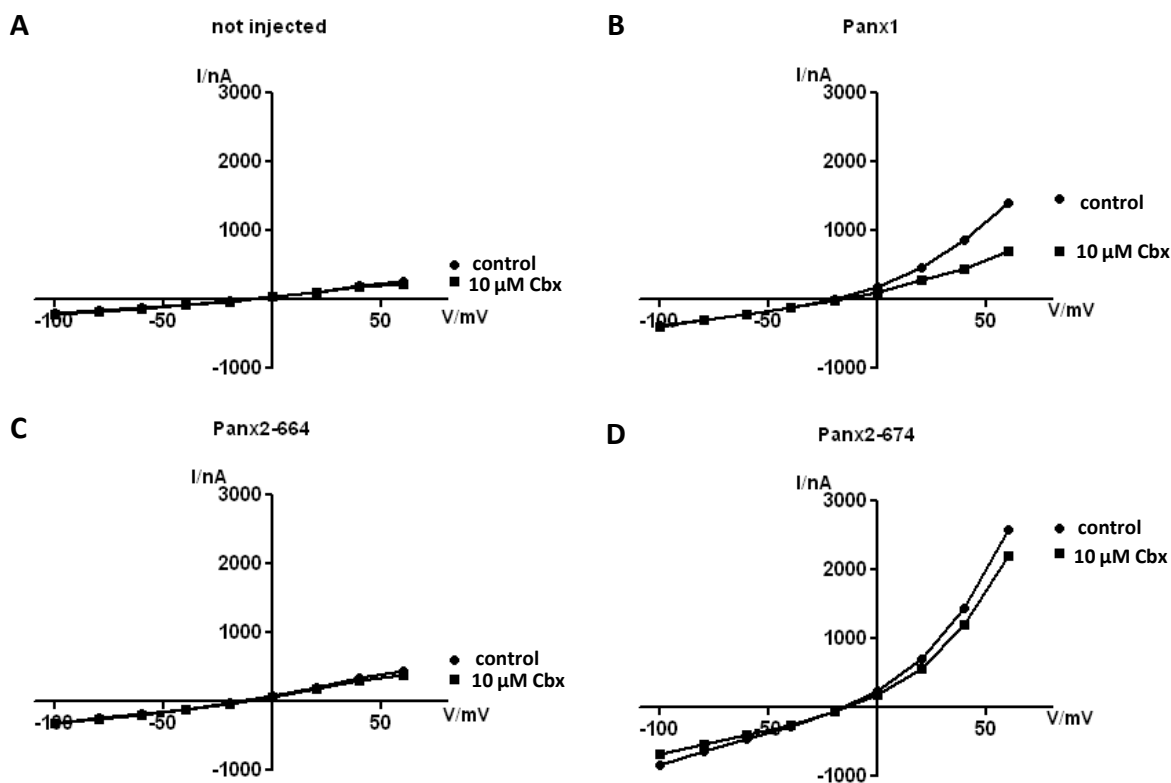


Figure 5.7: Comparison of the IV-relationship in *Xenopus laevis* oocytes expressing Panx2-664 and Panx2-674. Whole cell membrane currents from cRNA injected *Xenopus laevis* oocytes were recorded using the TEVC technique. Oocytes were clamped to -70 mV, voltage steps starting from -100 mV to $+60$ mV membrane potential were applied subsequently. IV-curves were calculated from corresponding current responses. ni = not injected. (A) Representative IV-curves from oocytes expressing Panx1 or under control conditions and Cbx inhibition as a reference curve (B) IV-curve from a uninjected oocyte as negative control (C) IV-curves from oocytes expressing rPanx2-664. Currents are small, the slope of the curve is linear (D) IV-curves from oocytes expressing rPanx2-674. Current amplitude is higher, the slope of the curve is exponential. Cbx application, however, does not influence Panx2-674 mediated currents.

inside of these vesicles (Ambrosi et al. 2010a). Up to now, Panx2 channel activity could not be measured using standard depolarization protocols. In the present work, however, current responses to the commonly used standard depolarization protocol were recorded, and Panx2-664 and Panx2-674 were compared with respect to their ability to form functional channels.

Application of depolarizing voltage steps to oocytes expressing Panx2-664 (see Fig. 5.7 C and 5.1 B) does not lead to current responses different from those recorded from uninjected cells (Fig. 5.7 A). The slope of the IV-curves is always linear and does not reveal a voltage gated channel activation. Oocytes expressing Panx2-674 show a distinctly different pattern: the slope of the IV-relationship increases exponentially at holding potentials $\sim \geq -20$ mV (Fig. 5.7 D). This resembles an activation pattern similar to Panx1 (Fig. 5.7 B).

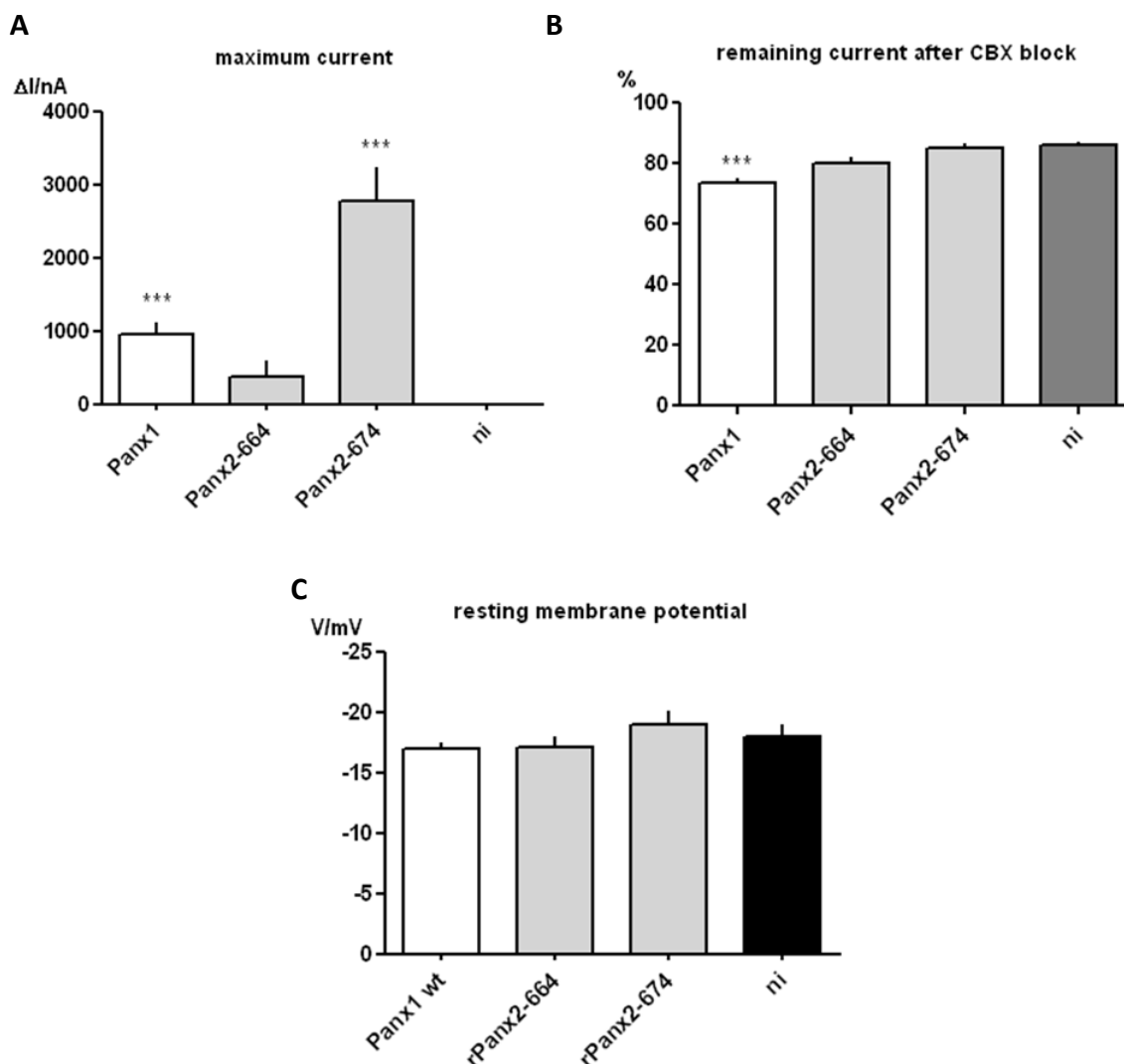


Figure 5.8: Comparison of the electrophysiological properties of Panx2-664 and Panx2-674 in *Xenopus laevis* oocytes. (A) Quantitative analysis of the maximum current measured at a membrane potential of +60 mV. The average maximum current of Panx2-674 expressing oocytes is three times higher than in Panx1 expressing oocytes. Currents were normalized to negative controls. (B) Quantitative analysis of the remaining current after inhibition of channel activity with Cbx (in % of control). Cbx sensitivity cannot be observed for Panx2.674, Panx2-664 and ni. (C) Quantitative analysis of the resting membrane potential. Panx1 n=232, Panx2-674 n=47, Panx2-664 n=54, ni n=106. ***P<0.001 **P<0.01 *P<0.05, SEM, significance vs. ni.

This observation leads to the conclusion that Panx2-674 forms functional, voltage gated channels. Interestingly, the currents measured in oocytes expressing Panx2-674 channels are ~ three times larger than Panx1 evoked currents (average currents: Panx1 = $972,9 \pm 145,2$ nA , Panx2-674 = $2780,4 \pm 468,5$ nA, normalized to ni). This raises the same questions about differences between Panx1 and Panx2-674 channels: (i) are there differences in channel gating? (ii) Is inactivation of Panx2-674 channels slower? (iii) Do they differ in response to Cbx? While Panx1 mediated currents can be inhibited to

an extent of 26,6% on average by Cbx application (Fig. 5.8 B), Panx2-674 mediated currents are Cbx-insensitive. Because the exact mechanism of Cbx inhibition is not known yet it is impossible to search for Cbx binding domains probably missing in Panx2. Anyway, other inhibitors have to be examined.

5.2.5 Panx2-674 pharmacology

Identification of agonists for channel proteins provides a useful tool for functional analysis of investigated proteins. An identified inhibitor allows to verify that measured effects can be subscribed to a specific protein, or to separate the participation of a certain channel to the current response in complex systems. Panx2-674 was shown to be insensitive to Cbx (Fig. 5.8 B). Therefore, several additional compounds were tested for possible inhibitory effects on currents recorded from Panx2-674 expressing oocytes. CoCl_2 was chosen because an inhibitory effect of cobalt ions on hemichannel activity in the zebrafish retina has been reported (Fahrenfort et al. 2004). LaCl_3 also is known to be a connexin hemichannel blocker (Anselmi et al. 2008), while the antimalarial quinine derivative mefloquine is described to block Panx1 (Iglesias et al. 2009). Octanol, a long chain alcohol, is a common gap junction inhibitor (Johnston et al. 1980)

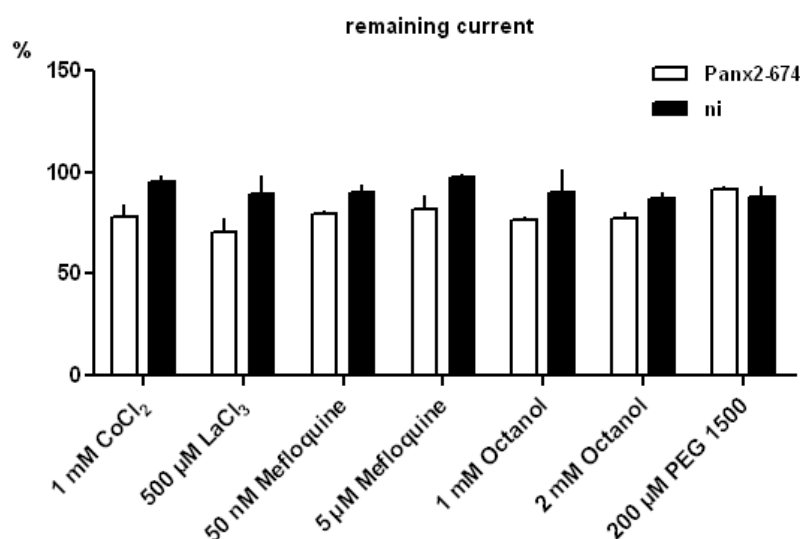


Figure 5.9: Effect of different compounds on Panx2-674. Current responses were recorded in *Xenopus laevis* oocytes expressing Panx2-674 before and after application of different compounds, uninjected oocytes were used as negative controls. A quantitative analysis of the remaining current after application of possible inhibitors was performed (in % of control).

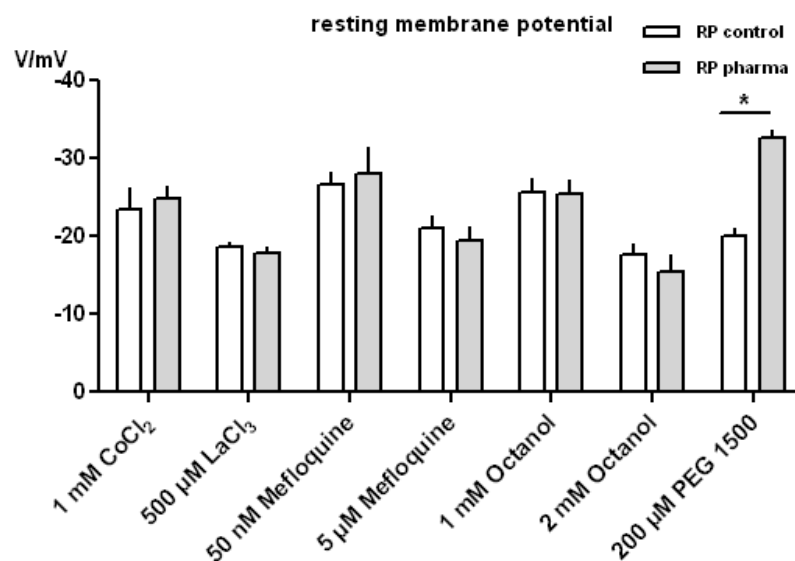


Figure 5.10: Effect of different compounds on resting potential. *Xenopus laevis* oocytes expressing Panx2-674 were incubated with different compounds, TEVC measurements were performed and the resting membrane potential was calculated before and after application of substances. ***P<0.001 **P<0.01 *P<0.05, SEM, significance Panx2-674 vs. ni.

Finally, PEG 1500 has been shown earlier to be able to block Panx1 induced currents (Bunse et al. 2009; Wang et al. 2007). Significant inhibition of Panx2-674 mediated currents could not be achieved with any of the compounds tested. Next, an endogenous inhibitor of pannexin channel activity was tested for possible inhibitory effects on Panx2-674.

Table 5.1: Inhibitory effect of different compounds. IV-curves were recorded from oocytes expressing Panx2-674 and uninjected cells before and after drug application. The average remaining current after drug application recorded in Panx2-674 expressing oocytes in comparison to uninjected cells is given, values in % of predrug.

Compound	Max. current after application of compound (% of predrug)	
	Panx2-674	uninjected oocytes
1mM CoCl ₂	77,90	88,04
500 μM LaCl ₃	70,84	88,95
50 nM Mefloquine	79,47	86,60
5 μM Mefloquine	81,66	104,78
1 mM Octanol	76,42	89,99
2 mM Octanol	77,59	86,73
200 μM PEG 1500	91,17	62,84

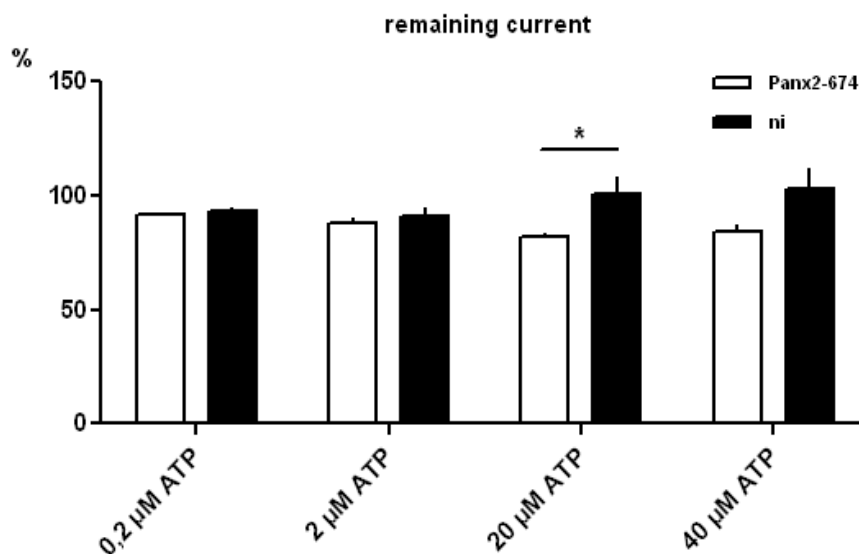


Figure 5.11: Effect of ATP on Panx2-674 mediated currents. Current responses were recorded in *Xenopus laevis* oocytes expressing Panx2-674 before and after application of ATP at different concentrations, uninjected oocytes were used as negative controls. Quantitative analysis of the remaining current after application of possible inhibitors was performed (in % of control). ***P<0.001 **P<0.01 *P<0.05, SEM, significance Panx2-674 vs. ni.

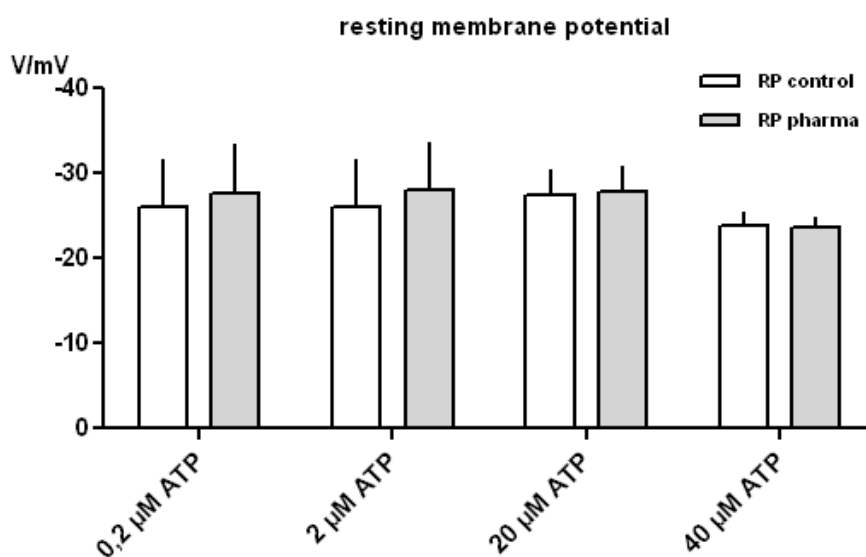


Figure 5.12: Effect of ATP on resting potential (A) *Xenopus laevis* oocytes expressing Panx2-674 were incubated with ATP at different concentrations, TEVC measurements were performed and the resting membrane potential was calculated before and after application of substances.

Therefore, the Panx1 channel modulator ATP (Dubyak 2009) was used as a potential inhibitor of Panx2-674 mediated currents in TEVC measurements. Figure 5.11 demonstrates that the application of ATP to oocytes expressing Panx2-674 at a concentrations of 0,2 or 2μM did not induce an inhibition of Panx2 mediated currents in response to depolarization. Application of 20 μM ATP slightly decreased current

amplitudes in comparison to control measurements before ATP application (81,7% vs 100,7% remaining current on average) with a significance of $P < 0,5$ while the application of ATP in a concentration of 40 μM does not lead to a significant decrease. The application of ATP did also not cause a shift in the cells membrane resting potential at all concentrations tested (Fig. 5.12). Because a mean reduction of 20% of the maximum current recorded in TEVC measurements at 20 μM , but not at 40 μM , is not sufficient to convincingly regard ATP as an inhibitor of Panx2 mediated currents, the search for an appropriate Panx2 channel blocker must be continued in the future.

5.3 Chimeras

5.3.1 Comparison of Panx1 and Panx2 protein structure

When comparing the protein structure of Panx1 and Panx2, alignment studies calculate a sequence homology of about 16% only. However, taking into account the different length of specific domains, obvious similarities remain. Both proteins have an intracellular aminoterminal domain of similar size, and both the extracellular and the intracellular loops as well as the four transmembrane domains are also comparable in length. The most striking difference is found in the size of the C-terminus. While Panx1 consists of 130 intracellular amino acids downstream TM4, the Panx2 proteins C-terminal tail consists of 358 aa, which is nearly three times the length of the respective Panx1 domain.

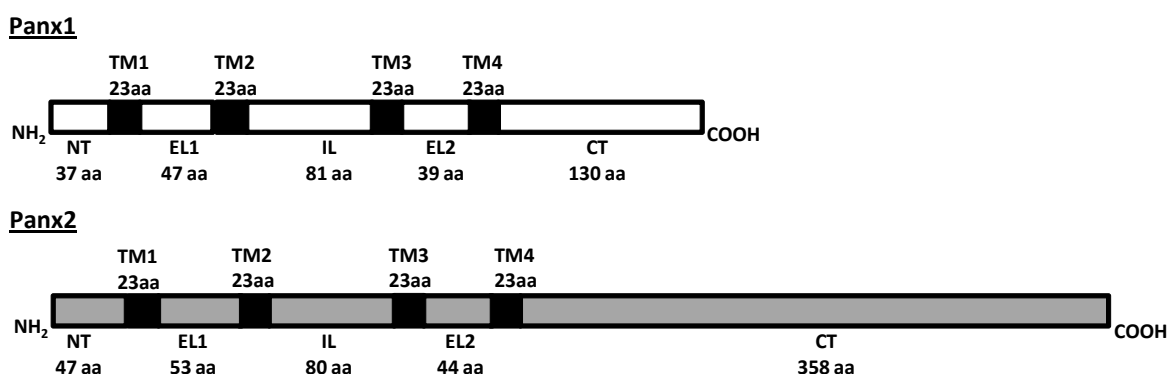


Figure 5.13: Comparison of the Panx1 and Panx2 protein length. Definition of domain borders for Panx1 and Panx2 corresponding to *ensembl* data. Linear representation of the protein domains are drawn to scale, the lengths reflect actual amino acid numbers. The transmembrane domains (TM), the extra- and intracellular loops (EL, IL) as well as the amino- and carboxyterminal domains (NT, CT) are indicated.

5.3.2. Construction of the Panx1-Panx2 chimeras

The protein sequences of Panx1 and Panx2-674 do not give any hint about the domains necessary for an efficient channel function. Which parts of the proteins are necessary for gating of the channel?

Therefore, a further aim of this thesis was to investigate, if an exchange of the C-termini of Panx1 and Panx2 in total or in parts would result in gain or loss of channel function, further attempt on the importance of length of the C-terminus was intended.

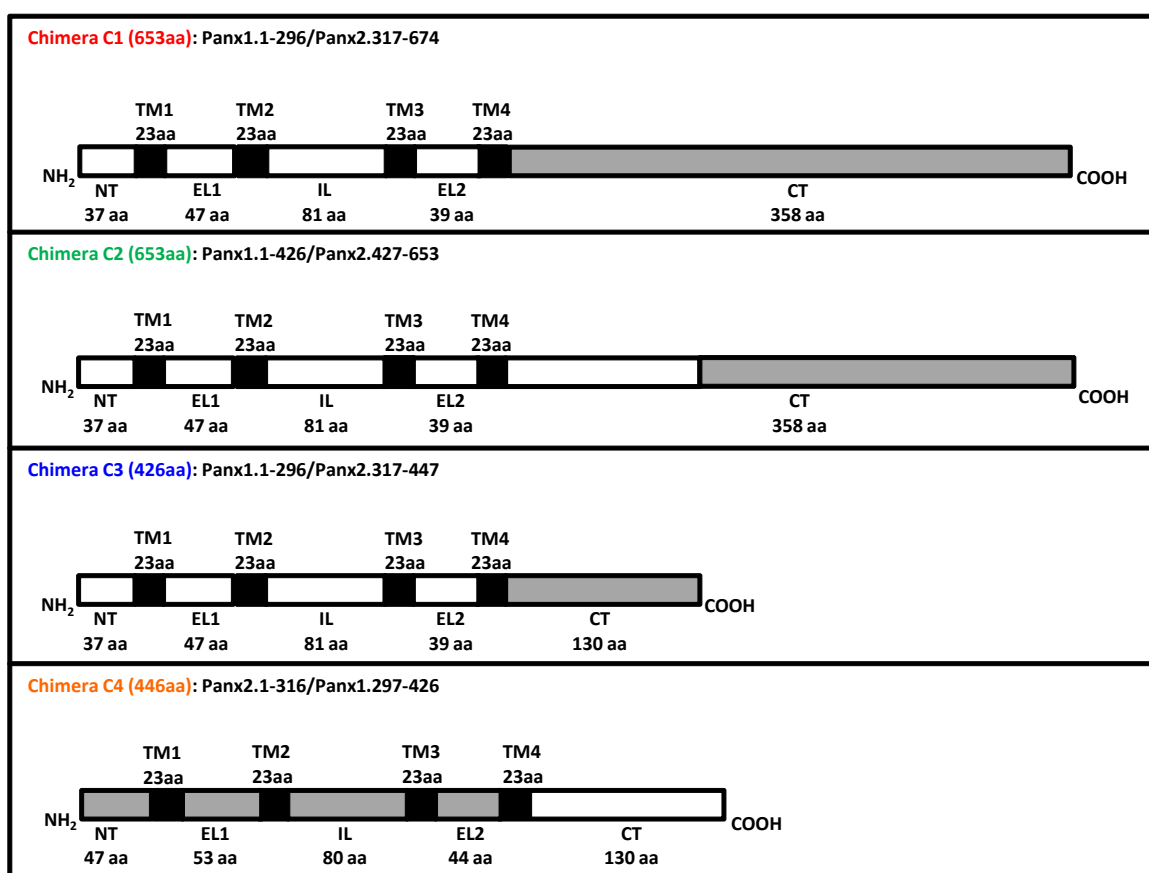


Figure 5.14: Design of the Panx1/Panx2 chimeras. Illustration of the chimeric proteins built from Panx1 and Panx2. Chimeras C1 and C2 (upper lanes) both start with Panx1 and are of the same size. In C1 the C-terminus of Panx1 is exchanged against the C-terminus of Panx2, while in C2 the Panx1 protein is prolonged by a part of Panx2. Chimera C3 (third lane) consists of Panx1 from N-terminus to TM4 and is prolonged by Panx2 to its original length of 426 aa. In Chimera C4 (bottom lane) the Panx2 C-terminal domain is exchanged against the respective Panx1 domain. For other conventions see Fig. 5.13

For this purpose, C-terminal domains were swapped via overlap extension PCR right behind the proteins' fourth transmembrane domains or further downstream. One experimental approach was to investigate the function of the C-terminal domain after a

complete exchange by using electrophysiological methods. For this purpose Chimeras C1(see Fig. 14, indicated in red) and C4 (yellow) were designed: C1 starts with Panx1 aa1- aa296 and is prolonged by the Panx2 C-terminus, which equals aa317- aa674. The resulting size of C1 was 653aa. The design of the 446 aa long chimeric protein C4 was inverted, the proteins starts with Panx2 aa1- aa316 which is extended by Panx1 aa297- aa426, resulting in a total length of 446aa. To answer the question whether Panx2 channel function depends on the specific length of the C-terminus or whether it depends on the amino acid sequence, chimera C2 (green) was designed. This protein has the same size as C1, but contains the full length Panx1 protein. It is extended with Panx2 aa427-aa653. To have a closer look on the influence of the size of the C-terminus, the Panx2 C-terminal domain was exchanged against the Panx1 respective domain and shortened to its length of 130 aa in chimera C3 (blue).

5.3.3 Expression of the chimeras in N2A cells and *Xenopus laevis* oocytes

To ensure that the chimeras are fully processed in common heterologous expression systems, evidence for expression had to be provided for all constructs. Therefore, oocytes that were injected with cDNA encoding chimeric proteins followed by cryosectioning and immunohistological staining.

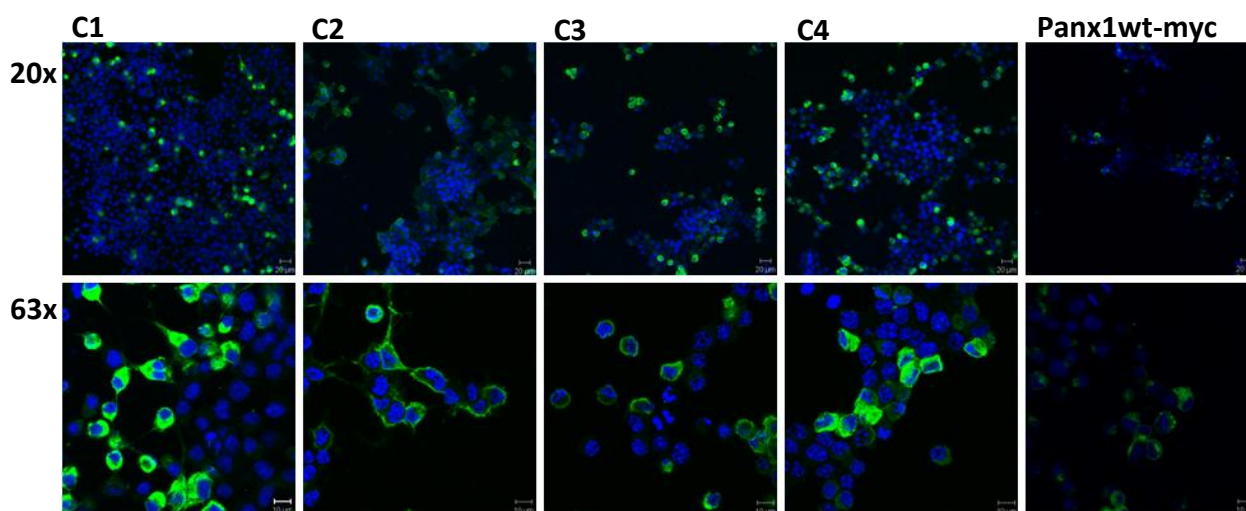


Figure 5.15: Expression analyses of Panx1/Panx2 chimeras in N2A cells. Cells were transfected with pSC-C1, pSC-C2, pSC-C3, pSC-C4 or pRK5rPanx1 and stained against c-myc 48h post transfection. Images were taken with a confocal microscope. The nuclei were stained with Hoechst 33342, the derived signal is shown in blue. Bars represent 20 μ m in the upper, 10 μ m in the lower panel.

Furthermore, all chimeras were cloned into plasmid vectors providing c-myc-tags and transfected into N2A cells, to confirm their expression in a mammalian system and to analyze protein trafficking and membrane internalization via immunocytochemical staining. Expression could be confirmed for all chimeric proteins, providing an important prerequisite for electrophysiological measurements. The expression rate is comparable to cell culture standards (Fig. 5.15 upper panel). High magnification images revealed an expression of all chimeras in the cell membrane, while C1, C3 and C4 show a cytosolic/ intracellular localization as well. From the immunostaining experiments, it is not possible to decide whether the protein is located in intracellular compartments such as the ER or Golgi apparatus or if it is dissolved in the cytosol or accumulated in vesicles. In micrographs of cells expressing C1 and C2 a localization in cellular processes can be observed.

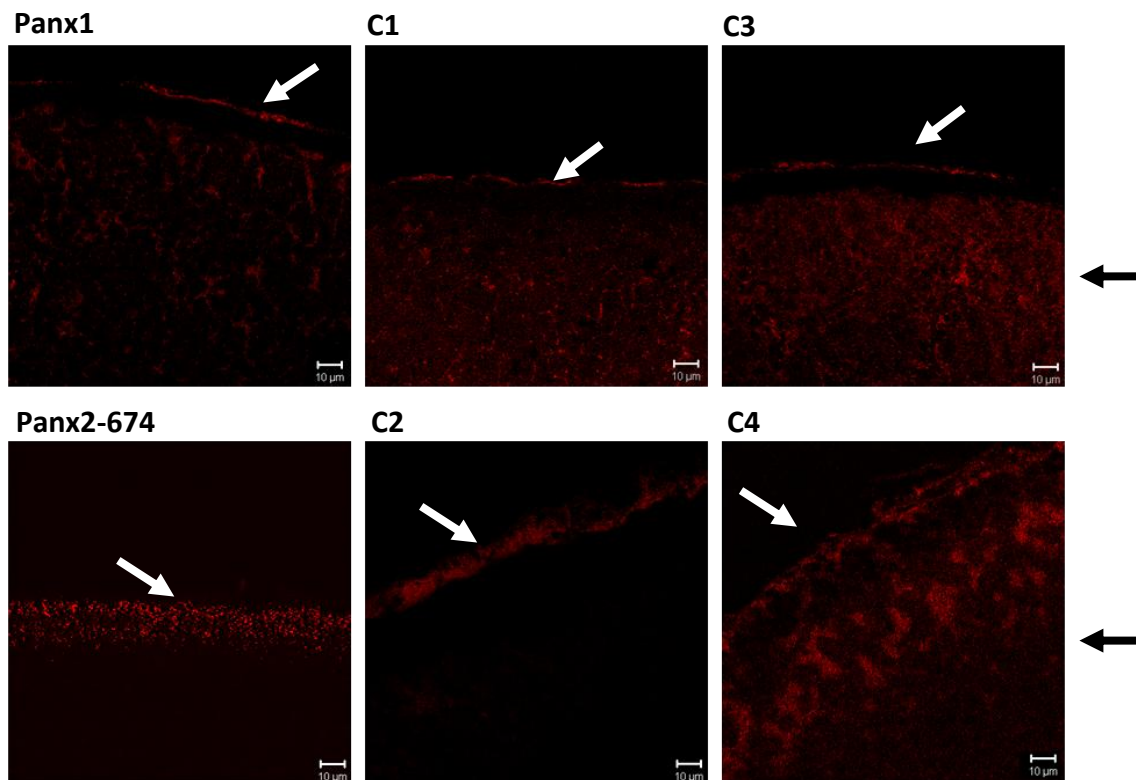


Figure 5.16: Expression analyses of Panx1/Panx2 chimeras in *Xenopus laevis* oocytes. cDNA injected oocytes were fixed with 2% paraformaldehyde and frozen. 12 µm thick cryostat sections were used for immunohistochemistry and confocal fluorescence microscopy. Due to protein domains containing antigen sequences that could be recognized by antibodies, α Panx1, α Panx2 or α -c-myc antibodies have been used. Bars as indicated, 10 µm. Note the staining of the cell membrane (white arrows), which can be separated from cytoplasmic staining (region indicated by black arrows).

5.3.4 The role of the C-terminus of Panx1 and Panx2 for channel gating

For an electrophysiological characterization all chimeric proteins were expressed in *Xenopus* oocytes. IV-curves were recorded under control conditions and in response to Cbx application. Panx1 wildtype and Panx2-674 (wildtype) were used as reference controls, for statistical analyses uninjected cells were used as negative control.

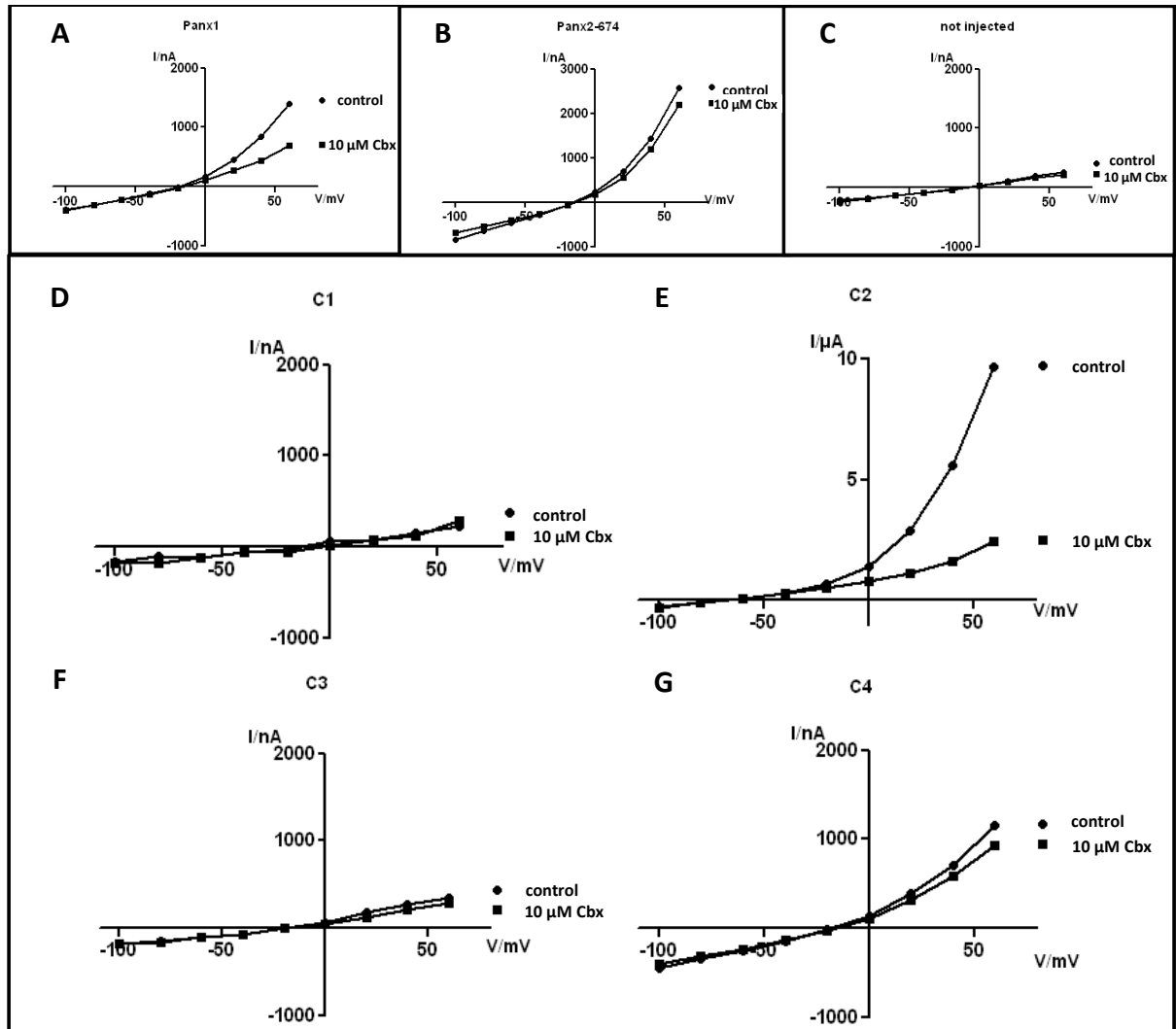


Figure 5.17: Representative IV-curves of Panx1/Panx2 chimeras 2 expressed in *Xenopus laevis* oocytes. Whole cell membrane currents from cDNA injected *Xenopus laevis* oocytes were recorded using the TEVC technique. Oocytes were clamped to -70 mV, voltage steps starting from -100 mV to +60 mV membrane potential were applied subsequently. IV-curves were calculated from corresponding current responses. ni = not injected. (A,B) Representative IV-curves from oocytes expressing either Panx1 or Panx2-674 under control conditions and in the presence of Cbx. Large outward currents can be achieved, but Cbx effects can be observed in A only. (C) IV-curve from a non injected oocyte as negative control (D-G) IV-curves from oocytes expressing one of four different chimeric proteins. Note the different scales.

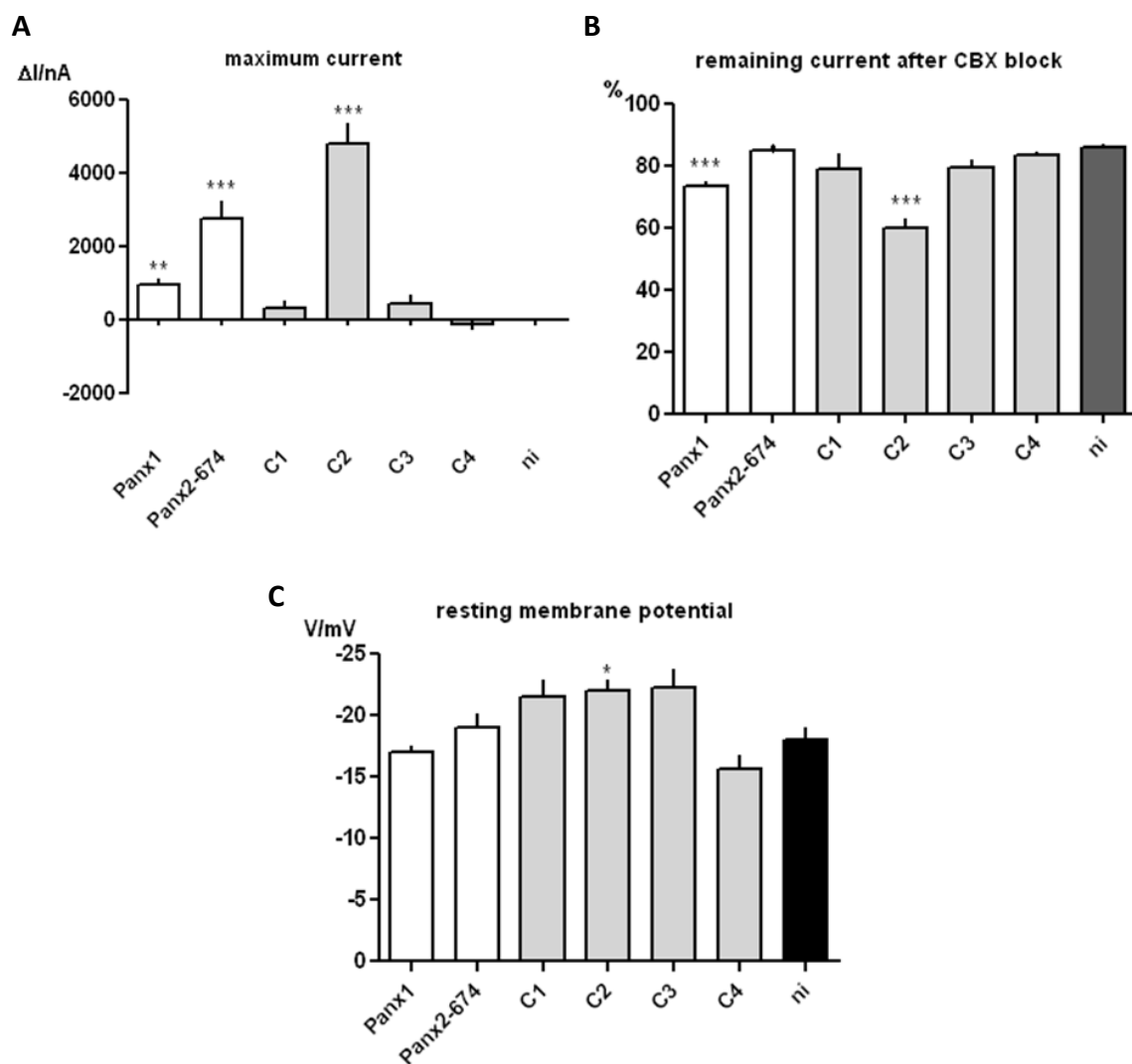


Figure 5.18: Electrophysiological characterization of chimeras of Panx1 and Panx2 expressed in *Xenopus laevis* oocytes. (H) Quantitative analysis of the maximum current measured at a membrane potential of +60 mV, currents were normalized to negative controls (I) Quantitative analysis of the remaining current after inhibition of channel activity with Cbx (in % of control). (J) Quantitative analysis of the resting membrane potential. Panx1 n=232, Panx2-674 n=47, C1 n=45, C2 n=79, C3 n=76, C4 n=17, ni n=106. ***P<0.001 **P<0.01 *P<0.05, SEM, significance vs. ni

Oocytes expressing chimera C1 (Panx1.1-296/Panx2.317-674) did not show current responses significantly different from uninjected cells. Although the slope of the IV-curves is not perfectly linear (5.17 D), the maximum current amplitude is comparable to negative controls. Furthermore, expression of C1 does not induce Cbx sensitivity or alterations in resting membrane potential. The replacement of the Panx1 C-terminus with the Panx2 C-terminal domain leads to a complete loss of voltage dependent gating. Channels formed by chimera C2 (Panx1.1-426/Panx2.427-653) alter the current-voltage relationship of recorded oocytes dramatically. First, the exponential slope of the IV-curve reveal very large outward currents, the current amplitude increase is highly

significant compared to negative controls. The channel responds to Cbx, the cells' resting membrane potential is altered slightly, but again in a range of nonbiological relevance. The current amplitude is even higher than the amplitude evoked by Panx1 or Panx2. Thus, the extension of Panx1 by a part of Panx2 leads to a gain in channel function. Oocytes expressing chimera C3 (Panx1.1-296/Panx2.317-447) seem to have a phenotype comparable to uninjected cells. No significant difference of any of the parameters analyzed could be observed. The exchange of the Panx1 C-terminal domain by the respective Panx2 sequence reduced in length to the original Panx1 C-terminus size of 130 aa also leads to a complete loss of channel function.

Expression of chimera C4 (Panx2.1-316/Panx1.297-426) also does not cause a change of the IV-curve, maximum currents, Cbx sensitivity or the cells resting potential. This shows that the Panx1 C-terminal domain, which is necessary for Panx1 channel function, loses its functionality when transferred to Panx2.

5.4 Truncation of the Panx1 C-terminal domain

The investigation of the chimeric proteins leads to the conclusion, that the C-terminal domain of Panx1 is crucial for the formation of a functional channel. Therefore, it was obvious to have a closer look at the properties of this domain, which consists of aa 297-426. Truncation of a protein provides the possibility to get insight into the functionality of the impaired domain. The Panx1 protein's intracellular C-tail consists of 130 aa in length. A shortening of this domain was achieved to address the following questions: (i) How long is the region of the C-tail, which is crucial for the formation of a functional channel? Assuming that a loss of function is caused if truncation of the C-terminal domain passes a critical limit, channel function could disappear when a certain length is reached. (ii) How does C-terminus truncation influence channel gating? (iii) Is Cbx sensitivity impaired when the C-tail domain is truncated and do Cbx induced effects disappear when a certain length is reached by truncation?

Beyond that, recent studies revealed a crucial role for Panx1 in apoptotic processes (Chekeni et al. 2010). When a cell undergoes apoptosis, caspase 3 and caspase 7 are activated. These caspases induce cleavage of Panx1 at two positions: the first cleavage site is located in the intracellular loop. The second cleavage site is located in the C-terminal domain at amino acid position 378. The respective motif recognized by caspases 3/7 consists of the four amino acids DxxD and is conserved through evolution

in vertebrates as well as in invertebrates. Cleavage at this position leads to a constitutively open Panx1 channel, that releases ATP and UTP to activate immune responses. Furthermore, because this channel opening is irreversible, Panx1 contributes to cell death itself, apart from activating phagocytes. It was a major aim of this thesis to define the region where Panx1 truncation leads to a constitutively open channel. Regarding caspase cleavage and the function of Panx1 in apoptosis, a truncation of the protein can be considered an analogue to mimicking a cleavage by effector caspases.

5.4.1 Design of Panx1 truncated versions

Truncations were performed by use of specific PCR primers, which were designed to amplify products of the intended size.

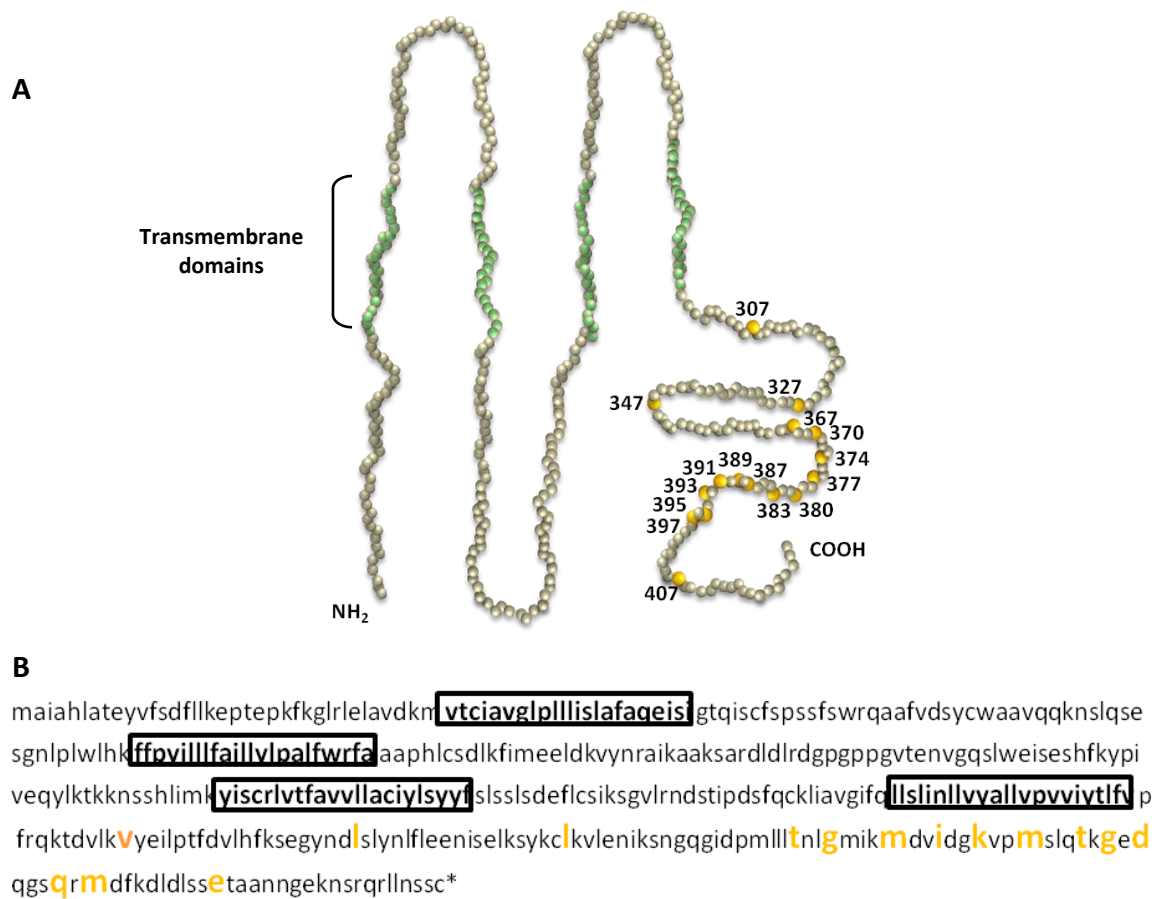


Figure 5.19: Position of the amino acids chosen for truncation of Panx1. (A) The graph depicts the topology of rPanx1. The amino acids forming the transmembrane domains are marked in green. The amino acids marking the truncation sites are depicted in yellow. (B) The amino acid sequence of rPanx1-wt. Amino acids providing transmembrane domains are encased, according to (A), the amino acids marking the end of a truncation construct are indicated in yellow.

The plasmid pCS2+ was used as vector backbone for all constructs to allow expression in mammalian cells as well as *in vitro* transcription for the generation of cRNA for injection into *Xenopus* oocytes.

rPax1 was shortened to the denoted lengths depicted in figure 5.19.

5.4.2 Electrophysiological characterization of truncated Pax1-forms in *Xenopus laevis* oocytes

After injection of cRNA, oocytes were incubated for ~60 hours to allow expression of the constructs investigated. During this time, oocytes expressing some of the truncated versions showed signs of severe cell degeneration. Therefore, it was not possible to electrophysiologically characterize these cells. Only oocytes expressing truncated forms of Pax1 which did not show signs of degeneration were chosen for TEVC recordings. The analysis of the maximum current evoked by expression of the different truncated versions differed significantly. Pax1-307 evoked average maximum currents of $5742,6 \pm 948,2$ nA which is significantly higher than those of uninjected cells or Pax1 mediated currents. Interestingly, the expression of the 20 aa longer protein Pax1-327 significantly reduces average maximum currents ($512,1 \pm 117,6$ nA). Pax1-347 and Pax1-367 evoked maximum currents comparable in size ($1513,6 \pm 938,4$ nA and $1342,6 \pm 340,7$ nA). Oocytes expressing Pax1-truncated versions larger than 367 aa and smaller than 397 aa could not be measured, because cells did not survive expression.

Surprisingly, while cells expressing Pax1-397 survive and evoke currents in a range of three times the magnitude of Pax1 evoked currents ($2652,9 \pm 886,9$ nA vs. $972,9 \pm 145,2$ nA), the addition of 10 aa to obtain Pax1-407 leads to even higher currents ($6878,6 \pm 522,1$ nA).

Regarding Cbx sensitivity, it turned out that three out of six truncated Pax1-forms tested were inhibited by Cbx. Inhibition of currents induced by Pax1-347, Pax1-397 and Pax1-407 was considerably stronger than Pax1 mediated currents (average reduction 46,2%, 68,2% and 52,7% vs. 28,8%, respectively).

Surprisingly, the intermediate form Pax1-367 did not respond to Cbx. Resting membrane potentials of oocytes expressing Pax1-307 and Pax1-367 were significantly more positive than those of uninjected cells ($-6,5 \pm 2,04$ mV and $-12,1 \pm$

0,83 mV vs. $-17,9 \pm 0,98$ mV), while Panx1 expression does not alter resting potential ($-16,9 \pm 0,6$ mV). Further, oocytes expressing Panx1-397 had membrane potentials significantly more negative than uninjected oocytes ($-24,3 \pm 1,19$ mV). All other constructs investigated did not affect the cells resting membrane potential.

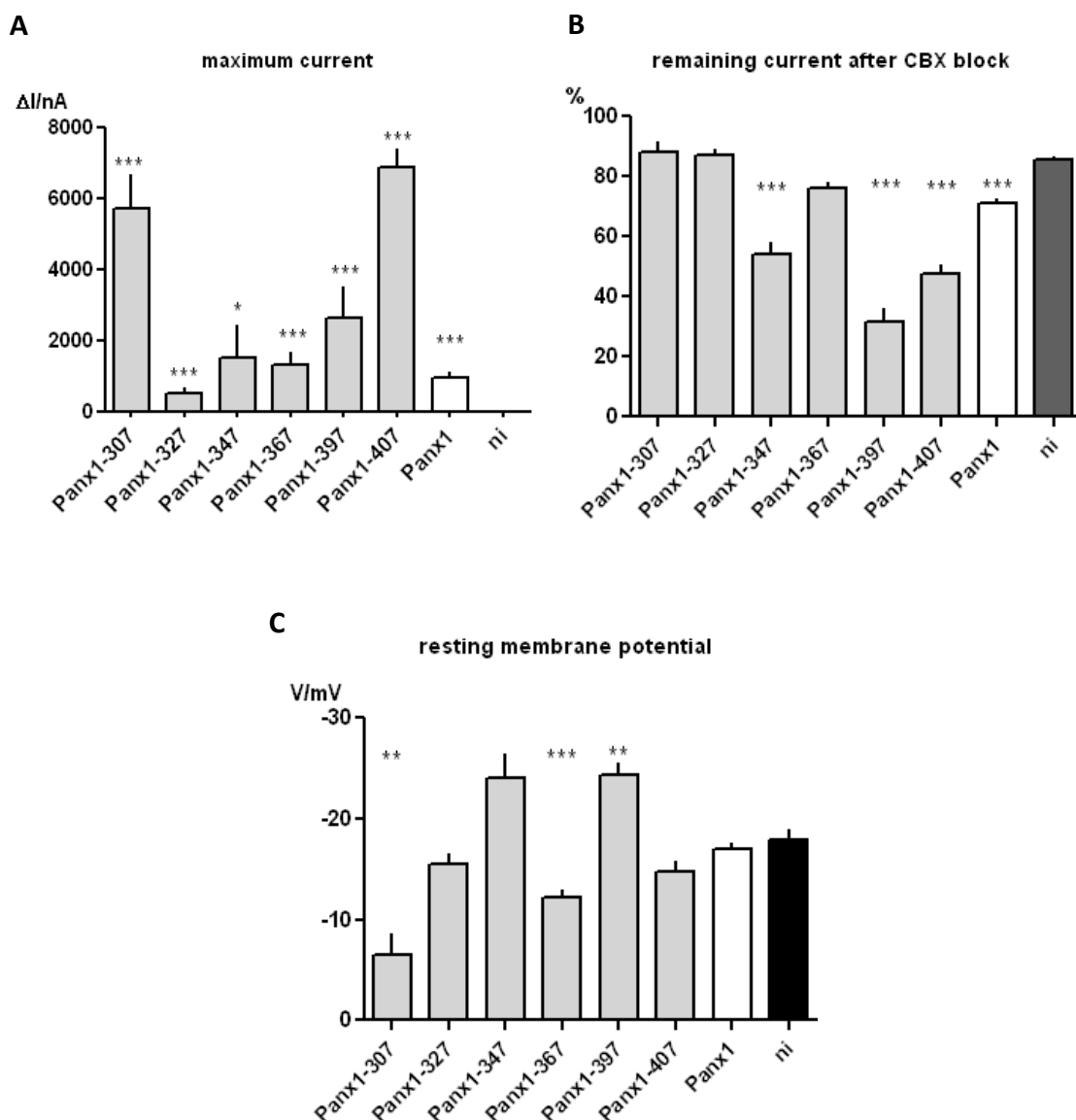


Figure 5.20: Comparison of the electrophysiological properties of truncated versions of Panx1 in *Xenopus laevis* oocytes. Whole cell membrane currents from cRNA injected *Xenopus laevis* oocytes were recorded using the TEVC technique. Oocytes were clamped to -70 mV, voltage steps starting from -100 mV to +60 mV membrane potential were applied subsequently. IV-curves were calculated from corresponding current responses. ni = not injected. (A) Quantitative analysis of the maximum current measured at a membrane potential of +60 mV, currents were normalized to negative controls. The maximum currents show a high variation in comparison to Panx1 expressing oocytes. (B) Quantitative analysis of the remaining current after inhibition of channel activity with Cbx (in % of control). Cbx sensitivity was observed in oocytes expressing Panx1-347, Panx1-397 and Panx1-407. (C) Quantitative analysis of the resting membrane potential, which is altered through expression of Panx1-307, Panx1-327 and Panx1-397. Panx1 n=232, Panx1-307 n=15, Panx1-327 n=41, Panx1-347 n=27, Panx1-367 n=43, Panx1-397 n=17, Panx1-407 n=37, ni n=106. ***P<0.001 **P<0.01 *P<0.05, SEM, significance vs. ni.

5.4.3 The role of Panx1 truncation for cellular survival in *Xenopus laevis* oocytes

The expression of truncated versions of Panx1 with sequences longer than 367 aa and shorter than 397 aa lead to oocytes, that either showed degeneration after incubation of 60 hours or were severely damaged by penetration with the recording electrode when trying to perform TEVC measurements, indicating an increase of fragility of the plasma membrane. In order to investigate the influence of a certain length of the Panx1 protein on cellular survival, truncated Panx1 forms with lengths spanning the range that was considered crucial for cellular survival were expressed in *Xenopus* oocytes. Oocyte viability was continuously monitored over a period of 96 hours after the injection of cRNA by visual inspection. The use of *Xenopus* oocytes has the advantage to allow inspections over a long time period due to their size and their general viability. Figure 5.21 shows oocytes expressing either the wildtype form of Panx1 or Panx1-387 as an example for protein-induced cell degeneration. Following an incubation period of 72 hours after cRNA injection, yolk is protruding from the ooplasm. This was regarded as a marker for cell death in the survival curves (Fig. 5.22). Furthermore, the rescue of cell degeneration by the presence of Cbx is illustrated.

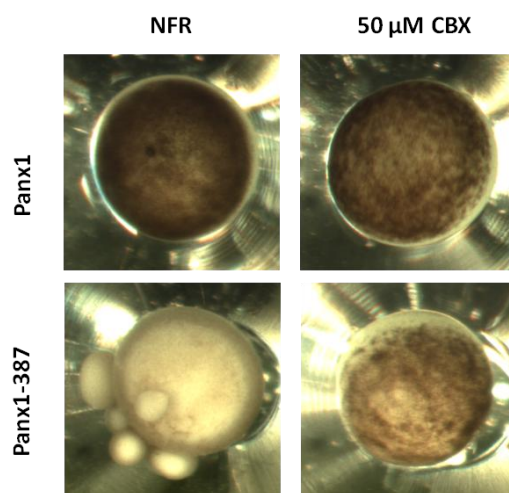


Figure 5.21: Morphological appearance of *Xenopus laevis* oocytes after expression of Panx1-truncated versions. Panx1 wt or Panx1-387 expressing oocytes, incubated either in Normal Frog Ringer (NFR, no treatment) or in NFR solution containing 50 μ M Cbx 72 h after injection. An oocyte was considered dead, when yolk was protruding from the ooplasm, as depicted in the lower left panel.

5. Results

To improve presentation, the survival curves of oocytes expressing Panx1 truncated versions inducing cell death of $\geq 25\%$ /96 hours are depicted in separate diagrams.

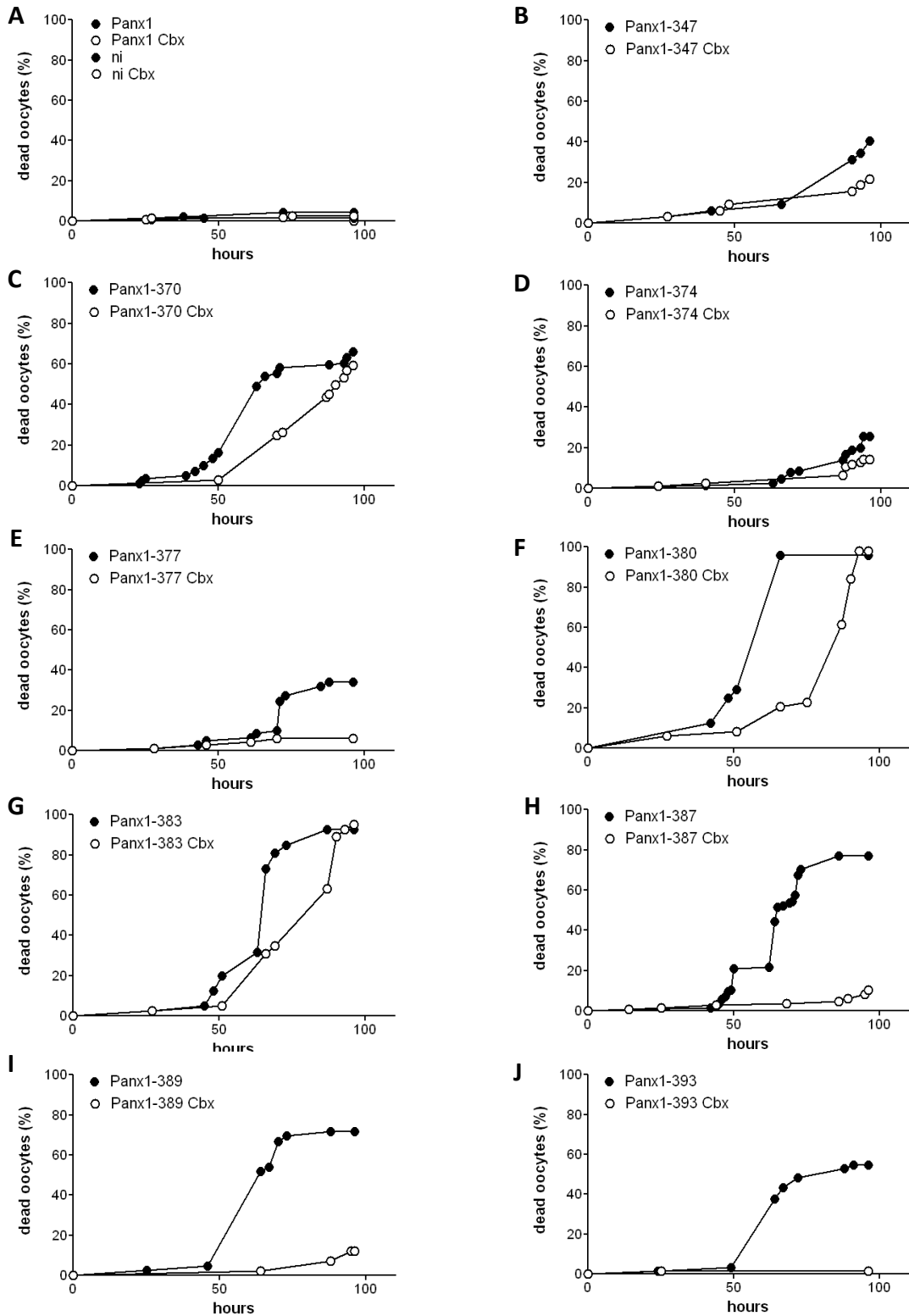


Figure 5.22: Induction of cell death by expression of truncated versions of Panx1. The oocytes were examined microscopically at four time points/day, the viability was determined according to morphological criteria. An oocyte was considered dead when yolk was protruding from the ooplasm. All oocytes were incubated in NFR and in NFR containing 50 μ M Cbx. (A) Panx1 injected and uninjected oocytes were used as controls.

The survival curves (Fig. 5.22 A-J) reveal specific differences regarding viability and Cbx sensitivity. Generally, cell degeneration starts to occur at about 48 h after injection, but only some constructs lead to rapid and substantial degeneration.

After 48h, degeneration started to progress differently for different constructs. In most oocytes, the breakdown of cellular homeostasis was decelerated by incubation with 50 μ M Cbx. However, degeneration could not be affected for some of the constructs. In conjunction with the results from the electrophysiological recordings, these findings indicate that Panx1-307, Panx1-327, Panx1-367, Panx1-370, Panx1-380 and Panx1-383 appeared Cbx insensitive (Fig. 5.22 and 5.23).

Data for oocyte survival when expressing truncated Panx1 channels are given in Table 5.2. Surprisingly, the amount of degenerated oocytes did not directly correlate with the length of the C-terminus.

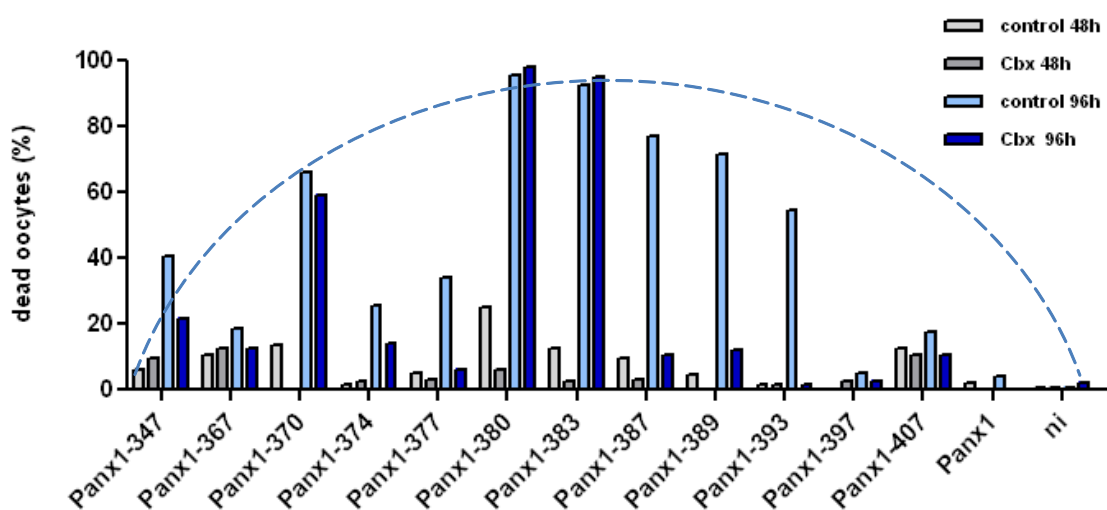


Figure 5.23: Induction of cell death in *Xenopus laevis* oocytes by expression of Panx1-truncated versions. Cell death of oocytes expressing truncated forms of Panx1 after 48 hours (grey) and 96 hours (blue). Panx1-347 n=67, Panx1-367 n=54, Panx1-370 n=111, Panx1-374 n=127, Panx1-377 n=145, Panx1-380 n=74, Panx1-383 n=67, Panx1-387 n=266, Panx1-389 n=86, Panx1-393 n=88, Panx1-397 n=131, Panx1-407 n=68, Panx1 n=96, ni n=270, results obtained in $n \geq 2$ independent experiments / construct.

For a demonstration of the influence of the position of the truncation, the mean percentage value obtained in the survival experiments ($n \geq 2$) is given in figure 5.23. Obviously, a symmetry in curve distribution is not given, indicating that there is no single peak in cell death increase. Starting with Panx1-347, successive elongation of the amino acid sequence does not impair oocyte viability at regular intervals up to a maximum of mortality followed by a stepwise reduction of cell death. Instead,

expression of Panx1-370 leads to 66,0% dead oocytes after 96h, which is one third more than in Panx1-347 expressing oocytes. Further elongation by only four amino acids reduces mortality in Panx1-374.

Table 5.2: List of constructs leading to breakdown of cellular homeostasis. Constructs leading to $\geq 25\%$ cell death are listed, sensitivity to Cbx inhibition is indicated in the last column.

Construct	% dead oocytes / 96h	Cbx sensitive
Panx1-347	40,6	+
Panx1-370	66,0	-
Panx1-374	25,6	+
Panx1-377	34,0	+
Panx1-380	95,8	-
Panx1-383	85,0	-
Panx1-387	77,2	+
Panx1-389	71,7	+
Panx1-393	54,5	+

Expression of Panx1-377, which marks the cleavage site for caspase 3 and 7, leads to an induction of cell death of 34,0 % only. The addition of three more amino acids leads to breakdown of homeostasis of nearly all cells (Panx1-380, 95,8% dead oocytes). Residue 380 seems to represent a critical point, since further addition of amino acids leads to stepwise decrease in mortality (85,0% to 54,5% in oocytes expressing Panx1-383 to Panx1-393 and intermediate forms). A total rescue of the lethal effect on *Xenopus* oocytes is provided at expression of Panx1-397.

5.4.4 The role of Panx1 truncation for cellular survival in N2A cells

From a comparative point of view, it is of interest to study the effect of Panx1 truncation also in a mammalian cell system. The differences observed by expression of the shorter Panx1 versions in oocytes provide an important insight into the function of domains of Panx1. Anyway, *Xenopus* oocytes are large and robust cells, that allow studying harmful proteins over a time period which is not comparable with the behavior

of mammalian cell systems. Therefore is of interest, if the expression of the truncated Panx1 forms evokes a comparable gradual effect regarding cellular survival in N2A cells.

For this reason, N2A cells were cotransfected with constructs encoding the truncated Panx1 versions and pEGFP, with Panx1 and pEGFP as positive control and pEGFP as negative control to adjust background. 24h post transfection, cells were collected and suspended in PBS.

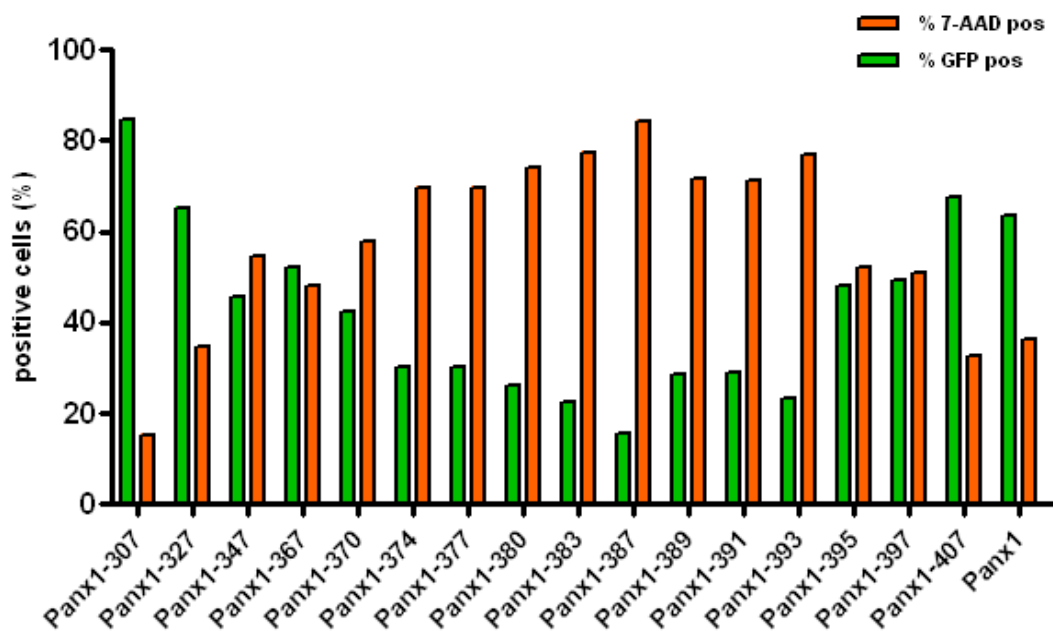


Figure 5.24: Induction of cell death in N2A cells by expression of Panx1-truncated versions. The percentage of cells sorted by FACS flow cytometry positive for either 7-Aminoactinomycin (7-AAD) or GFP are depicted. Cells positive for 7-AAD are considered dead, while cell populations positive for GFP are still alive. 10.000 cells counted / transfection, results obtained in two independent experiments.

Then, the fluorescent dye 7-Aminoactinomycin (7-AAD) was added to the cell suspension to stain dead cells, and afterwards cells were analyzed in the FACS flow cytometer. The measurement of GFP and 7-AAD is reciprocal, which provides an internal control for experimental conditions. The FACS analysis revealed a phasic behavior starting with a maximum of survival at Panx1-307 and a nadir at Panx1-387. Elongation from position Panx1-387 on provides a continuous rescue effect which at position Panx1-407 is identical with the wildtype Panx1 survival rate. Insofar the analyses of survival exploiting N2A cells is in total agreement with the data obtained in the oocyte expression system.

6. Discussion

6.1 Panx1 and Panx2 do not form functional heteromeric channels

When pannexins were first described by Panchin and colleagues (Panchin et al. 2000), Panx1 and Panx2 were assumed to form functional heteromeric channels. In the first study that experimentally addressed this issue, both proteins were expressed in *Xenopus* oocytes (Bruzzone et al. 2003), which resulted in a difference in current response when compared with oocytes expressing Panx1 only. From these results, the authors postulated that both proteins form heteromeric hemichannels that reveal functional differences in comparison to Panx1 homomeric channels.

In the present thesis a possible reciprocal influence of Panx1 and Panx2 on each other's channel properties was re-investigated. To achieve this goal, the results obtained by Bruzzone et al. (2003) should be confirmed and extended. As a first step, the existence of heteromeric Panx1/Panx2 channels were intended to be verified. As method of choice, *Xenopus laevis* oocytes were used as expression system and the use of the Roobocyte® system provided high throughput standardized TEVC measurements. *Xenopus* oocytes were injected with cRNA encoding either Panx1, Panx2-664 or both cRNAs. For these experiments, Panx2-664 was chosen to allow a comparison with results from the original publication by Bruzzone's group. Both cRNAs were injected in three different ratios to possibly affect the composition of the hexameric pannexon. A 3:1 ratio of Panx1 and Panx2 should represent the properties of channels formed mainly by Panx1 and less Panx2 or formed by Panx1 only. In case of injecting two cRNAs in an unequal ratio, the formation of homomeric channels cannot be excluded, nevertheless the existence of both types of pannexons, homomeric as well as heteromeric, in the oocyte is most likely.

The expression of both proteins in similar quantities should be achieved by injection of both cRNAs in an equal ratio, and the injection of a ratio 1:3, which is in favor of Panx2 expression, should allow recordings from oocytes expressing channels formed by Panx2 mainly or exclusively.

As a first result, it was successfully demonstrated that Panx1 expression in *Xenopus* oocytes leads to the formation of functional channels which are voltage gated and sensitive to inhibition by the gap junction blocker Cbx. In contrast, oocytes expressing

Panx2-664 did not show currents in response to depolarization; Panx2-664 does not form functional voltage gated channels. These findings are in line with results published previously, providing a stable control condition for the analysis of the recordings of heteromeric channels (Bruzzone et al. 2003; 2005).

Based on the working hypothesis that, depending on the ratio of RNAs injected, Panx1/Panx2 heteromeric channels could be forced to build hexamers consisting of varying amounts of Panx1 vs. Panx2, a decrease in current response was expected with decreasing amounts of Panx1 in the heteromer. The analysis of the maximum current recorded from oocytes expressing both proteins revealed that the Panx1-mediated current response disappeared completely upon co-expression of Panx1 and Panx2 at any ratio tested. Cells that were dedicated to express heteromeric channels did not show currents different from uninjected oocytes which were recorded as negative controls. Current amplitudes were not found to represent a function of the expected relative amount of Panx1 expressed. This is confirmed by a recent study, where after coexpression of Panx1 and, in this case, Panx2-674, current responses could not be evoked by depolarization, indicating an inhibitory effect of Panx2 on Panx1. It remains unclear, however, whether this inhibitory effect is caused by deficiencies in trafficking of Panx1/Panx2 channels or whether these channels are not functional, even when they are inserted into the cell membrane (Penuela et al. 2009).

It has been shown that Panx1 forms hexameric channels (Boassa et al. 2007), and Panx2 was reported to form octamers. This observation provides a likely explanation for the inability of Panx1 and Panx2 to form functional heteromeric channels, due to the differences in symmetry of the homomers (Ambrosi et al. 2010a). Furthermore, the authors purified Panx1/Panx2 heteromeric channels from overexpressing Sf9 cells. These cells were infected with baculovirus encoding Panx1 tagged with hexahistidine (6His) and untagged Panx2 protein, and protein complexes were purified over affinity columns binding the 6His-tagged Panx1. This approach allowed to isolate Panx1/Panx2 heteromeric channels. Interestingly, the authors could demonstrate that Panx1/Panx2 heteromers are very unstable and disaggregate after a few hours (Ambrosi et al. 2010a;b).

The described finding is of special interest, because the half-life of connexins can be very short, similarly to gap junctions which have been shown to have a half-life of ~2 hours only (Laird 2006; Crow et al. 1990). In contrast, Panx1 channels could be

followed up for ~15-18 hours before lysosomal degradation occurred (Boassa et al. 2007).

TEVC measurements performed during this thesis work provide no clue for the existence of functional heteromeric channels consisting of Panx1 and Panx2. Together with the published findings, these observations suggest that Panx1/Panx2 channels are non-functional when formed and are degraded very fast. This makes electrophysiological recordings in *Xenopus* oocytes impossible, when an incubation time of about 60 hours for stable protein expression is maintained.

Therefore, heteromeric channel formation between Panx1 and Panx2 can be considered to happen accidentally. A functional relevance for heteromeric Panx1/Panx2 channels in naturally existing biological systems can be excluded.

6.2 Panx2-674 forms functional, voltage gated channels

Panx2 is an integral membrane protein (Panchin, 2000, Dahl & Locovei 2006). This means that during or after synthesis, the protein has to be packed in a correct way, and trafficked to its target compartment. For this purpose, proteins in general contain target sequences that provide protein sorting and shuttling. It is well known that signal sequences for membrane transport are often localized in the amino terminus (Blobel et al. 1984). The genomic DNA encoding the Panx2 protein is located on chromosome 7 in the rat genome, the coding region is built by four exons. At mRNA level it is hard to distinguish between two possible start codons which could be used as a start site for gene expression, because both are localized on exon 2 and sequences that would hint on a particular start codon used for gene expression are not obvious. A Kozak sequence could not be found upstream the prospective start codons. To allow an experimental discrimination between the two ATG chosen for gene expression, they would have to be located on different exons. In that case, it would be possible to distinguish whether two different or only one isoform were expressed by use of alternative start codons on different exons. The fact that both prospective start codons are localized on the same exon makes discrimination via PCR-techniques, as demonstrated before, impossible (Buettner et al. 2000).

In this context, the strategy chosen in this thesis to determine the native form of Panx2 was a comparison of localization and function of both proteins, e.g. Panx2-664 and

Panx2-674. It was therefore intended to uncover if the elongation of Panx2-664, the Panx2 form formerly used in the literature, by ten amino acids to achieve the Panx2-674 form, leads to differences in localization and function.

In a first attempt, both proteins were expressed in N2A cells, and immunostained afterwards to allow an analysis via confocal microscopy.

In this experiment, differences in the expression pattern could be demonstrated successfully. Panx2-674 is localized in the plasma membrane. A cytosolic localization could not be detected. N2A cells expressing Panx2-664 showed a clear intracellular staining, with retain in intracellular compartments such as the endoplasmatic reticulum and Golgi. Shuttling to the plasma membrane is hardly visible under light microscopical conditions.

This result provides first evidence, that the N-terminus of Panx2-674 exhibits a signal sequence crucial for a targeting to the cell membrane, which is probably missing in Panx2-664.

To further investigate the localization of Panx2 in the cell membrane, FRIL experiments were performed. In the protocol commonly used to obtain FRIL specimen, cells are frozen quickly, fractured and shadowed with platinum/carbon layers to generate a replica. After this step, digestion of the sample from the replica is provided by addition of SDS detergent solution. For the staining of Panx2-664 and Panx2-674, this digestion was performed incompletely, resulting in a replica bound to one lipid monolayer, that still contains proteins accessible for antibodies.

N2A cells were transfected with plasmids encoding either Panx2-664 or Panx2-674 and subjected to FRIL. Electron microscopy of the cell's outer membrane allowed counting of gold particles / area. Thus, the rate of expression of Panx2-674 could be compared to the expression rate of Panx2-664.

Surprisingly, the quantification obtained by analysis of the EM pictures revealed a comparable density of protein internalized into the plasma membrane for both proteins, unless a tendency towards a higher Panx2-674 density was observed. As stated above, after analysis of the confocal images, it was assumed that the localization of Panx2-664 in the membrane would be significantly lower than for the longer Panx2-674 protein.

Taken together, the confocal imaging revealed that Panx2-674 was localized mainly inside the plasma membrane and less in the cytosol, while Panx2-664 was

predominantly localized in the cytoplasm or in intracellular compartments (which cannot be distinguished).

The quantitative analysis of the FRIL data revealed a surface localization for both proteins. It is an important finding to note, that both proteins seem to be targeted to the cell membrane to the same extent.

This means: (i) the N-terminus of Panx2-674 is not needed for internalization into the plasma membrane (ii) the difference in the N-terminus of the Panx2 forms does not influence the extent of internalization. Although confocal imaging revealed that a large part of Panx2-664 is retained intracellularly, still, the amount of particles in the membrane remains comparable to Panx2-674 expressing cells.

It may be speculated, that due to overexpression of the proteins a maximum of protein internalized into the cell surface is achieved. Given that the N-terminus does not influence the process of internalization into the plasma membrane, both proteins can be detected at the cell surface to the same extent. However, the fact that Panx2-664 is partly retained inside the cell while Panx2-674 is not, leads to the conclusion that (iii) the ten additional amino acids in the N-terminus of Panx2-674 leads to a more efficient protein shuttling and membrane targeting. This may also explain why Panx2-664 is localized intracellularly as well as on the cell surface. Possibly, a shuttling pathway from the ER via the Golgi apparatus to the membrane may be impaired in the short form. In Panx1, shuttling to the plasma membrane is mediated by glycosylation of the protein, as shown by Boassa et al., who postulated that N-glycosylation of Panx1 at residue 254 is necessary for membrane targeting, a finding validated by site directed mutagenesis studies (Boassa et al. 2007). In any case, the results of the present thesis identify the N-terminus of Panx2-674 as a crucial region for membrane targeting. It is of further interest, if glycosylation deficient mutants of Panx2-674 would also alter the spatial expression pattern.

A localization of Panx2-674 in the plasma membrane has not always been confirmed in the literature. Panx2-674 localization seems to be dependent on the cell type used for analysis. After expression in HEK 293T or NRK cells, Panx2-674 was localized in intracellular compartments, showing only little cell surface localization (Penuela et al. 2009). In contrast, transfection of HeLa cells resulted in a clear membranous staining in confocal imaging (Zappalà et al. 2007).

6.2.1. Electrophysiology of Panx2

Here, it is shown that Panx2-674 is capable of forming functional channels which open to a standard depolarization protocol, a phenomenon not observed so far (Ambrosi 2010a). Starting from a holding potential of -70 mV, voltage steps were applied from -100 mV to +60 mV in 20 mV increments and currents were recorded from *Xenopus* oocytes using the Roboocyte® system. The applied protocol is commonly used in electrophysiology and was sufficient to evoke Panx2-674 mediated currents. For a proper analysis of the currents, it was important to include a mathematical correction of the current amplitude with respect to a negative control in order to allow the background current of the oocytes to be evaluated. Therefore, it was important to also record from uninjected oocytes on every experimental day. The uninjected oocytes represent the background conductivity and a reference or background current can be calculated and subtracted from the currents recorded from oocytes expressing Panx2-674 (or every other protein of interest, respectively). This method allows to analyze the contribution of Panx2-674 to the total current response.

In general, when channel proteins are analyzed IV-relationships before and after application of an activating agonist are recorded. This allows to calculate and subtract the background conductivity individually for every single oocyte (Cavara et al. 2010). This method cannot be used for analysis of currents obtained from oocytes expressing pannexins, because specific agonists are not available. Furthermore, because channel gating by voltage is rather slow for pannexins, it is not possible to induce an on-off effect that allows separating an intrinsic background current from the current evoked by the pannexins. Therefore, currents were recorded from uninjected oocytes as a reference negative control and average background currents were calculated from these results.

During this thesis, Panx2-664 and Panx2-674 were compared. As revealed from TEVC recordings, only Panx2-674 formed functional voltage gated channels. Together with the results from the FRIL experiments it is likely that Panx2-664 can be considered not to be the native Panx2 protein, a conclusion consistent with recent findings (Ambrosi et al. 2010a). Membrane targeting of Panx2-664 seems impaired, but not disabled completely. The protein is incorporated into the plasma membrane, but seems not to form functional voltage gated channels. On the contrary, voltage gated channels are formed by Panx2-674, implicating that the N-terminus of Panx2-674 may have a

functional role in pore formation and/ or gating. The maximum currents mediated by Panx2-674 channels exceed the Panx1 evoked currents by a factor of three ($2780,4 \pm 468,5$ nA vs. $972,9 \pm 145,2$ nA on average). This finding provides a completely new insight into the importance of Panx2-channels in cellular conductance and excitability of the nervous system, given the expression of Panx2 in the CNS. Up to now, Panx2 was considered to mainly have accessory functions in Panx1 trafficking. Recent findings, however, demonstrated that Panx2 forms a channel with a pore diameter of ~ 30 Å, while the pore diameter of Panx1 is 19 Å (Ambrosi et al. 2010a). Panx1 is capable of releasing molecules of up to 1 kDa in size, and it is obvious to assume that Panx2 may release even bigger molecules and/or similar sized molecules at a higher rate. The observation, that Panx2 is able of forming channels exhibiting large currents is of special importance regarding excitability and also exchange of molecules.

Interestingly, Panx2-674 is not sensitive to any of the substances tested as possible channel blockers. Cbx, CoCl_2 , LaCl_3 , Mefloquine, PEG 1500 and Octanol were analyzed for inhibitory effects on Panx2-674, and none of these commonly used gap junction or Panx1 channel blockers was able to induce a significant inhibition. A first impression of LaCl_3 or Mefloquine being possible candidates for blocking Panx2-674 could not be confirmed.

Considering the large impact of Panx1 in ATP-mediated ATP-release (Thompson et al. 2006, Dubyak 2009, Qiu & Dahl 2009) and the regulation of Panx1 by ATP in a negative feedback loop, ATP was also tested as a compound that might have been capable of blocking Panx2-674 activity. Panx1 is activated by high levels of extracellular ATP as, for example, found under ischemic conditions and inactivated by rather low levels of ATP accumulating at the outside of the channel pore. Thus, in experiments on inhibitory effects on Panx2-674, ATP was tested at different concentrations ($0,2\mu\text{M}$ to $40\mu\text{M}$). As for the compounds described earlier, only a small inhibitory effect could be observed. The application of $20\mu\text{M}$ ATP led to a slight decrease in Panx2-674 evoked current. This decrease, although significant, still demonstrates an inhibition of only 20% of the maximum current. Therefore, it is difficult to postulate that ATP can be used as an inhibitor of the Panx2-674 protein. The search for a substance capable of blocking Panx2-674 mediated currents remains a fascinating question that may be solved in future studies.

6.3 Transplantation of domains of Panx1 and Panx2 causes loss of function, whereas prolongation of Panx1 by a domain of Panx2 leads to gain of function

To understand the molecular mechanisms underlying voltage-dependent gating of Panx1 and Panx2 channels, the interaction of different protein domains in forming the pore is of special interest. Domain swapping is an appropriate method to address this issue, as demonstrated in various experiments regarding the functionality of protein domains (Stern-Bach et al. 1994, Strutz-Seebohm et al. 2003)

During this thesis, four chimeric proteins have been designed. Expression was verified for all chimeras in N2A cells as well as in *Xenopus* oocytes, reflecting an adequate translation of the proteins. Further, confocal microscopy confirmed that all chimeras were internalized into the cell membrane or were expressed at the surface of *Xenopus* oocytes, respectively. These findings indicate, that non-functionality of chimeric proteins is not caused by insufficient expression or trafficking. It is necessary to mention, that the creation of chimeric proteins always bears a risk of losing functionality by the technique itself, because it can never be excluded that the borders chosen for exchanging domains are the reason for loss of function.

Our observations indicate, that only one out of four chimeras was capable of building a functional channel. In the following, the results obtained by TEVC recordings from oocytes expressing chimeras are discussed one by one.

Chimera C1 (653aa): Panx1.1-296/Panx2.317-674.

This chimera consists of the Panx1 aa sequence from the N-terminus to the predicted fourth transmembrane domain. The intracellular C-terminal part is taken from Panx2.

This protein did not form functional channels, which could be activated by depolarization. Assuming that Panx1 and Panx2-674 are forming voltage gated channels, the results lead to the conclusion that (i) the N-terminal part of Panx1 (residues 1-296) does not build functional channels with the C-terminus of Panx2, and (ii) *vice versa*, the C-terminus of Panx2 (residues 317-674) is not sufficient to form functional channels without at least parts of the internal N-terminal sequence.

Chimera C2 (653aa): Panx1.1-426/Panx2.427-653.

The design of this chimera was based on the entire Panx1 protein extended by a carboxyterminal part of Panx2. For extension, residues 427-653 of Panx2 were chosen, because they refer to the sequence starting right behind the respective length of Panx1. Furthermore, the length of C2 is adapted to the length of C1 to allow a comparison of the influence of the length of the C-terminal part. TEVC recordings revealed the formation of a functional channel that mediates large currents and is sensitive to Cbx. On average currents recorded from *Xenopus* oocytes expressing chimera C2 were even ~1,7 times larger than Panx2-674 evoked currents. Different explanations can be assumed for this channel behavior.

(a) The pore size could be influenced leading to an increase in channel conductance. (b) The channel's opening probability could be altered. (c) Channel closing could be inhibited by steric interaction of the elongation of the Panx1 wildtype protein by a part of the C-terminus of Panx2. Although the experiments do not give any clue about the reasons for the enlarged current response, it is a remarkable result that the extension of Panx1 by a part of Panx2 leads to a gain in function. This also indicates that this part of Panx2 does not have an inhibitory effect on Panx1 channel function, referring to published data where an inhibitory effect of Panx2 on Panx1 channel function is postulated (Penuela et al.2009).

Comparing these findings with the results obtained from chimera C1, it is now confirmed that Panx1 residues 297-426 are necessary for Panx1 channel formation. Furthermore, the missing functionality of C1 is not a consequence of the extended length of the C-terminus, since the C-termini of C1 and C2 are of the same length.

Chimera C3 (426aa): Panx1.1-296/Panx2.317-447.

The third chimera investigated was designed similar to chimera C1, but in this case the C-terminus was truncated so that a protein with the respective size of Panx1 was generated. Expression of chimera C3 did not lead to the formation of functional channels. An important consequence of this result, together with the findings described earlier, is that Panx1 can only form channels with its own C-terminus. Furthermore, the non-functionality of C1 is not caused by the length of the protein or, alternatively, shortening of C1 to the length of Panx1 does not lead to a rescue in function.

Chimera C4 (446aa): Panx2.1-316/Panx2.297-426.

The fourth chimera was designed to start with Panx2 from the amino terminus to the fourth transmembrane domain and the intracellular C-terminus taken from Panx1. TEVC measurements revealed that this chimera does not lead to the formation of functional channels. Obviously, although Panx1 and Panx2 are both capable of forming functional homomeric pannexons, expression of a chimera consisting of the N-terminus of one protein and the C-terminal part of the other protein leads to a complete loss of function, as can be seen from the results obtained from chimeras C1 and C4. This means, that in both proteins a functionally important interaction of the C- and the N-terminal part must take place that cannot be mimicked by the respective part of the other protein.

6.4 Truncation of Panx1 leads to differential effects on channel properties

As an important consequence of the results achieved with the chimeric proteins, the residues 297-426 of Panx1 moved into focus. Obviously, the C-terminal domain of Panx1 was necessary for channel function, and the question arose, which parts were crucial for channel formation and which parts were responsible for gating, voltage dependence and Cbx sensitivity. Further, the truncation of Panx1 by caspases 3/7 is part of apoptotic processes and causes recruitment of phagocytes by release of “find-me” signals from the cell (Chekeni et al. 2010). It was a main goal of this thesis to map the region of the aa sequence, where Panx1 truncation leads to cell death. In this context, it has to be considered that upon truncation and expression in *Xenopus* oocytes or mammalian cell culture the artificially open Panx1 channels cause cell death *per se*. In both heterologous expression systems, the immunologic response is not present, which means that after expression of truncated Panx1 forms a possible cell death is always mediated by altered channel properties. This allows to explore the Panx1 contribution solely, unaffected by influences of other processes.

Within the scope of this thesis, 16 truncated versions of Panx1 have been generated. Two different expression systems were used to analyze the effect of these proteins on cell viability as well as electrophysiological channel properties.

Expression of some proteins led to cell death in mammalian cells as well as in *Xenopus* oocytes, while others could be expressed in oocytes without causing degradation and

were used for TEVC recordings. In the following, the influence of the length of Panx1 on cellular survival and on channel gating properties will be discussed.

6.4.1 Electrophysiology of truncated proteins not lethal after expression in oocytes

First, truncation of Panx1 resulted in specific effects on channel gating depending on the site of truncation. A stepwise reduction of the length of the C-terminus did not simply lead to a loss of function. Instead, the results are far more irregular: the expression of Panx1-307, the shortest form generated, led to very large Cbx-insensitive currents. This result is likely to expect, considering that nearly the entire C-terminus is missing. Taking the survival of oocytes expressing Panx1-307 into account, a constitutive, permanent opening of the pore can be excluded. Thus, it may be assumed that the C-terminus is involved in closure of the pore after voltage gated opening. Upon truncation at residue 307, a part of the sequence crucial for subsequent closing of the channel is missing. One further important conclusion can be drawn from the finding that Panx1-307 is voltage gated: the voltage sensor of Panx1 seems not to be located in the C-terminal domain, but rather in the N-terminal part and/or the extra- and intracellular loops, considering that Panx1-307 is truncated only ten residues behind the fourth transmembrane domain.

Interestingly, currents recorded from oocytes expressing Panx1-327, -347 and -367 did not show large differences to currents recorded from oocytes expressing the full length Panx1 protein. This leads to the conclusion, that residues 308-327 are necessary and sufficient for proper channel gating. The addition of 20 to 40 residues does not inhibit this function.

In contrast, expression of Panx1-370 leads to significant cell death (66% dead oocytes on average). In this protein, only 3 aa more than in Panx1-367 are expressed and, obviously, the addition of residues 368-370 is sufficient to induce a conformational change causing a complete loss of channel regulation and breakdown of cellular homeostasis.

Next, stable current responses were obtained from oocytes expressing Panx1-397, while oocytes expressing Panx1 truncated forms between aa 367 and aa 397 did not survive and could not be used for electrophysiological measurements.

Oocytes expressing Panx1-397 exhibit large voltage gated current responses to depolarizing voltage steps of ~two times the magnitude of Panx1 mediated currents. It may be speculated that Panx1-397 is capable of forming a functional channel that can be gated and does not lead to cell death. The expression of Panx1-393 led to cell death of almost 54,5 % injected oocytes on average. This means that residues 394-397 are sufficient for a rescue of oocyte survival, the channel can be closed again, although complete channel function is not restored.

Surprisingly, oocytes expressing Panx1-407 show a very high current response with an average magnitude of nearly 7 μ A. It would have been reasonable to expect that an addition of further amino acids would cause stabilization of channel function and result in channel properties more similar to the full length Panx1 protein.

The difference of 10 residues between Panx1-397 and Panx1-407 leads to formation of a channel that does not cause cell death, but a conformational change must be induced that prevents proper channel gating.

6.4.2 Mortality induced by truncation of Panx1

The expression of truncated versions of Panx1 with lengths ranging from 370-393 aa show lethal effects upon expression in *Xenopus* oocytes as well as in N2A cells. In N2A cells, all 16 truncated versions of Panx1 were expressed and viability was investigated 24 hours post transfection. The FACS analysis revealed that, starting with Panx1-307, mortality increases with increasing prolongation und reaches a peak in cells expressing Panx1-387. Further prolongation of Panx1-constructs results in a steady decline of mortality until full length protein is reached. Interestingly, even expression of the wildtype Panx1 protein leads to a population of dead cells. One possible reason for this could be the procedure of collecting cells in preparing the samples for the FACS analysis, possibly Panx1 reacts to this mechanical stress. Further, impairment of the healthiness of cultured cells i.e. by transfection procedure, may lead to apoptosis in a small cell population, which results in Panx1 channel opening.

Regarding the truncated versions, it is remarkable that in N2A cells the length of Panx1 truncation is reflected in an almost symmetric distribution. This is given by the analysis of 7-AAD fluorescence which marks dead cells and which is reciprocal to the curve obtained from GFP fluorescence marking living cells. It is intriguing to note that Panx1-

377, the protein with the length that mimics a caspase cleaved channel, is not the most lethal protein. Instead, expression of Panx1-380, Panx1-383, Panx1-387 and Panx1-393 results in a slightly higher mortality, even though the differences are small (less than 15% dead cells).

The expression of truncated Panx1 proteins in *Xenopus* oocytes allows a more differentiated and more detailed analysis of the lethal effect induced by some forms. Figure 5.23 demonstrates, that after expression in oocytes, the distribution of oocyte degeneration is not revealing a symmetric curve progression anymore. Instead, Panx1-367, Panx1-374 and Panx1-377 show lower impairment of oocyte survival than would be expected from a symmetric distribution and from the results obtained in N2A cells. Expression of Panx1-367 leads to 18,7 % dead oocytes after 96h, which is quite low. The expression of Panx1-370 leads to a more than threefold increase in mortality, an effect which is restricted by the addition of four further amino acids. The expression of Panx1-374 results in a mortality of less than 25%, and the same result can be observed after expression of Panx1-377. Proteins with more than 380 residues lead to subsequent cell death. From that point, mortality is reduced continuously by the addition of further amino acids. When the full length Panx1 protein is expressed, no effect on oocyte viability can be observed. This underlines that Panx1 may be harmful for mammalian cell cultures whenever the cells are stressed by appropriate stimuli. Panx1-377 mimics a Panx1 protein cleaved by caspases 3/7 during apoptosis. When Panx1 is cleaved, the pore remains open and ATP and UTP are released from the cell (Chekeni et al. 2010). The results presented indicate that opening would be even more effective when the truncation by the caspases would occur upstream or downstream of the actual cleavage site DxxD.

The results obtained from the oocyte survival studies reveal that the critical region, i.e. the region where a putative caspase cleavage site does not lead to high mortality, is very small. In fact, only truncation at residues 367, 374 and 377 did not induce mortality leading to more than 25% dead oocytes. These findings unravel a highly conserved evolutionary mechanism. The exact position of the caspase cleavage site is crucial. If the motif DxxD was shifted just a few residues up- or downstream its actual position, cleavage would lead to formation of a pore with another conformation, an increased pore diameter is likely to consider: as a consequence, the release of the “find-me” signals ATP and UTP would be altered. The results demonstrate that the contribution of

the permanently open channel to cell death would increase dramatically. However, if the cells died too fast, less nucleotides could be released to activate phagocytes and, consequently, the activation of the immune response would be considerably altered. Thus, the exact position for the caspase cleavage site is of great importance and may have developed with strong selective pressure during evolution of the Panx1 protein.

6.4.3 Panx1 Cbx sensitivity

The mechanism of Cbx inhibition of Panx1 currents remains unknown to date (Bruzzone 2005). As demonstrated by oocyte survival, not all of the truncated Panx1 proteins responded to Cbx. While the inhibition of the lethal effect induced by the truncated constructs was nearly complete in some cases, other protein forms were not sensitive to Cbx or Cbx just delayed the initiation of cell death. The inhibitory effect of Cbx was observed when Panx1 was truncated to the lengths 347, 374, 377, 387, 389, 393, 397 and 407. No Cbx sensitivity was observed when Panx1 was truncated to the lengths 307, 327, 367, 370, 380 and 383. Thus, upon truncation of Panx1 behind the fourth transmembrane domain and stepwise elongation, Cbx sensitivity first occurs at a length of 347 residues, while 327 residues are not sufficient. This leads to the hypothesis that the Cbx interaction site must be found in the range between residues 327 and 347. It is conceivable to assume that the proteins Panx1-367, -370, -380 and -383 undergo a conformational change that masks the putative binding site. This would explain that these proteins do not respond to Cbx. Thus, these findings indicate a localization of a putative Cbx binding site in Panx1. The mechanism of protein folding and Cbx sensitivity is a complex topic. The results presented in this thesis provide new insight into the functionality of several subunits of Panx1, but other aspects also have a great impact on channel function. Recent findings examine the effect of substitution of single cysteines by serine in the Panx1 protein (Bunse et al., under submission). It turned out that the substitution of the cysteine residue at position 40 and the cysteine residue at position 346 lead to a constitutively open channel, comparable to the results obtained by Panx1 truncation. In the presented C40S mutant, the Cbx sensitivity was impaired. Taken together with the finding, that Panx1 residues 327 and 347 may constitute a Cbx binding site, it is obvious that the determination of the Cbx sensitivity to a single position or region would be pretermed. Therefore, the investigation of drug sensitivity of Panx1 remains an interesting task for future studies.

7. Outlook

For the first time, Panx2 has been shown to form functional, voltage gated channels in *Xenopus* oocytes responding to a standard depolarization protocol. This finding provides great potential for research in future Panx2 studies. Considering the involvement of Panx1 in the propagation of Ca^{2+} waves, Panx2 could be tested for a similar contribution in this pathway. Ca^{2+} imaging of mammalian cells overexpressing Panx2 could provide an insight into the participation of Panx2 in Ca^{2+} signaling. Further, a possible mechanosensitivity of Panx2 can be reconsidered. Dye uptake studies could be performed, taking into account that the Panx2 channel pore is of a diameter allowing the passage of molecules like ethidium bromide or others. Further attempts on the finding of a channel inhibitor should be made in future studies, allowing the identification of Panx2 mediated currents in complex systems. Another interesting point is given in the tumor suppressive effect of Panx2. Possibly, Panx2 could be involved in apoptotic processes similar to Panx1. It may be speculated, that residues 644-647 (DMGD) in the sequence of rPanx2-674 could be considered to be recognized by caspases. This putative cleavage site is located very close to the C-terminus of Panx2, an influence of a possible cleavage could be investigated by Panx2 truncation and its effect on cell viability. In summary, the finding that Panx2 forms functional, voltage gated channels allows for various experiments in the future.

Panx1 has been shown to influence cell viability in apoptotic processes by cleavage through effector caspases. During this thesis, the influence of the length of the C-terminus has been explored in truncation studies of Panx1. It is demonstrated, that, first, the expression of truncated Panx1-proteins can mimic the effect of caspase cleavage and, second, that mortality can be influenced by varying the length of truncated Panx1-forms. Previous studies have shown that Panx1 is downregulated in glioma cells, artificial upregulation was shown to be tumor suppressive. Furthermore, it is known that the release of ATP and UTP from cleaved Panx1 activates the immune system. Combining these previous findings with the findings from the present thesis lead to new working hypothesis, which is followed up in a project that just has started in cooperation with the Dept. of Virology, Ruhr University Bochum.

8. Summary

As a main goal of this thesis, the reciprocal influence of Panx1 and Panx2 was characterized. First, the possible formation of heteromeric channels consisting of both proteins, as described in recent publications preceding this thesis, was analyzed in coexpression studies in *Xenopus laevis* oocytes.

Coexpression was performed by injection of cRNA encoding either Panx1 or Panx2-664. Both cRNAs were injected in different ratios, so that a putative influence of the respective proteins on the channel properties of the pannexon could be monitored. Oocytes expressing either Panx1 or Panx2-664 were used as controls. TEVC recordings revealed the formation of voltage gated Panx1 channels mediating Cbx sensitive currents, while the expression of Panx2-664 did not induce the formation of functional channels.

Further measurements revealed a loss of function whenever both cRNAs were injected. An influence of the injection of cRNAs in different ratios was not detected. An altered channel behavior could not be observed, coexpression of both proteins led to recordings comparable to recordings obtained from uninjected oocytes. This result led to the conclusion, that Panx1 and Panx2 do not form functional heteromeric channels. Together with a finding published in parallel regarding a fast degradation of heteromeric Panx1/Panx2 channels, a physiological relevance of heteromeric channels can be excluded. If these channels are formed, it is likely to consider that this formation happens accidentally. A putative interaction of these two proteins must be found on another level.

The fact that Panx2-664 did not form functional channels gave reason to reinvestigate the nucleotide sequence encoding the Panx2 protein. It turned out, that two putative start codons are located in the genomic sequence, encoding proteins consisting of 674 or 664 amino acids. This observation was reflected in an update of the sequence published in ncbi and by an inconsistency throughout the literature regarding Panx2. The localization of both putative start codons on the same exon excluded the possibility of determining one start codon by common PCR techniques. Thus, a functional analysis of Panx2-674 and Panx2-664 was performed. Immunocytochemical staining revealed a different localization of both proteins after overexpression in N2A cells. Panx2-664 was localized mainly intracellularly, while Panx2-674 was localized mainly in the plasma

membrane. FRIL experiments were performed to unravel the cell surface distribution of both proteins. Interestingly, both proteins were detected in the plasma membrane and quantification revealed a comparable absolute cell surface expression, unless a tendency towards a slightly higher Panx2-674 density was observed.

In summary, the results led to the conclusion that the difference in the N-terminus of Panx2-664 and Panx2-674 is affecting a correct protein shuttling and membrane targeting, leading to a retain of an amount of Panx2-664 protein in intracellular compartments.

Next, Panx2-664 and Panx2-674 have been analyzed in TEVC recordings. Panx2-664 expressing oocytes did not show currents in response to depolarization, the expression of Panx2-664 did not induce the formation of functional channels.

It was shown for the first time, that Panx2-674 forms functional voltage-gated channels, that can be activated by a standard depolarization protocol. In comparison to Panx1, Panx2-674 mediated currents are very high, the maximum currents recorded from Panx2-674 expressing oocytes exceeded Panx1 evoked currents by a factor of three. Panx2-674 was not sensitive to Cbx, neither to other inhibitors that are commonly used to block Panx1 or gap junction proteins. Thus, CoCl_2 , LaCl_3 , Mefloquine, Octanol and PEG 1500 did not show any effect on the maximum current amplitude recorded from oocytes expressing Panx2-674. Also, ATP did not inhibit Panx2-674, excluding a mechanistic effect as described for Panx1. In summary, a blocker for Panx2-674 has not yet been found. In comparison to Panx2-664, Panx2-674 can be considered to be the native form of Panx2. The observation that Panx2-674 forms functional, voltage sensitive channels provides a new insight into the importance of this protein for cellular conduction and communication.

To further investigate on the reciprocal influence of Panx1 and Panx2, chimeric proteins consisting of Panx1 and Panx2-674 have been designed and analyzed in TEVC recordings. Chimeras with an exchange of the intracellular C-terminal domains of Panx1 and Panx2 did not form voltage sensitive channels, a chimera designed to have the size of Panx1 while consisting of both proteins also was non-functional. Only one out of four chimeras was functional, currents derived from this chimera were even ~1,7 times larger than Panx2-674 mediated currents. Here, Panx1 was extended by a part of Panx2 resulting in a gain of function, indicating that the extension alters channel formation. Additionally, it was obvious that in both proteins a functionally important

interaction of the C- and the N-terminal part must be provided to build functional channels.

By these studies, the C-terminal part of Panx1 moved into focus. Truncation of Panx1 was performed to address several questions. The part necessary for the formation of a functional channel was explored, the sensitivity of Panx1 to Cbx was investigated and finally, the influence of the length of Panx1 on cell viability was analyzed. Panx1 is known to be involved in apoptosis by influencing the immunologic response, the Panx1 protein is hydrolyzed by caspases at a cleavage site at residues 376-379. The importance of this cleavage and the position of the cleavage site was determined by expression of truncated Panx1 protein in *Xenopus* oocytes. Thus, oocytes expressing proteins not inducing cell degradation could be used for TEVC recordings, while oocytes showing signs of degradation after protein expression were monitored in kinetic studies. Further, all truncated Panx1 proteins were expressed in N2A cells and the influence on cell viability was analyzed via FACS. These studies unraveled several new findings: First, it became obvious that even a truncation of nearly the entire Panx1 C-terminal domain does not result in loss of channel formation, although gating is impaired. Therefore the voltage sensor of Panx1 must be localized between residues 1-306, i.e. the N-terminal part and/or the extra- and intracellular loops.

Further, Cbx sensitivity was dedicated to a certain region. In *Xenopus* oocytes, Cbx sensitivity could be observed in electrophysiological recordings as well as in survival studies, but not for all truncated proteins. By several observations, the Panx1 residues 327-347 could be linked to Cbx sensitivity.

The survival studies of the truncated Panx1 proteins in *Xenopus* oocytes and in N2A cells led to different results, because N2A cells were more sensitive to harmful proteins than oocytes. Expressing potentially harmful proteins in oocytes allowed a detailed insight into protein properties, while the expression in N2A cells reflected a native situation. A highly conserved evolutionary mechanism was unraveled, given that shifting the caspase cleavage site a few residues up- or downstream would result in increased cell death velocity. An altered nucleotide release would be the consequence, by formation of a pore with a different conformation, resulting in an altered immune response. Thus, the results obtained by truncation of Panx1 reveal a great importance of the exact position of the caspase cleavage site and reflect that Panx1 may have developed under strong selective pressure.

Zusammenfassung

Die Charakterisierung des reziproken Einflusses von Panx1 und Panx2 war eines der Hauptziele dieser Arbeit.

Zunächst wurde die Möglichkeit zur Formation heteromerer Kanäle aus beiden Proteinen in Koexpressionstudien in *Xenopus laevis* Oozyten analysiert, wie in jüngsten, dieser Arbeit vorangehenden Veröffentlichungen beschrieben. Die Koexpression wurde durch Injektion von Panx1 oder Panx2-664 codierender cRNA gewährleistet. Zur Beobachtung eines möglichen Einflusses der jeweiligen Proteine auf die Kanaleigenschaften des Pannexons wurden beide cRNAs in unterschiedlichen Verhältnissen injiziert. Zur Kontrolle dienten entweder Panx1 oder Panx2-664 exprimierende Oozyten. TEVC Messungen zeigten die Formation spannungsgesteuerter Panx1 Kanäle in der Ableitung Cbx sensitiver Ströme, während die Expression von Panx2-664 keine Formation funktioneller Kanäle induzierte.

Weiterführende Messungen zeigten einen Funktionsverlust bei Injektion beider cRNAs. Ein Einfluss von Injektion beider cRNAs in unterschiedlichen Verhältnissen wurde nicht detektiert. Ein verändertes Kanalverhalten wurde nicht beobachtet, Koexpression beider Proteine führten zu Messungen die denen uninjektierter Oozyten vergleichbar waren. Dieses Ergebnis führte zu dem Fazit, dass Panx1 und Panx2 keine funktionellen heteromeren Kanäle bilden. Zusammen mit einem parallel veröffentlichten Befund eine schnelle Degradierung heteromerer Panx1/Panx2 Kanäle betreffend kann eine physiologische Relevanz heteromerer Kanäle ausgeschlossen werden. Sofern diese Kanäle gebildet werden ist anzunehmen, dass die Formation zufällig geschieht. Eine mögliche Interaktion dieser beiden Proteine muss auf anderer Ebene gefunden werden.

Die Beobachtung, dass Panx2-664 keine funktionellen Kanäle bildete, gab Anlass zur wiederholten Untersuchung der Panx2 codierenden Nukleotidsequenz. Es stellte sich heraus, dass zwei mögliche Startcodons in der genomischen Sequenz vorliegen, die Proteine bestehend aus 664 oder 674 Aminosäuren codieren. Diese Beobachtung spiegelte sich in einer Aktualisierung der in *ncbi* veröffentlichten Sequenz sowie durch eine Inkonsistenz innerhalb der Panx2 betreffenden Literatur wider.

Die Möglichkeit zur Determinierung eines Startcodons mittels gebräuchlicher PCR-Techniken wurde durch die Lokalisation beider möglicher Startcodons auf demselben Exon ausgeschlossen. Daher wurde eine funktionelle Analyse von Panx2-664 und

Panx2-674 durchgeführt. Eine immunocytochemische Färbung überexprimierender N2A Zellen ergab eine unterschiedliche Lokalisation beider Proteine. Panx2-664 war hauptsächlich intrazellulär lokalisiert, während Panx2-674 hauptsächlich in der Plasmamembran lokalisiert war. Zur Untersuchung der Oberflächenverteilung beider Proteine wurden FRIL Experimente durchgeführt. Interessanterweise wurden beide Proteine in der Plasmamembran detektiert und die Quantifizierung ergab eine vergleichbare Expression an der Zelloberfläche, obschon eine Tendenz in Richtung einer erhöhten Panx2-674 Dichte erkennbar war.

Zusammenfassend führten die Ergebnisse zu der Schlussfolgerung, dass der Unterschied im N-Terminus von Panx2-664 und Panx2-674 sowohl einen korrekten Proteintransport als auch das Membrantargeting beeinflusst, was ein Zurückhalten eines Anteils von Panx2-664 Protein in intrazellulären Kompartimenten zur Folge hat.

Darauffolgend wurden Panx2-664 und Panx2-674 in TEVC Messungen analysiert. Panx2-664 exprimierende Oozyten zeigten als Reaktion auf Depolarisation keine Ströme, die Expression von Panx2-664 führte nicht zur Formation funktioneller Kanäle. Es konnte zum ersten Mal gezeigt werden, dass Panx2-674 funktionelle, spannungsgesteuerte Kanäle bildet, die durch ein Standardprotokoll zur Depolarisation aktiviert werden können.

Im Vergleich zu Panx1 sind Panx2-674 vermittelte Ströme sehr hoch, die Maximalströme, die von Panx2-674 exprimierenden Oozyten abgeleitet werden konnten, überstiegen Panx1 evozierte Ströme um das Dreifache.

Panx2-674 war nicht sensitiv gegenüber Cbx, ebenso wenig gegenüber anderen gebräuchlicherweise zur Blockierung von Panx1 oder Gap Junction-Proteinen genutzten Inhibitoren. So zeigten CoCl_2 , LaCl_3 , Mefloquin, Octanol und PEG 1500 keinerlei Effekt auf die Amplitude des Maximalstroms, der von Panx2-674 exprimierenden Oozyten abgeleitet werden konnte. Des Weiteren wurde Panx2-674 nicht durch ATP inhibiert, wodurch ein mechanistischer Effekt wie der für Panx1 beschriebene ausgeschlossen wurde.

Zusammenfassend ist ein Blocker für Panx2-674 noch nicht gefunden worden. Im Vergleich zu Panx2-664 kann Panx2-674 als native Form von Panx2 betrachtet werden. Die Beobachtung der Formation funktioneller, spannungsabhängiger Kanäle durch Panx2-674 vermittelt eine neue Sicht bezüglich der Wichtigkeit dieses Proteins für die zelluläre Leitfähigkeit und Kommunikation.

Zur weiteren Untersuchung des reziproken Einflusses von Panx1 und Panx2 wurden Chimäre, jeweils aus Panx1 und Panx2-674 bestehende Proteine entworfen und in TEVC Messungen analysiert. Chimären mit einem Austausch der intrazellulären C-terminalen Domänen von Panx1 und Panx2 bildeten keine spannungsabhängigen Kanäle, ebenso war eine Chimäre in der Größe von Panx1 bei Bestehen aus beiden Proteinen nicht funktional. Lediglich eine von vier Chimären war funktional, von dieser Chimäre abgeleitete Ströme waren tatsächlich ~1,7 mal größer als Panx2-674 vermittelte Ströme. Hier wurde Panx1 durch einen Teil von Panx2 verlängert, was in einer Funktionssteigerung resultierte und daraufhin deutete, dass die Extension eine Änderung der Kanalformation zur Folge hat. Zusätzlich wurde deutlich, dass in beiden Proteinen eine funktional wichtige Interaktion des C- und des N-terminalen Teils zur Bildung funktioneller Kanäle gegeben sein muss.

Durch diese Studien rückte der C-terminale Part von Panx1 in den Fokus. Zur Bearbeitung mehrerer Fragen wurden Trunkierungen von Panx1 durchgeführt. Der zur Formation funktioneller Kanäle notwendige Teil von Panx1 wurde untersucht, die Sensitivität von Panx1 gegenüber Cbx wurde erforscht und letztendlich wurde der Einfluss der Länge von Panx1 auf die Zellviabilität analysiert.

Bekanntermaßen ist Panx1 durch eine Einflussnahme auf die Immunantwort an der Apoptose beteiligt, das Panx1 Protein wird durch Caspasen an einer Schnittstelle bei den Aminosäureresten 376-379 hydrolysiert. Die Bedeutung dieser Spaltung und der Position der Spaltstelle wurde durch Expression trunkierter Panx1 Proteine in *Xenopus* Oozyten bestimmt. Oozyten, die Proteine bei Ausbleiben von Zelldegradation exprimierten, wurden für TEVC Messungen genutzt. Oozyten, die nach Proteinexpression Zeichen von Degradation zeigten, wurden in Studien hinsichtlich ihrer Kinetik beobachtet.

Des Weiteren wurden alle trunkierten Panx1 Proteine in N2A Zellen exprimiert und der Einfluss auf die Zellviability wurde mittels FACS analysiert. Diese Studien führten zu mehreren neuen Ergebnissen: zunächst wurde deutlich, dass sogar eine Trunkierung der nahezu gesamten Panx1 C-terminalen Domäne nicht in einem Funktionsverlust resultiert, obschon die Steuerung des Kanals beeinträchtigt ist. Daher muss der Spannungsensor von Panx1 zwischen Aminosäuren 1-306 lokalisiert sein, d.h. dem N-terminalen Teil und/oder den extra- und intrazellulären Schleifen.

Des Weiteren wurde die Cbx Sensitivität auf eine bestimmte Region festgelegt. In *Xenopus* Oozyten konnte eine Cbx Abhängigkeit sowohl in elektrophysiologischen Ableitungen als auch in Überlebensstudien beobachtet werden, jedoch nicht bei allen trunkierten Proteinen. Basierend auf verschiedenen Beobachtungen konnten die Panx1 Aminosäuren 327-347 der Cbx Sensitivität zugeordnet werden.

Die Überlebensstudien der trunkierten Panx1 Proteine in *Xenopus* Oozyten und in N2A Zellen führten zu unterschiedlichen Ergebnissen, da N2A Zellen sensibler auf schädigende Proteine reagierten als Oozyten.

Die Expression potentiell schädlicher Proteine in Oozyten erlaubte einen detaillierten Einblick

in die Eigenschaften der Proteine, während die Expression in N2A Zellen einer native Situation entsprach. So wurde ein hoch konservierter evolutionärer Mechanismus aufgedeckt, da eine Verschiebung der Caspase-Schnittstelle um einige wenige Aminosäuren stromauf- oder abwärts eine gesteigerte Geschwindigkeit des Zelltods zur Folge hat. Die Konsequenz wäre ein veränderter Nukleotidausstrom durch Formation einer Pore mit unterschiedlicher Konformation, resultierend in veränderter Immunantwort. Somit wird durch die mittels der Trunkierung von Panx1 gewonnenen Ergebnisse eine große Bedeutung der exakten Position der Caspase-Schnittstelle belegt und herausgestellt, dass sich Panx1 wahrscheinlich unter hohem selektivem Druck entwickelt hat.

9. References

- Ambrosi, C., Boassa, D., Pranskevich, J., Smock, A., Oshima, A., Xu, J., Nicholson, B. J., and Sosinsky, G. E. (2010). Analysis of four connexin26 mutant gap junctions and hemichannels reveals variations in hexamer stability. *Biophysical journal* 98, 1809-19.
- Ambrosi, C., Gassmann, O., Pranskevich, J. N., Boassa, D., Smock, A., Wang, J., Dahl, G., Steinem, C., and Sosinsky, G. E. (2010). Pannexin1 and Pannexin2 channels show quaternary similarities to connexons and different oligomerization numbers from each other. *The Journal of biological chemistry* 285, 24420-31.
- Anselmi, F., Hernandez V.H., Crispino G., Seydel A., Ortolano, S., Roper S. D., Kessaris N., Richardson W., Rickheit G., Mikhail A. Filippov M. A., Monyer H., and Mammano, F. (2008). ATP release through connexin hemichannels and gap junction transfer of second messengers propagate Ca^{2+} signals across the inner ear. *Proceedings of the National Academy of Sciences of the United States of America* 105, 18770-5.
- Bao, L., Locovei, S., and Dahl, G. (2004). Pannexin membrane channels are mechanosensitive conduits for ATP. *FEBS letters* 572, 65-8.
- Baranova, A., Ivanov D., Petrash, N., Pestova, A., Skoblov, M., Kelmanson, I., Shagin, D. Nazarenko, S., Geraymovych, E., Litvin, O., Tiunova, A., Born, T. L., Usman, N., Staroverov, D., Lukyanov, S. and Panchin, Y. (2004). The mammalian pannexin family is homologous to the invertebrate innexin gap junction proteins. *Genomics* 83, 706-16.
- Barbe, M. T., Monyer, H., and Bruzzone, R. (2006). Cell-cell communication beyond connexins: the pannexin channels. *Physiology (Bethesda, Md.)* 21, 103-14.
- Bennett, M. V. L., and Zukin, R. S. (2004). Electrical coupling and neuronal synchronization in the Mammalian brain. *Neuron* 41, 495-511.
- Bhalla-Gehi, R., Penuela, S., Churko, J. M., Shao, Q., and Laird, D. W. (2010). Pannexin1 and pannexin3 delivery, cell surface dynamics, and cytoskeletal interactions. *The Journal of biological chemistry* 285, 9147-60.
- Bianco, F., Pravettoni, E., Colombo, A., Schenk, U., Möller, T., Matteoli, M., and Verderio, C. (2005). Astrocyte-derived ATP induces vesicle shedding and IL-1 beta release from microglia. *The Journal of Immunology* 174, 7268-7277.
- Blobel, G., Walter, P., and Gilmore, R. (1984). Intracellular protein topogenesis. *Progress in clinical and biological research* 168, 3-10.

- Boassa, D., Ambrosi, C., Qiu, F., Dahl, G., Gaietta, G., and Sosinsky, G. (2007). Pannexin1 channels contain a glycosylation site that targets the hexamer to the plasma membrane. *The Journal of biological chemistry* 282, 31733-43.
- Boassa, D., Qiu, F., Dahl, G., and Sosinsky, G. (2008). Trafficking dynamics of glycosylated pannexin 1 proteins. *Cell communication & adhesion* 15, 119-32.
- Bruzzone, R., Barbe, M. T., Jakob, N. J., and Monyer, H. (2005). Pharmacological properties of homomeric and heteromeric pannexin hemichannels expressed in *Xenopus* oocytes. *Journal of neurochemistry* 92, 1033-43.
- Bruzzone, R., Hormuzdi, S. G., Barbe, M. T., Herb, A., and Monyer, H. (2003). Pannexins, a family of gap junction proteins expressed in brain. *Proceedings of the National Academy of Sciences of the United States of America* 100, 13644-9.
- Buettner, R., Papoutsoglou, G., Scemes, E., Spray, D. C., and Dermietzel, R. (2000). Evidence for secretory pathway localization of a voltage-dependent anion channel isoform. *Proceedings of the National Academy of Sciences of the United States of America* 97, 3201-6.
- Bunse, S., Molecular and functional analyses of the pannexins in the central nervous system.
- Bunse, S., Locovei, S., Schmidt, M., Qiu, F., Zoidl, G., Dahl, G., and Dermietzel, R. (2009). The potassium channel subunit Kvbeta3 interacts with pannexin 1 and attenuates its sensitivity to changes in redox potentials. *The FEBS journal* 276, 6258-70.
- Bunse, S., Schmidt, M., Hoffmann, S., Engelhardt, K., Zoidl, Georg, and Dermietzel, R. Single cysteines in the extracellular and transmembrane regions modulate pannexin1 channel function. Under submission.
- Cao, F., Eckert, R., Elfgang, C., Nitsche, J. M., Snyder, S. A., H-Ulser, D. F., Willecke, K., and Nicholson, B J (1998). A quantitative analysis of connexin-specific permeability differences of gap junctions expressed in HeLa transfectants and *Xenopus* oocytes. *Journal of Cell Science* 111 (Pt 1, 31-43.
- Cavara, N. a, Orth, A., Hicking, G., Seebohm, G., and Hollmann, M. (2010). Residues at the tip of the pore loop of NR3B-containing NMDA receptors determine Ca^{2+} permeability and Mg^{2+} block. *BMC neuroscience* 11, 133.
- Chekeni, F. B. et al. (2010). Pannexin 1 channels mediate “find-me” signal release and membrane permeability during apoptosis. *Nature* 467, 863-867.
- Clapp, T. R., Yang, R., Stoick, C. L., Kinnamon, S. C., and Kinnamon, J. C. (2004). Morphologic characterization of rat taste receptor cells that express components of the phospholipase C signaling pathway. *The Journal of comparative neurology* 468, 311-21.

- Crow, D. S., Beyer, E. C., Paul, D. L., Kobe, S. S., and Lau, A. F. (1990). Phosphorylation of connexin43 gap junction protein in uninfected and Rous sarcoma virus-transformed mammalian fibroblasts. *Molecular and cellular biology* 10, 1754-63.
- Dahl, G., and Locovei, S. (2006). Pannexin: to gap or not to gap, is that a question? *IUBMB life* 58, 409-19.
- Dando, R., and Roper, S. D. (2009). Cell-to-cell communication in intact taste buds through ATP signalling from pannexin 1 gap junction hemichannels. *The Journal of physiology* 587, 5899-906.
- DeFazio, R., Dvoryanchikov, G., Maruyama, Y., Kim, J. W., Pereira, E., Roper, S. D., and Chaudhari, N. (2006). Separate populations of receptor cells and presynaptic cells in mouse taste buds. *The Journal of neuroscience : the official journal of the Society for Neuroscience* 26, 3971-80.
- Dermietzel, R., and Spray, D. C. (1993). Gap junctions in the brain: where, what type, how many and why? *Trends in Neurosciences* 16, 186-192.
- Dinarello, C. (2005). Blocking IL-1 in systemic inflammation. *The Journal of experimental medicine* 201, 1355-9.
- Dubyak, G. R. (2009). Both sides now: multiple interactions of ATP with pannexin-1 hemichannels. Focus on " A permeant regulating its permeation pore: inhibition of pannexin 1 channels by ATP". *American Journal of Physiology- Cell Physiology* 296, C235.
- Dvorientchikova, G., Ivanov, D., Panchin, Y., and Shestopalov, V. I. (2006). Expression of pannexin family of proteins in the retina. *FEBS letters* 580, 2178-82.
- Dvorientchikova, G., Ivanov, D., Pestova, A., and Shestopalov, V. (2006). Molecular characterization of pannexins in the lens. *Molecular vision* 12, 1417-26.
- Elfgang, C., Eckert, R., Lichtenberg-Fraté, H., Butterweck, a, Traub, O., Klein, R., Hülser, D. F., and Willecke, K. (1995). Specific permeability and selective formation of gap junction channels in connexin-transfected HeLa cells. *The Journal of cell biology* 129, 805-17.
- Elliott, M. R., Chekeni F. B., Trampot P. C., Lazarowski E.R., Kadl A., Walk S.F., Park D., Woodson I. R., Ostankovich M., Sharma P., Lysiak J.J., Kendall T., Harden K., Leitinger N., and Ravichandran K. S. (2009). Nucleotides released by apoptotic cells act as a find-me signal to promote phagocytic clearance. *Nature* 461, 282-6.
- Enkvist, M. O., and McCarthy, K. D. (1992). Activation of protein kinase C blocks astroglial gap junction communication and inhibits the spread of calcium waves. *Journal of neurochemistry* 59, 519-26.

- Fahrenfort, I., Sjoerdsma, T., Ripps, H., and Kamermans, M. (2004). Cobalt ions inhibit negative feedback in the outer retina by blocking hemichannels on horizontal cells. *Visual Neuroscience* 21, 501-511.
- Ferrari, D., Pizzirani, C., Adinolfi, E., Lemoli, R. M., Curti, A., Idzko, M., Panther, E., and Di Virgilio, F. (2006). The P2X7 receptor: a key player in IL-1 processing and release. *Journal of immunology (Baltimore, Md. : 1950)* 176, 3877-83.
- Harris, A. L. (2001). Emerging issues of connexin channels: biophysics fills the gap. *Quarterly reviews of biophysics* 34, 325-472.
- Harris, A. L. (2007). Connexin channel permeability to cytoplasmic molecules. *Progress in Biophysics and Molecular Biology* 94, 120-143.
- Hassinger, T. D., Guthrie, P. B., Atkinson, P. B., Bennett, M. V. L., and Kater, S. B. (1996). An extracellular signaling component in propagation of astrocytic calcium waves. *Proceedings of the National Academy of Sciences of the United States of America* 93, 13268-13273.
- Hu, X., and Dahl, G. (1999). Exchange of conductance and gating properties between gap junction hemichannels. *FEBS letters* 451, 113-7.
- Hu, X., Ma, M., and Dahl, G. (2006). Conductance of connexin hemichannels segregates with the first transmembrane segment. *Biophysical journal* 90, 140-50.
- Hua, V. B., Chang, A. B., Tchieu, J. H., Kumar, N. M., Nielsen, P. A., and Saier, M. H. (2003). Sequence and phylogenetic analyses of 4 TMS junctional proteins of animals: connexins, innexins, claudins and occludins. *The Journal of membrane biology* 194, 59-76.
- Huang, Y. A. N., Grinspan, J. B., Abrams, C. K., and Scherer, S. S. (2007). Pannexin1 is Expressed by Neurons and Glia but Does Not Form Functional Gap Junctions. *Cultures* 56, 46-56.
- Huang, Y.-J., Maruyama, Y., Dvoryanchikov, G., Pereira, E., Chaudhari, N., and Roper, S. D. (2007). The role of pannexin 1 hemichannels in ATP release and cell-cell communication in mouse taste buds. *Proceedings of the National Academy of Sciences of the United States of America* 104, 6436-41.
- Iglesias, R., Locovei, S., Roque, A. P., Dahl, G., Spray, D. C., and Scemes, E. (2008). P2X7 receptor-Pannexin1 complex: pharmacology and signaling. *American journal of physiology. Cell physiology* 295, C752-60.
- Iglesias, R., Spray, D. C., and Scemes, E. (2009). Mefloquine blockade of Pannexin1 currents: resolution of a conflict. *Cell communication & adhesion* 16, 131-7.
- Iwamoto, T., Nakamura, T., and Doyle, A. (2010). Pannexin 3 regulates intracellular ATP/cAMP levels and promotes chondrocyte differentiation. *Journal of Biological Chemistry*. 285, 18948–18958.

- Iwatsuki, K., Ichikawa, R., Hiasa, M., Moriyama, Y., Torii, K., and Uneyama, H. (2009). Identification of the vesicular nucleotide transporter (VNUT) in taste cells. *Biochemical and Biophysical Research Communications* 388, 1-5.
- Johnston, M., Simon, S., and Ramon, F. (1980). Interaction of anaesthetics with electrical synapses.
- Kienitz, M.-C., Bender, K., Dermietzel, Rolf, Pott, L., and Zoidl, Georg (2010). Pannexin 1 constitutes the large-conductance cation channel of cardiac myocytes. *The Journal of biological chemistry*.
- Klebe, R., and Ruddle, F. (1969). Neuroblastoma: Cell culture analysis of a differentiating stem cell system. *Journal of Cellular Biology* 43:69A.
- Lai, C. P. K., Bechberger, J. F., and Naus, C. C. (2009). Pannexin2 as a novel growth regulator in C6 glioma cells. *Oncogene* 28, 4402-8.
- Lai, C. P. K., Bechberger, J. F., Thompson, R. J., MacVicar, B. , Bruzzone, R., and Naus, C.C. (2007). Tumor-suppressive effects of pannexin 1 in C6 glioma cells. *Cancer research* 67, 1545-54.
- Laird, D. W. (2006). Life cycle of connexins in health and disease. *The Biochemical journal* 394, 527-43.
- Litvin, O. (2006). What is hidden in the pannexin treasure trove: the sneak peek and the guesswork. *Journal of Cellular and Molecular Medicine* 10.
- Locovei, S., Scemes, E., Qiu, F., Spray, D. C., and Dahl, G. (2007). Pannexin1 is part of the pore forming unit of the P2X(7) receptor death complex. *FEBS letters* 581, 483-8.
- Locovei, S., Wang, J., and Dahl, G. (2006a). Activation of pannexin 1 channels by ATP through P2Y receptors and by cytoplasmic calcium. *FEBS letters* 580, 239-44.
- Ma, M., and Dahl, G. (2006). Cosegregation of permeability and single-channel conductance in chimeric connexins. *Biophysical journal* 90, 151-63.
- Ma, W., Hui, H., Pelegrin, P., and Surprenant, A. (2009). Pharmacological characterization of pannexin-1 currents expressed in mammalian cells. *Journal of Pharmacology and Experimental Therapeutics* 328, 409.
- MacVicar, B. a, and Thompson, R. J. (2010). Non-junction functions of pannexin-1 channels. *Trends in neurosciences* 33, 93-102.
- Martinon, F., and Tschopp, J. (2004). Inflammatory caspases: linking an intracellular innate immune system to autoinflammatory diseases. *Cell* 117, 561-574.
- Nishida, M., Sato, Y., Uemura, A., Narita, Y., Tozaki-Saitoh, H., Nakaya, M., Ide, T., Kazuhiro, K., Inoue, K., Nagao, T., and Kurose, H. (2008). P2Y6 receptor-

- Galphal2/13 signalling in cardiomyocytes triggers pressure overload-induced cardiac fibrosis. *The European Molecular Biology Organization Journal* 27, 3104-3115.
- Panchin, Y., Kelmanson, I., Matz, M., Lukyanov, K., Usman, N., and Lukyanov, S (2000). A ubiquitous family of putative gap junction molecules. *Current Biology* 10, R473-4.
- Pelegrin, P., and Surprenant, A. (2007). Pannexin-1 couples to maitotoxin- and nigericin-induced interleukin-1beta release through a dye uptake-independent pathway. *The Journal of biological chemistry* 282, 2386-94.
- Pelegrin, P., and Surprenant, A. (2006). Pannexin-1 mediates large pore formation and interleukin-1beta release by the ATP-gated P2X7 receptor. *The EMBO journal* 25, 5071-82.
- Penuela, S., Bhalla, R., Gong, X.-Q., Cowan, K. N., Celetti, S. J., Cowan, B. J., Bai, D., Shao, Q., and Laird, D. W. (2007). Pannexin 1 and pannexin 3 are glycoproteins that exhibit many distinct characteristics from the connexin family of gap junction proteins. *Journal of cell science* 120, 3772-83.
- Penuela, S., Bhalla, R., Nag, K., and Laird, D. W. (2009). Glycosylation Regulates Pannexin Intermixing and Cellular Localization. *Molecular Biology of the Cell* 20, 4313- 4323.
- Peter, C., Wesselborg, S., and Lauber, K. (2010). Apoptosis: Opening PANdora`s BoX. *Current biology : CB* 20, R940-2.
- Phelan, P., and Starich, T. A. (2001). Innexins get into the Gap. *BioEssays news and reviews in molecular cellular and developmental biology* 23, 388-396.
- Qiu, F., and Dahl, Gerhard (2009). A permeant regulating its permeation pore: inhibition of pannexin 1 channels by ATP. *American journal of physiology. Cell physiology* 296, C250-5.
- Ray, A., Zoidl, G., Weickert, S., Wahle, P., and Dermietzel, R. (2005). Site-specific and developmental expression of pannexin1 in the mouse nervous system. *The European journal of neuroscience* 21, 3277-90.
- Scemes, E., Spray, D. C., and Meda, P. (2009). Connexins, pannexins, innexins: novel roles of "hemi-channels". *Pflügers Archiv : European journal of physiology* 457, 1207-26.
- Scemes, E., Suadicani, S. O., Dahl, G., and Spray, D. C. (2007). Connexin and pannexin mediated cell-cell communication. *Neuron glia biology* 3, 199-208.
- Schenk, U., Westendorf, A. M., Radaelli, E., Casati, A., Ferro, M., Fumagalli, M., Verderio, C., Buer, J., Scanziani, E., and Grassi, F. (2008). Purinergic control of T cell activation by ATP released through pannexin-1 hemichannels. *Science signaling* 1, ra6.

- Shestopalov, V. I., and Panchin, Y. (2008). Pannexins and gap junction protein diversity. *Cellular and molecular life sciences : CMLS* 65, 376-94.
- Silverman, W. R., Rivero Vaccari, J. P. de, Locovei, S., Qiu, F., Carlsson, S. K., Scemes, E., Keane, R. W., and Dahl, G. (2009). The pannexin 1 channel activates the inflammasome in neurons and astrocytes. *The Journal of biological chemistry* 284, 18143-51.
- Silverman, W., Locovei, S., and Dahl, G. (2008). Probenecid, a gout remedy, inhibits pannexin 1 channels. *American journal of physiology. Cell physiology* 295, C761-7.
- Stern-Bach, Y., Bettler, B., Hartley, M., Sheppard, P., O'Hara, P., and Heinemann, S. (1994). Agonist selectivity of glutamate receptors is specified by two domains structurally related to bacterial amino acid-binding proteins. *Neuron* 13: 1345-1357.
- Strutz-Seebohm, N., Werner, M., Madsen, D., Seebohm, G., Zheng, Y., Walker, C., Maricq, A., and Hollmann, M. (2003). Functional analysis of *Caenorhabditis elegans* glutamate receptor subunits by domain transplantation. *J Biol Chem* 278: 44691-44701.
- Suadicani, S. O., Brosnan, C. F., and Scemes, E. (2006). P2X7 receptors mediate ATP release and amplification of astrocytic intercellular Ca²⁺ signaling. *The Journal of neuroscience : the official journal of the Society for Neuroscience* 26, 1378-85.
- Thompson, R. J., Jackson, M. F., Olah, M. E., Rungta, R. L., Hines, D. J., Beazely, M., MacDonald, J. F., and MacVicar, B. (2008). Activation of pannexin-1 hemichannels augments aberrant bursting in the hippocampus. *Science (New York, N.Y.)* 322, 1555-9.
- Thompson, R. J., Zhou, N., and MacVicar, B. (2006). Ischemia opens neuronal gap junction hemichannels. *Science (New York, N.Y.)* 312, 924-7.
- Vanden Abeele, F., Bidaux, G., Gordienko, D., Beck, B., Panchin, Y. V., Baranova, A. V., Ivanov, D. V., Skryma, R., and Prevarskaya, N. (2006). Functional implications of calcium permeability of the channel formed by pannexin 1. *The Journal of cell biology* 174, 535-46.
- Vogt, A., Hormuzdi, S. G., and Monyer, H. (2005). Pannexin1 and Pannexin2 expression in the developing and mature rat brain. *Brain research. Molecular brain research* 141, 113-20.
- Wang, J., and Dahl, G. (2010). SCAM analysis of Panx1 suggests a peculiar pore structure. *The Journal of general physiology* 136, 515-27.
- Wang, J., Ma, M., Locovei, S., Keane, R. W., and Dahl, G. (2007). Modulation of membrane channel currents by gap junction protein mimetic peptides: size matters. *American journal of physiology. Cell physiology* 293, C1112-9.

- Werner, R., Levine, E., Rabadan-Diehl, C., and Dahl, G (1989). Formation of hybrid cell-cell channels. *Proceedings of the National Academy of Sciences of the United States of America* 86, 5380-4.
- Wurch, T., Lestienne, F., and Pauwels, P. J. (1998). A modified overlap extension PCR method to create chimeric genes in the absence of restriction enzymes. *Biotechnology techniques* 12, 653–657.
- Zappalà, a, Li Volti, G., Serapide, M. F., Pellitteri, R., Falchi, M., La Delia, F., Cicirata, V., and Cicirata, F. (2007). Expression of pannexin2 protein in healthy and ischemized brain of adult rats. *Neuroscience* 148, 653-67.
- Zhang, L., Deng, T., Sun, Y., Liu, K., Yang, Y., and Zheng, X. (2008). Role for nitric oxide in permeability of hippocampal neuronal hemichannels during oxygen glucose deprivation. *Journal of neuroscience research* 86, 2281-91.
- Zoidl, G., Petrasch-Parwez, E., Ray, A., Meier, C., Bunse, S, Habbes, H.-W., Dahl, G., and Dermietzel, R (2007). Localization of the pannexin1 protein at postsynaptic sites in the cerebral cortex and hippocampus. *Neuroscience* 146, 9-16.
- Zoidl, G., Kremer, M., Zoidl, C., Bunse, S., and Dermietzel, R. (2008). Molecular diversity of connexin and pannexin genes in the retina of the zebrafish *Danio rerio*. *Cell communication & adhesion* 15, 169-83.

Curriculum vitae

Name	Kathrin H. Engelhardt
Date of birth	30.06.1981
Place of birth	Dortmund
Nationality	German

Education

Since October 2007	Doctoral thesis at the Department of Neuroanatomy and Molecular Brain Research, under supervision of Prof. Dr. R. Dermietzel; Title: “Molecular and functional analysis of communicating channels”
Since October 2010	Doctoral stipend of the Heinrich & Alma Vogelsang Stiftung
October 2007 – October 2010	Doctoral stipend of the Graduiertenkolleg 736: “Development and plasticity of the nervous system: Molecular, synaptic and cellular mechanisms”
August 2006 – July 2007	Diploma thesis “Immunogenität und Wirksamkeit genetischer Impfstoffe gegen das Respiratorische Syncytialvirus” in the Dept. of Molecular and Medical Virology
October 2001-August 2006	Studies for the diploma of biology at the Ruhr-University Bochum, Germany
1987 – 2001	Goethe Gymnasium Dortmund and Primary school Kirchhörde, Dortmund

Acknowledgements

I thank...

Prof. Dr. R. Dermietzel for giving me the opportunity to work in this department, for his constant interest in the progress of my studies and for much support and helpful ideas. Thanks for encouraging me to develop new ideas and, especially, for support in keeping the focus in experimental design.

PD Dr. M. Schmidt for cosupervision of this thesis, and for much help beyond. Thank you for discussions, encouragement and for the tremendous support regarding all electrophysiological matters. At this point, I would like to thank you and also the Ecocyte Bioscience company for giving me the opportunity to use the Robocyte System.

Prof. Dr. P. Wahle for giving me the opportunity to take part in the Graduate School 736, for funding, but most important, for scientific education.

PD Dr. G. Zoidl and Dr. S. Bunse for help and advice in molecular biologic questions and many fruitful discussions.

Dr. M. Tenbusch for support regarding the FACS analysis and for conceptual help regarding not only this thesis, but also further projects planned in cooperation.

For excellent technical help:

H.W. Habbes in immunohistochemistry, L. Augustinowski and A. Ludwig in FRIL experiments, S. Schreiber-Minjoli and J. Willms in cell culture, C. Zoidl, S. Peuckert and S. Wulf for help in molecular biological regards, and H. Schulze for providing artwork.

Dr. N. Prochnow for introducing me to the electrophysiology on N2A cells.

PD Dr. C. Theiss for support with the confocal LSM microscope.

M. Wüthrich and B. Vornefeld for help regarding computer problems.

U. Becker and M. Birkelbach for caring about all administrative matters.

The Vogelsang Stiftung for funding.

... all the colleagues, that I was lucky to get to know during the time I spent in this department. Thank you for the nice atmosphere. Thank you for help in scientific questions, but also for encouragement, for distraction, for arguments and for making a day at work feel nice.

... at last, I would like to take the opportunity to thank my family.

I thank my parents for the persistent, stubborn believe in my skills.

I thank my sister for so many times of encouragement, for help in chemical questions, and for an overall basic understanding of chemistry, which I would not have reached alone.

I again thank Dr. M. Tenbusch, for being at my side at this thesis work, for patience, and for taking care.

Erklärung

Hiermit erkläre ich, dass ich die Arbeit selbständig verfasst und bei keiner anderen Fakultät eingereicht und dass ich keine anderen als die angegebenen Hilfsmittel verwendet habe. Es handelt sich bei der heute von mir eingereichten Dissertation um sechs in Wort und Bild völlig übereinstimmende Exemplare. Weiterhin erkläre ich, dass digitale Abbildungen nur die originalen Daten enthalten und in keinem Fall inhaltsverändernde Bildbearbeitung vorgenommen wurde.

Bochum, den
